Catalytic Oxidations in Dense Carbon Dioxide†

Tsunetake Seki‡ and Alfons Baiker*

Institute for Chemical and Bioengineering, Department of Chemistry and Applied Biosciences, ETH Zurich, Hönggerberg, HCI, CH-8093 Zurich, Switzerland

Received June 9, 2008

Contents

1. Introduction

Supercritical carbon dioxide ($scCO_2$) has been proven to offer a number of interesting opportunities as a medium for performing various catalytic reactions.[1] Particularly, its great miscibility with gaseous reagents as well as organic compounds has led to exceedingly high-speed reaction rates that are hardly achievable in conventional liquid solvents due to inherent gas−liquid mass transport limitations. Earlier accounts on important issues on the catalytic reactions using gaseous reagents mainly involve hydrogenation of organic compounds,[2] carbon monoxide,[3] and carbon dioxide,[4] while studies on the catalytic oxidation using molecular oxygen, namely, aerobic oxidations in $scCO_2$, came into focus more recently,[5] though a few older studies on this topic exist. Compared to hydrogenations which are often monotonously accelerated when the concentration of H_2 in the vicinity of catalyst is increased, aerobic oxidations show a complex behavior. The miscibility of organic substrates and catalysts with molecular oxygen is crucial to achieve higher oxidation rate, but the metal component(s) of catalysts tend to undergo

† This article is part of the Facilitated Synthesis special issue.
* To whom correspondence should be addressed. E-mail: baiker@chem.ethz.ch.
‡ Research Fellow of the Japan Society for the Promotion of Science.

10.1021/cr8004058 CCC: $71.50
Published on Web 04/15/2009

Tsunetake Seki, born in Tsukuba, Japan, in 1978, completed his undergraduate and Master's degrees at Hokkaido University under the direction of Prof. Hideshi Hattori, and his Ph.D. degree at the University of Tokyo in 2006 under the supervision of Prof. Makoto Onaka. From 2005 to 2010, he was appointed Research Fellow of the Japan Society for the Promotion of Science, and he is currently engaged in the development of both heterogeneous and homogeneous catalysis in supercritical fluids, under the supervision of Prof. Alfons Baiker (ETH Zurich) and Prof. Takao Ikariya (Tokyo Institute of Technology). His research interests also include heterogeneous acidic and basic catalysis, spectroscopy of solid surfaces and gas-expanded liquids, synthesis of mesoporous oxides and their application to catalytic reactions, and design of metal complex catalysts.

Alfons Baiker (1945) studied chemical engineering at ETH Zurich and earned his Ph.D. degree in 1974. After several postdoctoral stays at different universities, he finished his habilitation at Stanford University (California) and returned to ETH in 1980, where he started his own research group, focusing on heterogeneous catalysis and reaction engineering at the Department of Chemistry and Applied Biosciences. He moved up the ranks to become Full Professor in 1990. His research interests, documented in more than 770 publications in refereed journals and numerous patents, are centered around catalyst design and novel catalytic materials, mechanisms and kinetics of catalytic surface processes, asymmetric hydrogenation, selective oxidation, environmental catalysis, chiral surfaces, in situ spectroscopy, and the application of supercritical fluids in catalysis. His goal is to further the scientific basis needed for developing environmentally benign chemical processes which make optimal use of raw materials and energy.

overoxidation if contacted with too high O_2 concentration by virtue of $scCO_2$, leading to the catalyst deactivation. The following arguments have been brought up as possible merits of using $scCO_2$ as medium for catalytic aerobic oxidations: (i) CO_2 is abundantly available and cheap, (ii) CO_2 is nontoxic and environmentally benign, (iii) CO_2 is in the highest oxidation state of carbon and hence nonflammable and nonreactive even under oxidative conditions, (iv) $scCO_2$ is greatly miscible with gaseous O_2 as well as organic substrates due to its density being intermediate between gaseous CO_2 and liquid CO_2, thereby eliminating the gas−liquid boundary, (v) the high diffusivity and low viscosity of $scCO_2$ enhance the mass transfer of reactants and products in the porous network of heterogeneous catalysts, while its liquid-like density is sufficient to extract products from the catalyst surface, (vi) the relatively high heat conductivity of $scCO_2$ leads to better dissipation of reaction heat generated during oxidations, (vii) separation of products and solvent ($scCO_2$) can easily be performed by depressurization, and the separated CO_2 can be reused by pressurization, and finally, (viii) the tunable physical properties of $scCO_2$ by changing pressure and temperature allow us to use it at various conditions. Currently, only aqueous media[6a,b] and supercritical water[1b,6c−e] seem to rival $scCO_2$ as ideal solvents for catalytic oxidations. However, the higher polarity of aqueous media enhances metal leaching of heterogeneous catalysts and even brings about fatal structural collapse. In addition, the selectivity to aldehydes in the oxidation of alcohols can often be significantly lowered in aqueous media, because carboxylic acids are formed via the hydration of aldehydes. Supercritical water has been demonstrated to be a useful medium for destructive oxidation of organic pollutants but probably is not applicable for a wide range of synthetic oxidations due to the severe conditions. The high-pressure conditions are certainly a demerit of $scCO_2$, but this could be offset by a number of other favorable properties of the medium.

In the present review, we focus on both homogeneous and heterogeneous catalytic oxidations in dense CO_2, covering the work published until early 2008. Examples of the use of diluted peroxides such as aqueous H_2O_2 and *t*-BuOOH are also shown, though most work so far used molecular oxygen as oxidant. The oxidations in CO_2-expanded liquids (CXLs) are also considered.[7] Finally, we discuss the potential and limitations of the dense CO_2 as media for catalytic oxidations.

2. Properties of Carbon Dioxide−Molecular Oxygen Mixtures

2.1. Phase Behaviors

2.1.1. Critical Constants of the CO_2−O_2 Mixtures

The presence of O_2 alters the critical point of CO_2 (P_c = 7.375 MPa, T_c = 30.9 °C, ρ_c = 468 kg m^{-3}).[8] Experimental data on the critical properties of binary mixtures composed of CO_2 and O_2 are compiled in a recent review by Abdulagatov et al.[9] Figures 1 and 2 compare the changes of critical pressure and temperature of CO_2−O_2 and CO_2−H_2 mixtures with the molar percent of O_2 and H_2, while in Figure 3 is plotted the variation of critical pressure of CO_2−O_2 mixtures as a function of critical temperature, based on the data set given by Booth and Carter,[10] Zenner and Dana,[11] and Tsang and Streett.[12] As emerges from Figures 1 and 2, there is a striking difference in the change of critical point between the CO_2−O_2 and CO_2−H_2 systems, particularly at higher O_2 and H_2 molar percents. Aerobic oxidations in dense CO_2 are typically performed with a small mole fraction of O_2 (<10 mol % O_2). However, even in the oxidations with relatively large amounts of O_2, the presence of O_2 raises the critical pressure only a bit from that of pure CO_2 (Figure 1). This is in contrast to the behavior of the CO_2−H_2 system, where H_2 significantly increases the critical pressure as its content increases.

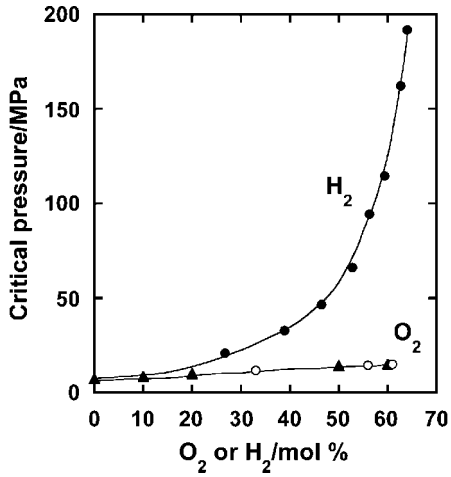

Figure 1. Variation of the critical pressure of CO_2-O_2 and CO_2-H_2 mixtures as a function of the amount of coexisting O_2 or H_2. Data taken from refs 10 (filled triangle), 11 (open circle), and 12 (filled circle).

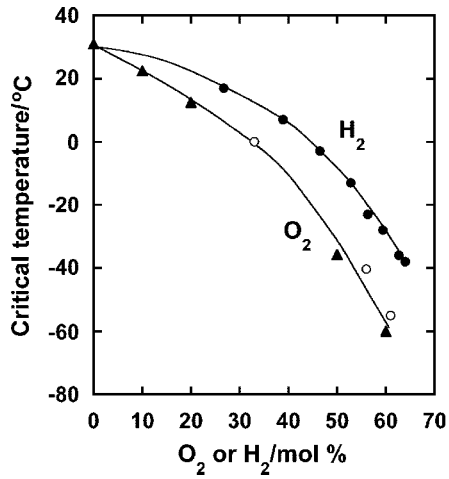

Figure 2. Variation of the critical temperature of CO_2-O_2 and CO_2-H_2 mixtures as a function of the amount of coexisting O_2 or H_2. Data taken from refs 10 (filled triangle), 11 (open circle), and 12 (filled circle).

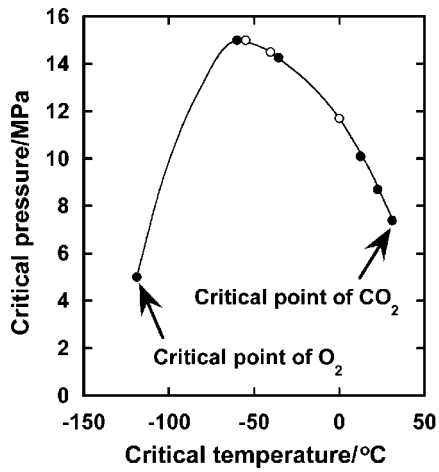

Figure 3. Variation of the critical pressure of CO_2-O_2 mixture as a function of its critical temperature. Data taken from refs 10 (filled circle) and 11 (open circle).

2.1.2. Phase Behaviors of the Reacting Systems

The miscibility of CO_2 and O_2 is not the sole factor determining the phase behavior of reaction mixtures, because the mixtures also contain reactants, catalysts, and, in some cases, promoters. Prediction of the phase behavior of a reaction mixture is usually difficult, owing to the very limited number of equation of states available and to the complex composition which changes with reaction time. However, information of the phase behavior is easily available by direct visual observation of the mixture using a reactor equipped with windows (material, e.g., sapphire).[13] Most researchers who performed oxidations in $scCO_2$ actually relied on this primitive but reliable way to systematically understand the catalytic performance−phase behavior relationships. The combined use of *in situ* transmission infrared and attenuated total reflection infrared spectroscopy (ATR-IR) also furnishes information of phase behavior, which is more reliable than visual observation, which strongly depends on the subjectivity of the observer. Figure 4 shows an example of an *in situ* IR cell designed for this purpose.[1k,14] These spectroscopic techniques do not miss even very small droplets of insoluble organic substances attached on the wall of a reactor, which are normally invisible with human eyes. The composition of the mixture inside the pores of heterogeneous catalysts can also be examined by using catalyst-coated ATR-IR crystals (see section 3.1.2.4).[1k,14]

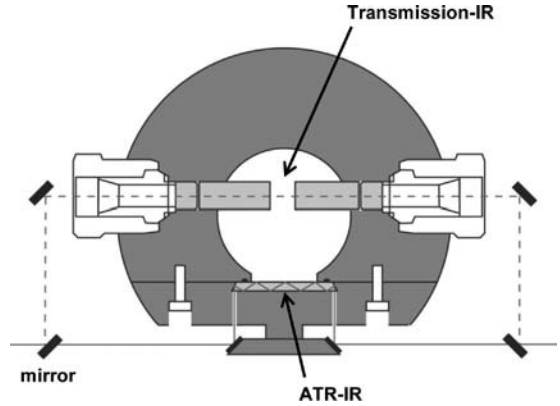

Figure 4. Schematic view of the combined cell used for the visual observation, transmission infrared spectroscopy, and attenuated total reflection infrared (ATR-IR) spectroscopy (for details, see ref 14a). Reprinted with permission from ref 14a. Copyright 2003 American Institute of Physics.

2.2. Reaction of Carbon Dioxide with Molecular Oxygen

CO_2 is a fully oxidized compound and is likely not to react directly with O_2 at normal temperatures. However, oxygen-exchange between CO_2 and O_2 has been observed over certain metal oxides. Kiyoura, for example, reported that the catalytic activity of metal oxides for the oxygen-exchange at 150−600 °C increases in the order of $TiO_2 < V_2O_5 < Cr_2O_3 < Fe_2O_3 < NiO < MnO_2 < Co_3O_4$.[15] Iwata and co-workers also described the ^{15}O-exchange reactions between CO_2 and O_2 over copper- and manganese-mixed oxide.[16] These exchange reactions are suggested to involve the oxygen-exchange between metal oxides and gases (CO_2 and O_2), as shown in Scheme 1. Note that these studies were performed with low pressure, gaseous CO_2, and no data is currently available on the oxygen-exchange between dense CO_2 and O_2. However, it is expected by analogy that a similar exchange occurs also in dense CO_2. Since metal oxides are used as catalyst supports or as catalysts in heterogeneous catalytic aerobic oxidations, systematic studies of the effect of such oxygen-exchange processes on the oxidation catalysis

Scheme 1. Catalytic Oxygen-Exchange between CO_2 and O_2 over Metal Oxides

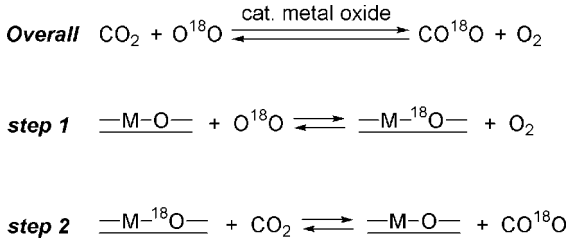

Scheme 2. General Reaction Pathways in the Aerobic Oxidation of Primary Alcohols in $ScCO_2$

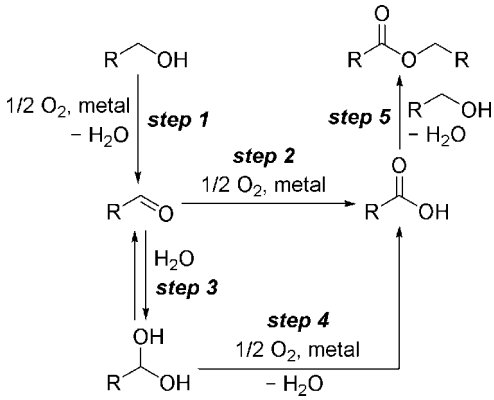

would be desirable. Particularly, for those catalysts which are prone to exchange oxygen atoms with reactants (e.g., Fe_2O_3, $Bi_2O_3-MoO_3$), such fundamental work seems to be indispensable to gain a thorough understanding of the governing reaction mechanism.

3. Aerobic Oxidation of Alcohols

Selective aerobic oxidation of alcohols to aldehydes or ketones has been widely studied not only in conventional liquid solvents but also in $scCO_2$ using both batch and continuous-flow reactors. Products usually observed in the primary alcohol oxidation with metal catalyst, and their formation routes, are depicted in Scheme 2.[17,18] The key to achieve high selectivity to aldehyde is to suppress the formation of carboxylic acid, which further reacts with reactant alcohol to yield ester, leading to a further decline of the aldehyde selectivity. Two paths are considered for the carboxylic acid formation from the aldehyde product, but the route via the hydration of aldehyde is considered to take place much faster. Hence, $scCO_2$ seems to be more suitable for the oxidation of primary alcohols compared to aqueous medium, which is also considered to be an ideal medium for oxidations, due to its nonflammability and nontoxicity.[6] For supported-metal heterogeneous catalysts, $scCO_2$ also should play an important role in extracting byproduct water from catalyst surfaces.[19]

3.1. Supported Palladium and Platinum Catalysts

The catalytic behavior of supported palladium and platinum particles for the aerobic oxidation of alcohols in dense CO_2 has widely been investigated, owing to their high activity and selectivity. Examples of the use of palladium or platinum complexes are comparatively rare. The oxidation over supported palladium or platinum catalysts in dense CO_2 seems to proceed by essentially the same mechanism as that in conventional liquid solvents, embracing the following main steps: (i) dehydrogenation of reactant alcohol on a palladium surface and (ii) oxidative removal of the adsorbed hydrogen atoms formed in step (i) and/or of the strongly adsorbed poisoning species such as carbon monoxide (oxidative surface cleaning).[17] In organic solvents, the oxidative conditions often afford solvent-derived byproducts, because solvents also undergo oxidations. However, in dense CO_2, the formation of CO_2-derived byproducts is typically not observed due to the inertness of CO_2 under oxidative conditions, indicating that dense CO_2 serves as an absolutely inert solvent for the oxidations over supported palladium and platinum catalysts. Apparently, the main roles of dense CO_2 are to enhance the miscibility of reactants (alcohols and O_2) and to promote the mass transfer of the reactants and products in the vicinity of the catalyst surface as well as inside the pores of catalyst, by virtue of its low viscosity and high diffusivity.

The palladium or platinum-catalyzed oxidations have been performed using both batch and continuous-flow reactors. The setup and operation of batch reactor systems are relatively simple, but studies with continuous-flow reactors are more attractive in view of possible application to large-scale processes in industry. In the following, the results gathered with batch reactors and continuous-flow reactors are separately introduced in that order.

3.1.1. Batch Reactor Investigations

3.1.1.1. Teflon-Coated Pd/C and Pt/C Catalysts. In the oxidation of alcohols, the presence of even a small quantity of water leads to the formation of carboxylic acids via hydration of the aldehyde products (Scheme 2).[17,18] Elimination of water formed during the alcohol oxidation from the catalyst surface is thus crucial to achieve high aldehyde yields. It is well-known that dense CO_2 can dry wet materials,[19] but its drying effect would be insufficient to suppress the formation of carboxylic acids. One interesting approach to enhance the water desorption was pursued by Tsang and co-workers, who used hydrophobic Teflon-coated Pd/C and Pt/C catalysts.[20] As shown in Table 1, drastic increases in the conversion of the aerobic oxidation of 9-anthracene methanol in $scCO_2$ were observed when the graphite-supported metal catalysts were coated with 1% Teflon, possibly due to the hydrophobic character promoting the elimination of water from the catalyst surface (entry 1 vs 2; entry 3 vs 4). The Teflon coating, however, also brings about significant decreases in surface area and metal dispersion of the parent catalysts. Thus, above 1%, the conversion decreased sharply (Figure 5).[21] The surface Teflon probably blocks the pores of the parent catalysts. In addition, sintering of the surface metals was promoted during the Teflon-coating process, as observed by TEM.[21] It is noteworthy that *n*-decanol could also selectively be oxidized to *n*-decanal at high conversion over the Teflon-coated Pt/C (Table 1, entry 5), because the aerobic oxidation of aliphatic alcohols is usually sluggish and nonselective. Interestingly, the increase in conversion with CO_2 pressure was much more pronounced for the Teflon-coated catalysts than for the Teflon-free ones, probably due to the difference in the water-desorption behaviors. The O_2 pressure was also a crucial parameter, which is related to the overoxidation of the supported metals. Thus, when the oxidation was performed over Pt/Teflon−C with 10.0 MPa of CO_2, an equivalent molar quantity of gaseous oxygen to the alcohol afforded the best result, even allowing the catalysts to be reused without serious loss of

Table 1. Aerobic Oxidation of Alcohols to the Corresponding Aldehydes in $ScCO_2$ (Data Taken from Ref 20)[a]

entry	catalyst (surface area $m^2\ g^{-1}$)	reactant	temperature (°C)	product	conversion (%)	selectivity (%)
1[b]	Pt/C (121)	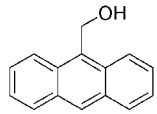	65	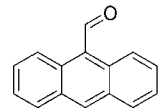	45 (100[c])	>99 (~65[c])
2	Pt/Teflon–C[d] (75)	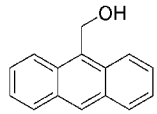	65	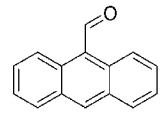	96	>99
3	Pd/C (805)	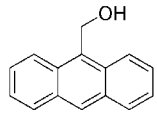	65	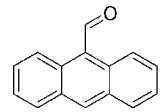	22	>99
4	Pd/Teflon–C[d] (687)	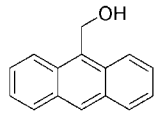	65	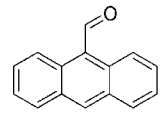	97	>99
5[e]	Pt/Teflon–C[d] (75)	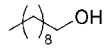	60		92	92

[a] Reaction conditions: batch reactor volume, 100 mL; catalyst (5% noble metal), 100 mg; substrate, 0.29 mmol; O_2, 0.5 MPa; CO_2, 15.0 MPa; reaction time, 24 h. The reaction mixture except for the solid catalyst formed a single homogeneous phase. [b] CO_2, 14.4 MPa. [c] The oxidation was performed in 100 mL of water using 60 mg of the alcohol dissolved in 5 mL of THF and 400 μL of Triton X-114 as a surfactant. [d] Teflon content, 1%. [e] CO_2, 11.0 MPa.

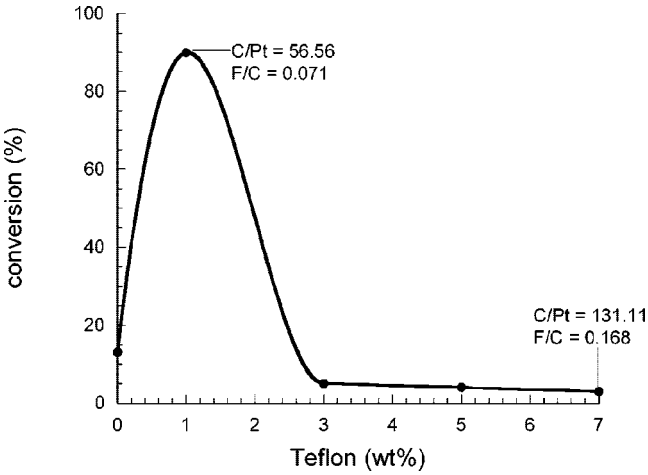

Figure 5. Variation of the conversion as a function of the amount of Teflon loaded for the aerobic oxidation of 9-anthracene methanol. Reaction conditions: catalyst (5% Pt/C), 100 mg; substrate, 0.29 mmol; O_2, 0.5 MPa; reaction temperature, 65 °C; reaction time, 24 h. 100% selectivity to the corresponding aldehyde at all Teflon contents. Reprinted with permission from ref 21. Copyright 2004 Elsevier Ltd.

activity. The 5%-Pt/1%-Teflon−C catalyst was also applied for the aerobic oxidation of *meso*-hydrobenzoin in $scCO_2$.[21] Several oxidation products such as deoxybenzoin, benzil, *trans*-stilbene epoxide, benzaldehyde, and benzoic acid were formed, and the product distribution (selectivity) could be tuned through the change of pressure and temperature. This is a good demonstration of the oxidation product control by virtue of the tunable solvent property of dense CO_2.

3.1.1.2. Oxidation of Propanols over Pt/C Catalyst. Gläser and co-workers performed the selective oxidation of propanols using carbon-supported 5% Pt catalyst.[22] The reaction was performed at 40 °C in a 100-mL reactor, using 13 mmol of alcohol and 250 mg of catalyst with various O_2 and CO_2 pressures. Based on calculations using the Patel−Teja equation of state, the reaction mixture except for the solid catalyst was estimated to be homogeneous under all the conditions applied (total pressure ≥10.0 MPa). The 5% Pt/C showed very good performance for the oxidation of 2-propanol and could give acetone in quantitative yield under optimal conditions, e.g., O_2 mole fraction 1.0%, total pressure 16.5 MPa, and reaction time 450 min. As observed by Baiker et al. for the continuous oxidation of a similar aliphatic alcohol, 2-octanol (see section 3.1.2.3), the reaction rate strongly depended on the O_2 concentration, reaching a maximum at a certain O_2 pressure. Overoxidation of Pt particles on the surface was probably related to the decrease in the product yield at higher O_2 pressures. The authors also performed the Pt/C-catalyzed oxidation in aqueous medium, which also is considered to be an ideal medium for oxidations. However, worse results were obtained. Particularly, deactivation of the catalyst was more significant in water than in $scCO_2$. Although the exact amount of leached metal was not reported for both media, there would probably be a striking difference in these amounts between the polar

Table 2. Aerobic Oxidation of Alcohols Using Poly(ethylene glycol)-Stabilized Palladium Nanoparticles in $ScCO_2$ (Data Taken from Ref 23)[a]

entry	reactant	temperature (°C)	time (h)	product	conversion (%)	selectivity (%)
1	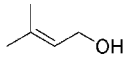	65	1.5	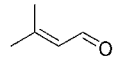	99.2	99.3
2	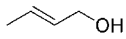	65	1.5	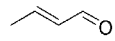	100	98.1
3	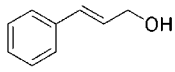	65	1.5	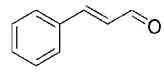	99.8	99.2
4	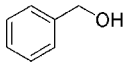	80	13	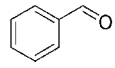	96.2	98.8
5	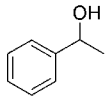	80	13	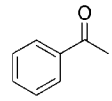	56.9	98.8
6	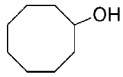	80	26	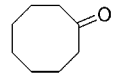	99.5	98.9
7	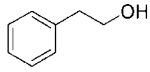	80	13	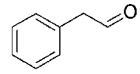	45.8	95.5
8	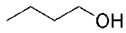	80	4	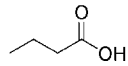	65.5[b]	57.5[b,c]

[a] Reaction conditions: batch reactor volume, 10 mL; Pd catalyst, 0.1 mmol; substrate, 1.99 mmol; CO_2-O_2 mixture (CO_2/O_2 = 92:8), 5.50 g. Conversion and selectivity from the second run are given. [b] Data obtained in the first run. [c] Butyric acid butyl ester and butanal were formed possibly via the pathways shown in Scheme 2.

aqueous medium and the apolar dense CO_2 medium. The 5% Pt/C−O_2−$scCO_2$ system was also successfully applied to the oxidation of 1-propanol to 1-propanal, although the oxidation rate was much slower compared to that obtained with 2-propanol. The sole byproduct was 1-propanoic acid, which started to form after a long induction period (after 800 min), suggesting that the fixed-bed continuous-flow oxidation of terminal alcohols to the corresponding aldehydes is feasible with carefully set reaction parameters, affording low conversion and short residence time. Macro-, meso-, and microporous silica-supported Pt catalysts were also tested in the oxidation of 2-propanol, but their performances were inferior to that of 5% Pt/C.

3.1.1.3. Palladium Nanoparticle Catalysts Stabilized in Poly(Ethylene Glycol). Leitner and co-workers found that the giant palladium cluster, $[Pd_{561}phen_{60}(OAc)_{180}]$, dispersed in poly(ethylene glycol) (PEG), efficiently catalyzes the aerobic oxidation of alcohols in $scCO_2$.[23] At the initial stage of the reaction, the Pd particles were agglomerated (average size 3.6 nm) but dissociated into uniformly dispersed small particles (average size 2.9 nm) as the reaction proceeded, possibly due to the mechanical stress induced by the stirring and to the enhanced mass transfer in the CO_2-expanded PEG, which has lower viscocity than the parent PEG. The resultant small Pd nanoparticles exhibit much higher activity than the initial agglomerated ones, and hence, the reaction possessed a long induction period. Representative results of the aerobic oxidation of alcohols are shown in Table 2. Owing to the long induction period, the results obtained from the second run using the same Pd particles and PEG as used for the first run were given, where the product extraction of the first run was conducted with $scCO_2$ (80 °C, 14.5 MPa, 7 h). The extraction was selective for the alcohols and carbonyl products, leaving the Pd and PEG in the batch reactor. As emerges from Table 2, the catalytic system was effective, particularly for the oxidation of allyl alcohols to the corresponding α,β-unsaturated aldehydes (entries 1, 2, and 3). Other alcohols, except for 1-butanol, were also selectively oxidized to the desired carbonyl products, although the reaction rates were lower. For comparison, the oxidation of 3-methyl-2-butene-1-ol (the substrate shown in entry 1) was also performed over other heterogeneous Pd catalysts such as Pd/C and Pd/Al_2O_3, but their activities and selectivities in $scCO_2$ and even in $scCO_2$-expanded PEG were inferior to those of the Pd nanoparticles in $scCO_2$-expanded PEG. It is also noteworthy that the palladium nanoparticles were reported to be ineffective for the oxidation of benzyl alcohols in conventional organic solvents, whereas in $scCO_2$-expanded

PEG they promoted the reaction with excellent selectivity at moderate to high conversions, indicating a favorable effect of the dense CO_2-swollen liquid. Finally, the authors also succeeded in performing the continuous oxidation of benzyl alcohol over the Pd particle−PEG−$scCO_2$ system, which was performed at 80 °C and a total pressure of 13.2 or 15.5 MPa (CO_2/O_2 pressure ratio 92:8), employing a flow rate of the alcohol of 0.5 mL h^{-1} and an exit flow rate of 5 L h^{-1}. No deactivation of the catalyst was observed for at least 36-h time-on-stream at both total pressures. The conversion was, however, higher at 13.2 MPa than at 15.5 MPa, probably due to the high concentration of benzyl alcohol in the CO_2-expanded PEG phase (where the oxidation took place) at lower pressures. The authors attributed the high activity and long-term stability mainly to the high dispersion of the Pd clusters.

3.1.1.4. Oxidation of *m*-Hydroxybenzyl Alcohol over Alumina- and Carbon-Supported Transition-Metal Catalysts. Itoh and co-workers investigated the oxidation of *m*-hydroxybenzyl alcohol over supported 5% transition-metal catalysts.[24] The reaction was typically carried out at 120 °C for 15 min in a 50-mL reactor, using 0.05 g of catalyst, 0.016 mol of the reactant, 0.5 MPa of O_2, and 20 MPa of CO_2. Under these conditions, the yield of *m*-hydroxybenzaldehyde increased in the order Rh/Al_2O_3 (no activity) < Pt/Al_2O_3 (1.4%, TON: 56) < Ru/C (4.5%, TON: 44) < Pt/C (6.3%, TON: 573), Rh/C (7.9%, TON: 670), Pd/Al_2O_3 (8.0%, TON: 69) < Ru/Al_2O_3 (11.9%, TON: 82) < Pd/C (18.6%, TON: 2136), indicating that carbon serves as a better support compared to Al_2O_3, except for the case of Ru. The detected byproducts were phenol and *m*-cresol, of which yields were a few percents. Thus, CO_2 was speculated to form as the major byproduct, compensating for the ill-matched mass (carbon) balance between before and after the reaction. The oxidation over Pd/C was also conducted in water and methanol, but lower yields and TONs compared to those achieved in $scCO_2$ were obtained. The reaction profile with Pd/C in $scCO_2$ for 0−60 min revealed that the oxidation to *m*-hydroxybenzaldehyde, phenol, and *m*-cresol apparently stopped after 5 min, whereas the reactant alcohol was steadily consumed. XRD analysis of the recovered catalyst showed intense diffractions of PdO species, indicating that the reduction of PdO to active metallic Pd by adsorbed hydrogen atoms, which were released from the reactant alcohol, was sluggish in the oxidation. The effect of reaction temperature was investigated in the range 100−140 °C, showing that the conversion increased with increasing temperature, while the increase of the selectivity to *m*-hydroxybenzaldehyde was observed only up to 120 °C, above which it stayed constant. The increment of temperature thus accelerated only the paths for byproduct formations. The O_2 pressure was altered in the range 0−2 MPa at a constant CO_2 pressure of 20 MPa, revealing that the conversion increased with increasing O_2 pressure and that the aldehyde selectivity showed a maximum at 0.5 MPa. The effect of CO_2 pressure was also investigated in the range 0.1−20 MPa at a constant O_2 pressure of 0.5 MPa. With 0.1 MPa of CO_2, combustion of the reactant occurred and no organic solids were obtained. Increasing the CO_2 pressure suppressed the combustion, possibly due to the high thermal conductivity of dense CO_2. The conversion showed a maximum at 10 MPa, while the aldehyde selectivity reached a maximum at 0.7 MPa (∼25%), which did not change with a further increase of CO_2 pressure. Although the actual phase behaviors were not reported due to the upper temperature limit of the apparatus, only a small amount of *m*-hydroxybenzyl alcohol dissolved in $scCO_2$, even at 30 MPa, when the visual observations were performed at 80 °C with a 10-mL cell and 0.05 g of the alcohol. Thus, the authors suggested that the reaction mixture consisted of two phases, i.e., the CO_2-expanded alcohol phase and the CO_2-rich phase, under the reaction conditions. The reusability of the Pd/C catalyst was investigated using the spent one dried at 60 °C overnight. Both the conversion and selectivity decreased after the first run, but they were almost the same in the second and third runs. Since the active Pd sites for the oxidation to the aldehyde were deactivated in just 5 min in the first run performed for 15 min, the overnight drying could probably partially convert the oxidized Pd atoms to the active metallic Pd. The XRD patterns of the dried catalyst were, however, not reported. The oxidation of benzyl alcohol was also investigated over Pd/C under identical conditions: 120 °C, 15 min, 0.05 g of the catalyst, 0.016 mol of the reactant, 0.5 MPa of O_2, and 20 MPa of CO_2. Compared to *m*-hydroxybenzyl alcohol, benzyl alcohol was much more reactive, and the yield of benzaldehyde was over 80%. Since the yields of the other recovered products, benzene and toluene, were very low, the authors speculated that the main byproduct was CO_2. The reaction profile in the range 0−60 min showed that the conversion to benzaldehyde, benzene, and toluene stopped after 5 min. On the other hand, the reactant alcohol was steadily consumed with reaction time, indicating that only the sites active for the CO_2 formation functioned after 5 min. XRD analysis of the spent Pd/C showed almost the same patterns as that of the corresponding fresh catalyst, of which behavior was in contrast to that of the catalyst used for the oxidation of *m*-hydroxybenzyl alcohol. However, deactivation of the Pd/C observed in the oxidation of benzyl alcohol and *m*-hydroxybenzyl alcohol seems to be caused by the overoxidation of active metallic Pd atoms. The Pd oxidation in the reaction of *m*-hydroxybenzyl alcohol was significant, leading to the formation of bulk PdO, which was detected even by XRD.

3.1.2. Continuous-Flow-Reactor Investigations

3.1.2.1. Total Oxidation of Ethanol over Pt/TiO_2 Catalyst. Zhou and Akgerman performed the aerobic oxidation of ethanol in a fixed-bed continuous flow reactor at 150−300 °C and a total pressure of 8.96 MPa.[25] Their goal was to establish kinetic models for the total oxidation to CO_2 as well as the partial oxidation to acetaldehyde in $scCO_2$, because the total oxidation of ethanol had widely been investigated due to the importance of the alcohol as a blend in gasoline, but it had never been tested in $scCO_2$. A commercially available 4.45% Pt/TiO_2 catalyst (1.5−9.1 mg, diluted with glass beads) and a reactant feed composed of ethanol and O_2 with a molar ratio of 1:5 were applied. Then, the flow rate was within the range of 3.51−6.31 mol h^{-1}, and the CO_2/O_2 molar ratio was approximately 99:1. In addition to CO_2, acetaldehyde (up to ca. 30% yield) and a small amount of carbon monoxide (<2% yields) were detected as byproducts under the conditions applied. However, such partially oxidized products could further be converted to CO_2 and H_2O by either increasing temperature or increasing the catalyst amount with excess O_2. Thus, at 300 °C and a contact time W/F_{E0} (W, catalyst amount (g); F_{E0}, inlet molar flow rate of ethanol) of 0.814 g h mol^{-1}, the yield of acetaldehyde dropped to almost 0% at 100% ethanol conversion, indicating that the total oxidation of

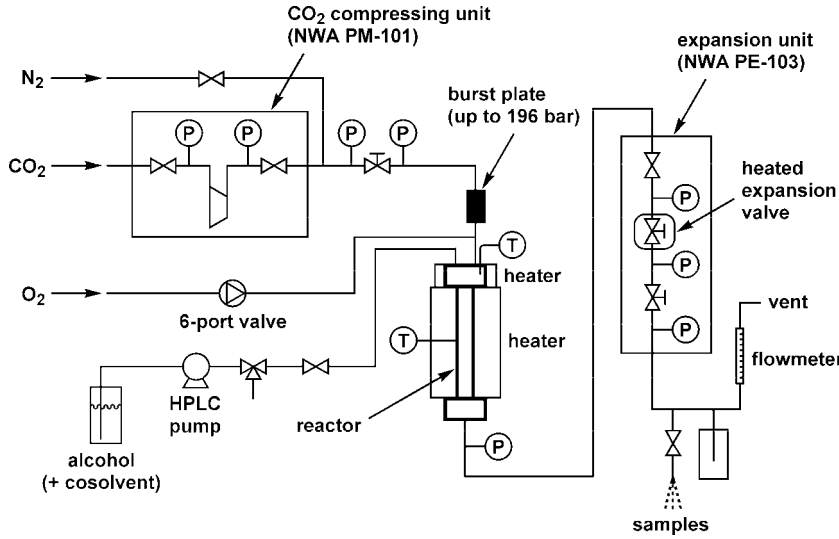

Figure 6. Schematic view of a typical fixed-bed continuous-flow-reactor system used for the aerobic oxidation of alcohols in dense CO_2.

ethanol took place. The kinetic model based on the Langmuir−Hinshelwood-type mechanism for the direct ethanol oxidation and assuming dehydrogenation of an ethoxy intermediate as the rate-determining step for the partial oxidation to acetaldehyde accurately predicted the experimental data. A kinetic model was proposed also for the oxidation of acetaldehyde to CO_2, which was based on the assumption that both acetaldehyde and O_2 were adsorbed dissociatively. This model could also predict the conversion of acetaldehyde accurately.

3.1.2.2. Oxidation of Benzyl Alcohol over Alumina- and Carbon-Supported Transition-Metal Catalysts. Baiker's group investigated the catalytic performance of supported Pd, Pt, and Ru catalysts for the aerobic oxidation of benzyl alcohol.[26] The continuous-flow-reactor system depicted in Figure 6 was used. Typically, 5 g of a commercially available catalyst was loaded in the reactor and was reduced in a stream of H_2 at 100 °C for 2 h prior to use. The contact time *W*/*F*, total pressure, and reactor temperature were 1.02 g h mol^{-1}, 9.5 MPa, and 80 °C, respectively, and the feed flow consisted of 5 mol % of benzyl alcohol, 2.5 mol % of O_2, and 92.5 mol % of CO_2. Under the standard conditions, 0.5% Pd/Al_2O_3 catalyst afforded the highest conversion (13.5%) with a benzaldehyde selectivity of 95.6%, whereas 0.5% Pt/Al_2O_3 and 0.5% Ru/Al_2O_3 gave the aldehyde in <1% yields, indicating that the use of palladium is crucial for the aerobic alcohol oxidation in dense CO_2. The 0.5% Pd/Al_2O_3 catalyst also exhibited a long lifetime, maintaining its activity for at least 75-h time-on-stream. Similarly, 0.5% Pd/C could be successfully applied with a slightly lower conversion (7.4%) and selectivity (97.1%), showing that the nature of the support is of secondary importance. The major byproducts given by the Pd catalysts were benzoic acid and benzyl benzoate, which were formed by the mechanism shown in Scheme 2. The effect of changing one of the following parameters, temperature, *W*/*F*, and O_2 concentration, on conversion and selectivity was investigated in the range 60−100 °C, 0.5−2.7 g h mol^{-1}, and 0−7.5 mol %, respectively, under conditions otherwise identical with the standard ones. The conversion increased, while the selectivity decreased with increasing one of the three parameters in the given ranges. On the other hand, changing the total pressure in the range 6.5−12.5 MPa at 60 or 80 °C had almost no effect on conversion and selectivity. One obvious result, however, was that the conversion reached a maximum at 10.0−11.5 MPa. The standard conditions were selected to perform the oxidation isothermally. By increasing temperature, *W*/*F*, and O_2 concentration, the conversion with 0.5% Pd/Al_2O_3 could be increased up to 56% with a benzaldehyde selectivity of 96%. This approach, however, was accompanied by the generation of high temperature due to the highly exothermic oxidation, and the insufficient heat transfer inside the reactor prevented the attempt to increase the conversion further.

Scheme 3. Products Formed in the Continuous Aerobic Oxidation of 2-Octanol over Pd/Al_2O_3 Catalyst

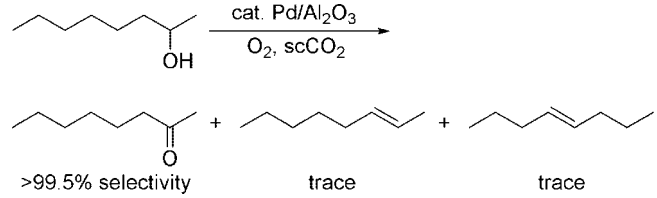

3.1.2.3. Oxidation of 1- and 2-Octanol over Pd/Al_2O_3. The same group applied the 0.5% Pd/Al_2O_3 catalyst also for the oxidation of long-chain aliphatic alcohols such as 1- and 2-octanol.[27] The oxidations were performed with the same continuous-flow-reactor system (Figure 6). The standard conditions were 5 g of catalyst (the catalyst prereduced in a stream of H_2 at 100 °C for 2 h), a total pressure of 9.5 MPa, a reactor temperature of 120 °C, a contact time *W*/*F* of 1.02 g h mol^{-1}, and a feed flow consisting of 5 mol % alcohol, 2.5 mol % O_2, and 92.5 mol % CO_2. These values were selected to minimize the temperature gradient in the catalyst bed owing to the highly exothermic oxidation. Under these conditions, 2-octanol was oxidized to 2-octanone in almost 100% selectivity, accompanied by the formation of a trace amount of alkenes (Scheme 3). Both temperature and contact time *W*/*F* were important parameters, and their increases in the respective ranges 60−130 °C and 0.7−2.7 g h mol^{-1} led to an increase of the 2-octanone yield, where the other parameters were equal to those of the standard conditions. The effect of changing the total pressure was investigated in the range 6.5−13.5 MPa. The 2-octanone yield then depended on the set of other parameters, and its change with the pressure was difficult to interpret. However, it is obvious that the total pressure is less important compared to the

Scheme 4. Products Formed in the Continuous Aerobic Oxidation of 1-Octanol over Pd/Al_2O_3 Catalyst

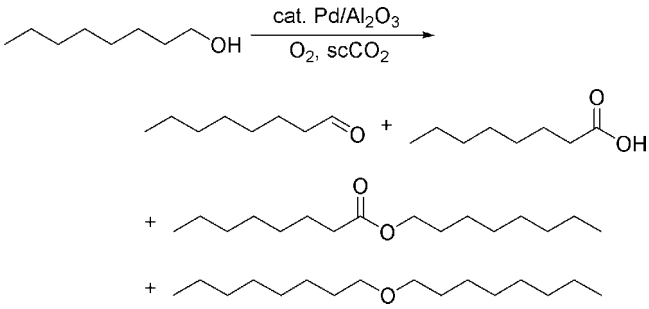

temperature and *W*/*F*, because the yield change by altering the total pressure was less prominent. Visual observation of the phase behaviors revealed that the mixture was composed of two phases, i.e., a 2-octanol-rich phase and a CO_2-rich phase, over the whole temperature and pressure ranges investigated. The O_2 concentration in the feed flow affected strongly the 2-octanone yield. Changing the O_2 amount from 0 to 15 mol % under the standard reaction conditions revealed that the yield reached a maximum at 7.5−10 mol %, above or below which the yield dropped drastically. The sharp decline of the yield at higher O_2 concentrations was attributed to overoxidation of the reduced Pd metal surface. The yield of 2-octanone could be increased up to 46% by applying higher *W*/*F* (2.71 g h mol^{-1}), temperature (140 °C), and total pressure (11.0 MPa) without any loss of the selectivity (still >99.5%). However, the attempt to enhance the conversion was accompanied by the formation of a temperature gradient in the catalyst bed. It is noteworthy that no deactivation of 0.5% Pd/Al_2O_3 was observed over a time-on-stream of 110 h, demonstrating the high stability of the catalyst under the oxidative conditions. In contrast to 2-octanol, 1-octanol afforded many byproducts under otherwise similar conditions (Scheme 4). This was explained by the rapid hydration of 1-octanal, leading to the byproduct formations (Scheme 2). The highest selectivity to 1-octanal was 73% at 3.3% conversion, where the reaction was performed at 80 °C and a total pressure of 11.0 MPa with 5 g of 0.5% Pd/Al_2O_3 and with the feed composition being 3 mol % 1-octanol, 6 mol % O_2, and 91 mol % CO_2. The low conversion could be improved by applying higher temperature and *W*/*F* at the cost of selectivity (e.g., 22.0% conversion and 27% selectivity at 140 °C and a *W*/*F* of 2.71 g h mol^{-1}). The total pressure, on the other hand, seems to have only a marginal effect on conversion and selectivity. Summarizing these results, the combination of 0.5% Pd/Al_2O_3 and dense CO_2 is promising for the aerobic oxidation of aliphatic secondary alcohols to the corresponding ketones, achieving even higher selectivity compared to the cases of the formerly developed catalytic systems operating at atmospheric pressure.

3.1.2.4. *In Situ* Spectroscopy during the Benzyl Alcohol Oxidation over Pd/Al_2O_3: Insight into the Effect of the Oxidation State of Supported Metals and the Phase Behaviors on the Reaction. Grunwaldt et al. constructed an "*in situ*" high-pressure flow cell for X-ray absorption spectroscopy (XAS), which allowed us to uncover the oxidation state of supported metals during the continuous aerobic oxidation in dense CO_2.[28] The experimental setup is depicted in Figure 7. The cell has a volume of 0.5 mL and contains two 3-mm thick beryllium windows with a diameter of 10 mm on both sites of the catalyst compartment. Catalyst, 0.5% Pd/Al_2O_3 prereduced with H_2 at 100 °C, with a sieved

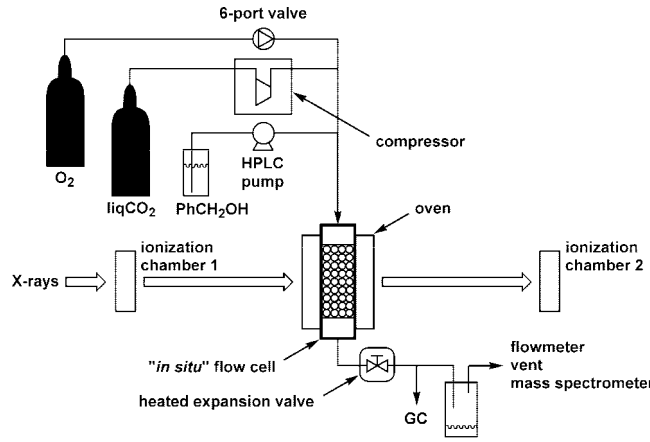

Figure 7. Fixed-bed continuous-flow-reactor system used for *in situ* X-ray absorption spectroscopy during aerobic oxidation of benzyl alcohol.

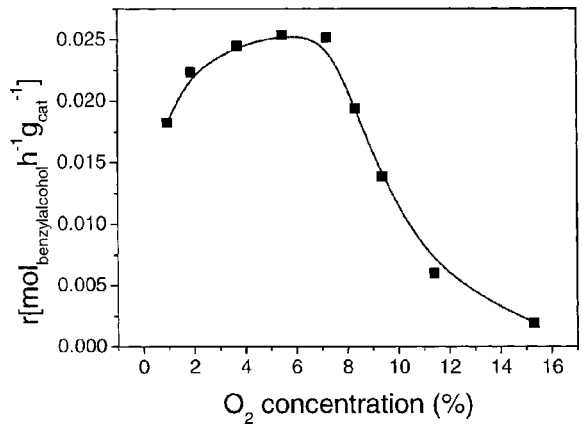

Figure 8. Variation of the oxidation rate as a function of O_2 concentration in the feed. Reaction conditions: Reaction temperature, 80 °C; total pressure, 15.0 MPa; total flow rate, 0.11 mol min^{-1} (benzyl alcohol concentration 1.9%); catalyst, 5 g of 0.5% PdO_x/Al_2O_3, over several days of equilibrated catalyst. Reprinted with permission from ref 28. Copyright 2003 Plenum Publishing Corporation.

fraction of ca. 0.5 mm was filled in the cell, and the oxidation of benzyl alcohol to benzaldehyde served as a test reaction. The continuous catalytic oxidation using the reactor system shown in Figure 6 revealed a strong dependence of the oxidation rate on the O_2 concentration in the feed, as shown in Figure 8. Note that similar results were obtained also for other heterogeneously catalyzed aerobic oxidations of alcohols in $scCO_2$ (for example, see sections 3.1.1.2 and 3.1.2.3). Since O_2 is a reactant for aerobic oxidation, the rate drop at lower O_2 concentration is reasonable. On the other hand, a few reasons had been proposed for the rate decrease at higher O_2 concentrations: (i) a phase behavior change due to the decreased CO_2 density (note that the total pressure was constant at any O_2 concentration) and (ii) overoxidation of the supported palladium. The "*in situ*" high-pressure XAS was a powerful tool for elucidation of the latter phenomenon. Figure 9 shows the X-ray absorption spectra under various conditions. The spectra are somewhat noisy, probably due to the unsteady operation of the compressor. As the oxidized part of the Pd particles increases, the absorption at 24.36−24.37 keV increases, while that at 24.37−24.40 keV decreases. A crucial point emerging from the figures is that the spectrum measured under reaction conditions (spectrum 3) is similar to that of the freshly reduced catalyst (spectrum 1). This indicates that the main part of the Pd particles was

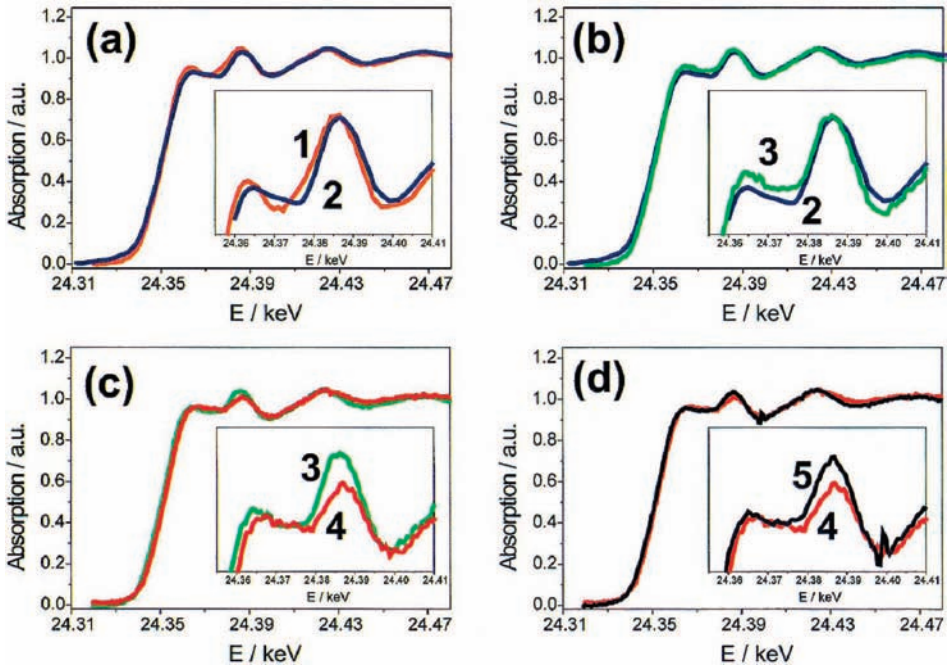

Figure 9. X-ray absorption spectra of 0.5% PdO_x/Al_2O_3 under various conditions. Spectrum (1) reduced catalysts in a stream of H_2 at 100 °C at normal pressure; (2) at 80 °C, 15.0 MPa total, only CO_2 in the feed, total flow rate 0.11 mol min^{-1}; (3) during the oxidation of benzyl alcohol under the following conditions: 80 °C, 15.0 MPa total, total flow rate 0.11 mol min^{-1}, alcohol concentration in the feed 1.9%, O_2 concentration 0.95%; (4) after stop of the alcohol feed and thus the following conditions: 80 °C, 15.0 MPa total, total flow rate 0.11 mol min^{-1}, O_2 concentration 1.9%; (5) during the oxidation of benzyl alcohol after the oxidation step (4) under the following conditions: 80 °C, 15.0 MPa total, total flow rate 0.11 mol min^{-1}, alcohol concentration 1.9%, O_2 concentration 1.9%. Reprinted with permission from ref 28. Copyright 2003 Plenum Publishing Corporation.

Scheme 5. Structure−Activity Relationship during the Aerobic Oxidation of Benzyl Alcohol in $ScCO_2$ over Supported Pd Catalysts

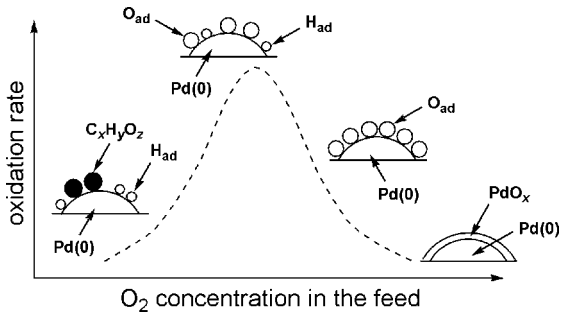

metallic even under the oxidative conditions. Another point is that the process was reversible. Even though the catalyst was oxidized upon stopping the benzyl alcohol feed and thus during exposure only to O_2/CO_2 flow, it could be rereduced by restart of the alcohol feed (see spectrum profile change 3 → 4 → 5). Benzyl alcohol can reduce the Pd particles, because it undergoes dehydrogenation on the surface of palladium. The authors also succeeded in monitoring the reduction of Pd particles by the benzyl alcohol/CO_2 feed. Strictly, however, the "reversible" process described above is irreversible, because the catalytic activity was lowered by the alcohol-feed stop. The lower reduction power of benzyl alcohol compared to molecular hydrogen was also demonstrated by the authors. Based on the spectroscopic results, a relation among the state of the palladium surface, O_2 concentration, and oxidation rate was proposed, which is shown in Scheme 5. The presence of O_2 is proposed to be important also for the removal of surface carbonate species (oxidative surface cleaning).[17]

As described above, the XAS investigations indicate that the Pd particles on alumina are mainly metallic under the alcohol oxidation conditions. However, there also exist oxidized Pd species during the oxidation in $scCO_2$, and the fraction of these species becomes greater as the O_2 concentration is increased.[29] As shown in Figure 10a, the increase of O_2 content from 0.5 to 5.5% resulted in the intensity increase and decrease in the 24.36−24.37 and 24.38−24.40 keV regions, respectively. In addition, the k^1-weighted Fourier-transformed EXAFS spectra in Figure 10b show that the backscattering of palladium decreased as the conditions became more oxidative. These results clearly indicate that the oxidized part of Pd particles became greater when the O_2 content was increased. More importantly, the partial Pd oxidation, in which oxygen atoms are adsorbed or even incorporated as ions in the surface and subsurface regions of Pd particles, is indispensable for higher activity (Scheme 5). This is in contrast to the alcohol oxidation in conventional organic solvents, where even such a small extent of Pd oxidation led to a fatal deactivation of the catalyst. The $scCO_2$ medium thus renders the supported Pd catalysts more tolerant for oxygen.

The authors later reported the effect of changing various reaction parameters on the continuous catalytic oxidation of benzyl alcohol.[30] A strong dependence of the conversion on the contact time W/F was observed, as shown in Figure 11, which also demonstrated that single homogeneous phase operation is a necessary prerequisite to achieve the highest oxidation rates under the conditions applied. Note here that a decrease in W/F corresponds to an increase of the CO_2 concentration in the feed and thus a decrease of the alcohol and O_2 concentrations, because only the CO_2 flow rate was altered. Intriguingly, when similar conversion-versus-W/F plots were made for the operation at a slightly lower

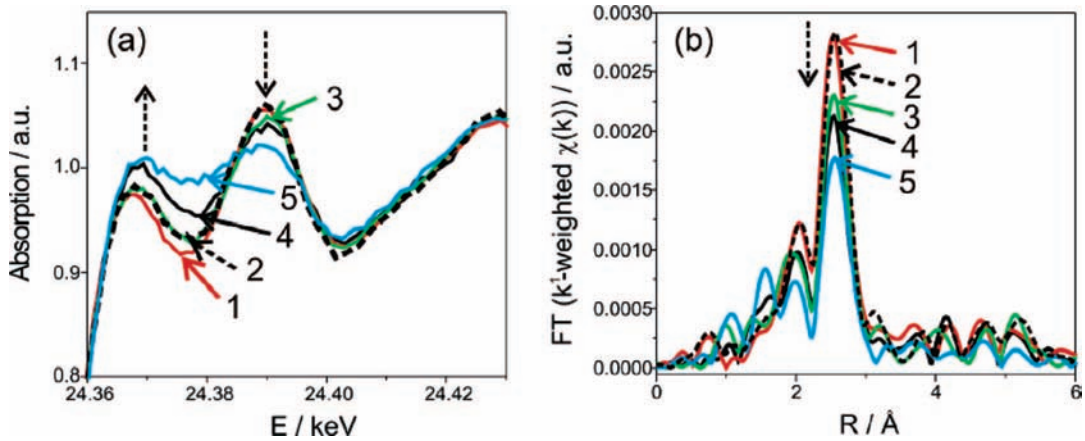

Figure 10. Comparison of the (a) XANES region and (b) k^1-weighted Fourier-transformed EXAFS spectra of 0.5% Pd/Al_2O_3 at 80 °C and a total pressure of 15.0 MPa. Spectrum 1, in CO_2 after reduction in 5% H_2/He; 2, in 0.9% benzyl alcohol/CO_2; 3, in 0.9% benzyl alcohol/0.5% O_2/CO_2; 4, in 0.9% benzyl alcohol/5.5% O_2/CO_2; 5, in 2.5% O_2/CO_2. Reprinted with permission from ref 29. Copyright 2006 American Chemical Society.

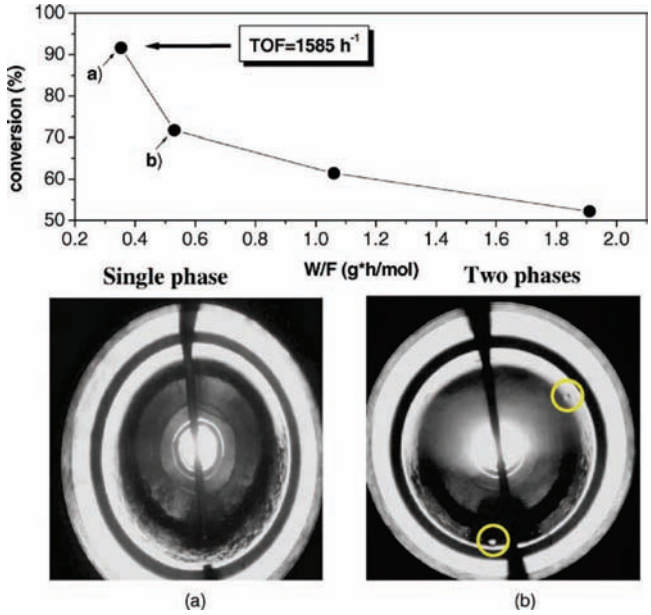

Figure 11. Variation of the conversion as a function of the contact time *W*/*F*. The *W*/*F* was altered by changing the flow rate of CO_2. Reaction conditions: Reaction temperature, 80 °C; total pressure, 15.0 MPa; catalyst, 5 g of 0.5% Pd/Al_2O_3; alcohol feed rate, 0.002 mol min^{-1}; O_2 feed rate, 0.001 mol min^{-1}. Snapshot (a): phase behavior of the mixture composed of 0.43% O_2, 0.86% benzyl alcohol, 98.71% CO_2 at 80 °C and 15.0 MPa total. Snapshot (b): phase behavior of the mixture composed of 0.65% O_2, 1.3% benzyl alcohol, 98.05% CO_2 at 80 °C and 15.0 MPa total. Reprinted with permission from ref 30. Copyright 2004 Elsevier Ltd.

temperature of 70 °C, significant drops in the conversion were observed in the whole *W*/*F* range. The authors attributed this unique behavior to the large difference in the reduction rate of palladium particles by benzyl alcohol between 70 and 80 °C. Actually, *in situ* X-ray absorption spectroscopy uncovered that the Pd reduction with the alcohol starts taking place only at temperatures above 70 °C. The O_2 concentration in the feed was also changed under conditions that were a bit different from those employed in Figure 8. Thus, the oxidation was performed with various O_2 concentrations in the feed (0.43−15.5 mol %), employing 2.5 g of 0.5% Pd/Al_2O_3 diluted with 1.5 g of Al_2O_3, a benzyl alcohol feed rate of 2 mmol min^{-1}, and a CO_2 flow rate of 0.1 or 0.233 mol min^{-1}. Under these conditions, the oxidation rate reached a maximum at ca. 6 mol % O_2 in the feed, and then the highest TOF of 1859 h^{-1} was achieved with a CO_2 feed rate of 0.1 mol min^{-1}. Above 6 mol % of O_2, the oxidation rate dropped drastically regardless of the CO_2 feed rate. This behavior is a general trend of aerobic oxidation in dense CO_2 using supported-metal catalysts and attributed to the over-oxidation of the palladium particles (for example, see sections 3.1.1.2 and 3.1.2.3). With a CO_2 flow rate of 0.233 mol min^{-1}, another maximum of the oxidation rate appeared at the lowest O_2 concentration of 0.43 mol %, affording a turnover frequency (TOF) of 1701 h^{-1}. Since the reaction mixture formed a single homogeneous phase only at this O_2 concentration, elimination of the gas−liquid mass transfer resistance seems to enhance the oxidation. However, the TOF was still lower than that observed at an O_2 concentration of ca. 6 mol %, and thus, phase behavior is not the sole factor that affects the oxidation rate.

The total pressure was also found to be a crucial parameter in the continuous catalytic aerobic oxidation of benzyl alcohol.[31] Figure 12 shows the effect of total pressure on the oxidation rate at 80 °C. The other reaction parameters are specified in the figure caption. As emerges from the figure, a small increase of the total pressure from 14.0 to 15.0 MPa led to a steep increase of the oxidation rate, whereas the selectivity to benzaldehyde in the whole pressure range investigated was almost constant around a value of 95%. The byproducts were benzoic acid and benzyl benzoate, which were formed by the mechanism shown in Scheme 2. Parallel phase behavior observation revealed the presence of a few droplets of benzyl alcohol at 14.0 MPa, whereas at 15.0 MPa the drops completely disappeared. Hence, it was proposed that the increase of oxidation rate with pressure was caused by the enhanced mass transfer of benzyl alcohol, owing to its complete dissolution in the dense CO_2 phase. In addition to visual observation, infrared spectroscopy was applied, employing a high-pressure cell, which allows us to measure both transmission and ATR-IR spectra (Figure 4).[14] This spectroscopic investigation is much more reliable compared to subjective visual observation, particularly when insoluble substances are present as invisible small droplets. The used cell had a screw-type-manual-pump structure, and the pressure inside could be changed by increasing or decreasing the cell volume. The IR spectroscopy also afforded results consistent with those of the visual observation, i.e., the importance of a single homogeneous phase for the higher oxidation rate. Since the insoluble liquid substance

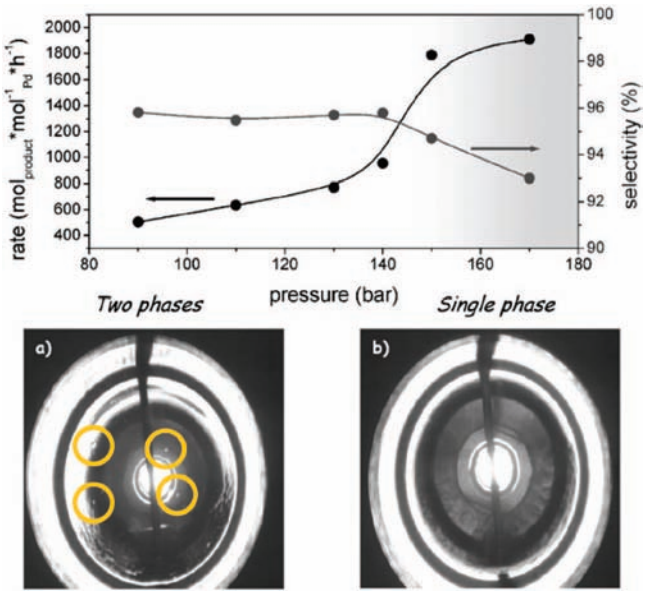

Figure 12. Variation of the oxidation rate and selectivity as a function of the total pressure. Reaction conditions: Reaction temperature, 80 °C; catalyst, 2.5 g of 0.5% Pd/Al_2O_3 diluted with 1.5 g of Al_2O_3; total flow rate, 0.236 mol min^{-1}; alcohol concentration, 0.9 mol %; O_2 concentration, 0.45 mol %. Snapshot (a): 14.0 MPa total. Snapshot (b): 15.0 MPa total. Reprinted with permission from ref 31. Copyright 2005 Royal Society of Chemistry.

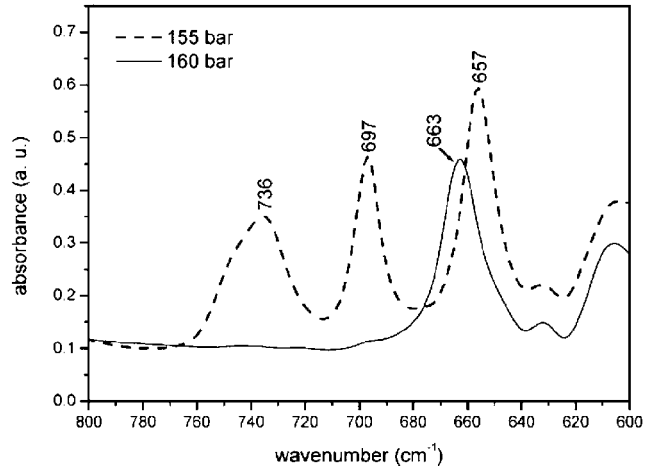

Figure 13. Comparison of the ATR-IR spectra of 0.9 mol % benzyl alcohol in CO_2 at 15.5 and 16.0 MPa at 80 °C in the region of the aromatic deformation bands (736 and 697 cm^{-1}) and of the ν_2 band of CO_2 (ca. 660 cm^{-1}) recorded in the presence of a catalyst layer of 0.5% Pd/Al_2O_3 on the ZnSe ATR-IR crystal. Reprinted with permission from ref 31. Copyright 2005 Royal Society of Chemistry.

stays on the wall of the cell, the decrease of the ATR-IR band intensities due to benzyl alcohol corresponds to the dissolution of the alcohol in dense CO_2. On the other hand, such dissolution would lead to the increase of the transmission-IR bands of benzyl alcohol. In addition, the ν_2 band of CO_2 in CO_2-expanded benzyl alcohol was found to shift to a lower wavenumber compared to that of pure CO_2. Thus, the presence of CO_2-expanded benzyl alcohol was demonstrated for the benzyl alcohol (0.9 mol %)−CO_2 system below 15.0 MPa at 80 °C, whereas above 15.0 MPa the spectra implied the complete dissolution of the alcohol in dense CO_2. It is interesting to note that the change of the bands in intensity and wavenumber with pressure was reversible for the catalyst-free system; depressurization resulted in the appearance of the same spectra obtained before pressurization. In Figure 13 are shown the ATR-IR spectra obtained with the ATR-IR crystal (ZnSe) coated with a thin catalytic layer of 0.5% Pd/Al_2O_3. Note the significant change in the spectrum between 15.5 and 16.0 MPa, indicating that this small increase in pressure caused the complete dissolution of benzyl alcohol in dense CO_2 in the pores of the catalyst. A similar spectral change was observed for the system without catalyst as mentioned above, but the change occurred at a slightly lower pressure (∼15.0 MPa) in the absence of catalyst, possibly due to the different phase behavior in the small pores of the catalyst compared to that in the open space (the case without catalyst). In the presence of the catalyst, the ATR-IR spectra exhibited irreversible behavior for the pressure change, in contrast to those recorded without catalyst. The *in situ* IR spectroscopy was also successfully applied for monitoring changes which occurred during the oxidation. Thus, the mixture composed of 1 mol % benzyl alcohol, 1 mol % O_2, and dense CO_2 with a total pressure of 15.0 MPa at 80 °C was brought in contact with the catalytic layer of 5% Pd/Al_2O_3 covering the ZnSe ATR-crystal. A clear decrease and increase of the transmission-IR bands attributed to benzyl alcohol and benzaldehyde, respectively, were observed with reaction time, while ATR-IR bands changed only at the end of the reaction, i.e., disappearance of the benzyl alcohol bands and appearance of the bands due to the adsorbed benzoic acid. The ATR-IR spectra also revealed the absence of benzaldehyde in the pores of the catalyst during the oxidation, indicating that the aldehyde was extracted from the surface by dense CO_2 immediately after its formation and quickly diffused out of the catalyst pores. The authors proposed that this would be an important reason why the high selectivity to benzaldehyde could be achieved in dense CO_2 medium. Applying a lower pressure of 12.0 MPa, however, led to the appearance of the benzaldehyde ATR-IR bands, indicating the sluggish mass transfer of the aldehyde at lower CO_2 densities. The selectivity to benzaldehyde at this pressure was equal to that obtained at 15.0 MPa (see Figure 12), indicating that the further reaction of the aldehyde over the catalyst surface was still suppressed. The oxidation rate, on the other hand, was much lower at 12.0 MPa than at 15.0 MPa, which was attributed to the slower mass transfer of benzaldehyde as well as benzyl alcohol in the catalyst pores at 12.0 MPa. The combined transmission-IR/ATR-IR study also revealed the behavior of byproduct water during the oxidation. While ATR-IR showed water bands which were unchanged during the whole reaction time, the transmission-IR band of water, i.e., the ν_2 bending vibration at 1604 cm^{-1}, increased with reaction time, indicating that not all but a part of the water formed during the oxidation is desorbed from the catalyst surface and dissolved in the dense CO_2. The water strongly adsorbed is assumed to be on the support Al_2O_3 surface, while that adsorbed on palladium particles is considered to be smoothly extracted in dense CO_2. The facilitated extraction of water as well as benzaldehyde in $scCO_2$ would account for the high selectivity to benzaldehyde, because further reaction of benzaldehyde involves the hydration of the aldehyde (Scheme 2). Concerning the byproduct bands, ATR-IR spectra showed the adsorbed benzoic acid only at the end of the reaction, whereas no such bands appeared in transmission-IR spectra over the whole reaction time.

Baiker and co-workers compared the catalytic performances of Ru/Al_2O_3 and Pt/Al_2O_3 with that of Pd/Al_2O_3 for the continuous catalytic oxidation of benzyl alcohol to

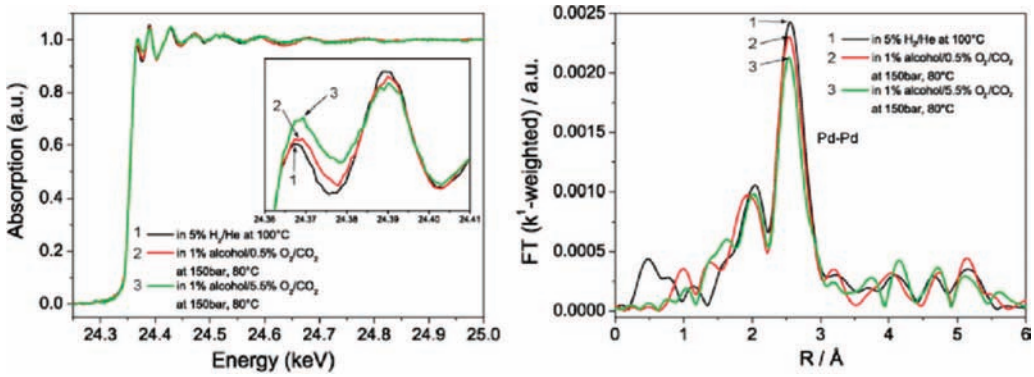

Figure 14. EXAFS spectra at the Pd K-edge (a) and the corresponding Fourier-transformed EXAFS spectra (b) recorded with the *in situ* XAS cell shown in Figure 7 during the aerobic oxidation of benzyl alcohol over 0.5% Pd/Al_2O_3 under different reaction conditions. Reprinted with permission from ref 32. Copyright 2006 Elsevier Ltd.

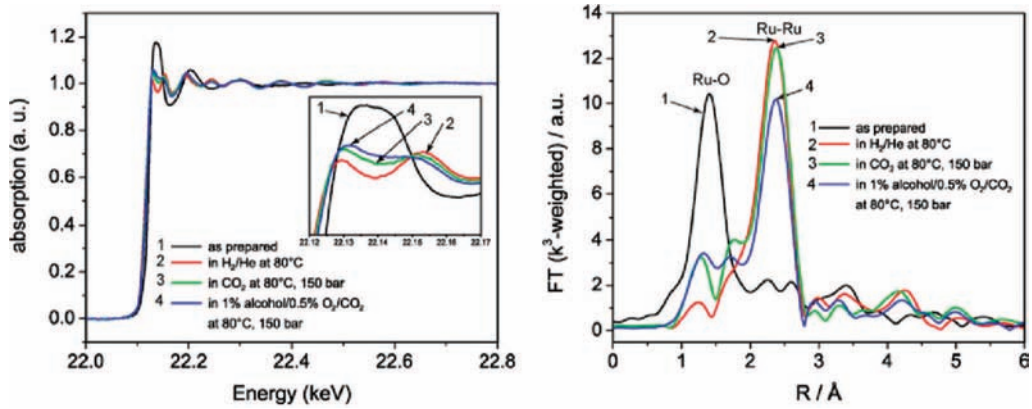

Figure 15. EXAFS spectra at the Ru K-edge (a) and the corresponding Fourier-transformed EXAFS spectra (b) recorded with the *in situ* XAS cell shown in Figure 7 during the aerobic oxidation of benzyl alcohol over 0.5% Ru/Al_2O_3. Reprinted with permission from ref 32. Copyright 2006 Elsevier Ltd.

benzaldehyde in $scCO_2$.[32] Although Ru/Al_2O_3 and Pt/Al_2O_3 have been reported to be active for the oxidation in conventional liquid solvents, they did not show activity in $scCO_2$ when the reaction was performed at 80 °C and at a total pressure of 15.0 MPa using the 0.5% metal-loaded catalysts prereduced with H_2 at 100 °C, 1 mol % of the reactant, and 0.5 mol % of O_2. In contrast, 0.5% Pd/Al_2O_3 yielded benzaldehyde in 94.7% selectivity at 48.3% conversion under identical conditions. The activity order among the catalysts was previously observed by the same group (see section 3.1.2.2). The difference in catalytic behavior among the catalysts was examined in terms of phase behavior, oxidation state of the metals, and degradation products poisoning active site. The phase behavior is usually crucial for reactions in SCFs, but its effect seems to be negligible for explaining the different catalytic behaviors observed, because the oxidations were conducted under identical conditions. In addition, *in situ* ATR-IR spectroscopy using the cell shown in Figure 4 revealed that there was no significant difference in phase behavior inside the catalyst pores between Pd and Pt catalysts. The oxidation state of the metals of catalysts was investigated using *in situ* X-ray absorption spectroscopy (XAS), which allows us to gain information on the oxidation state during the prereduction and oxidation reactions. The continuous-flow XAS cell shown in Figure 7 was used, where the fixed catalyst could be treated under various liquid and gas flows. The measurements revealed that the 0.5% Pd catalyst was reduced to a large extent under H_2/He at 100 °C, whereas the temperature was too low to reduce the 0.5% Ru and 0.5% Pt catalysts; these two metals were fully reduced only at a higher temperature of 180 °C. The measurement under stoichiometric reaction conditions (1% benzyl alcohol/0.5% O_2/CO_2 at 80 °C and 15.0 MPa) showed that the Pd catalyst prereduced at 100 °C was oxidized only to a small extent (Figure 14). The Ru catalyst reduced at 180 °C, however, was oxidized to a large extent under the oxidation conditions (Figure 15), whereas hardly any change in the oxidation state was observed for the Pt catalyst reduced at 180 °C (Figure 16). Thus, the easily oxidized Ru and the high stability of the corresponding oxidized particles were suggested to be at the origin of the low catalytic activity of Ru/Al_2O_3. On the other hand, these factors were not crucial for the Pt catalyst, which showed a similar redox behavior as that of the Pd catalyst. *In situ* ATR-IR spectroscopy uncovered the adsorption of carbon monoxide on the Pt surface during the oxidation, indicating that the CO blocks the active sites, leading to the low activity of the Pt catalyst. It is also noteworthy that the activity of the Pt catalyst could be enhanced by increasing the oxygen concentration, possibly due to the smoother removal of the surface carbonaceous species.[17] The authors thus concluded that the relatively high stability of palladium toward the redox process and the efficient removal of carbonate species originating from the degradation of benzaldehyde in the presence of molecular oxygen account for the high activity of the Pd/Al_2O_3 catalyst.

Although $scCO_2$ itself could afford better results than conventional organic solvents for the continuous Pd/Al_2O_3-catalyzed aerobic oxidation of benzyl alcohol, its use with toluene cosolvent further enhances the conversion.[33] The continuous oxidation performed on the system shown in Figure 6 at 80 °C and a total pressure of 15.0 MPa (CO_2

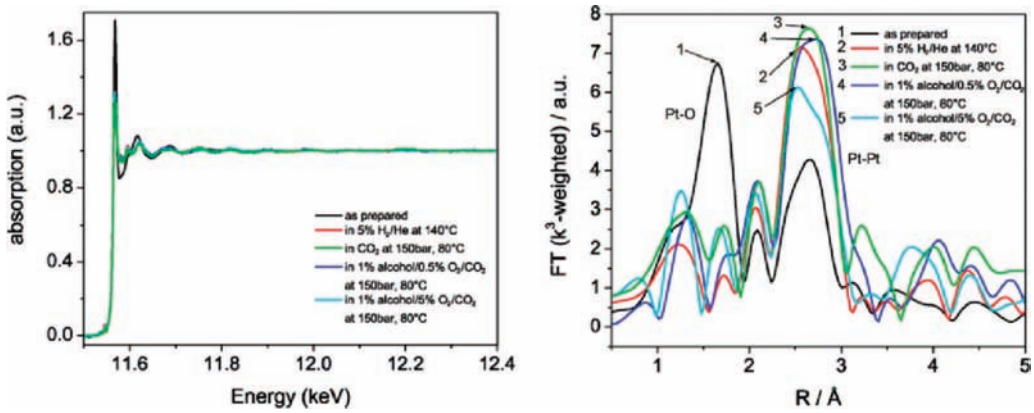

Figure 16. EXAFS spectra at the Pt L_3-edge (a) and the corresponding Fourier-transformed EXAFS spectra (b) recorded with the *in situ* XAS cell shown in Figure 7 during the aerobic oxidation of benzyl alcohol over 0.5% Pt/Al_2O_3 under different reaction conditions. Reprinted with permission from ref 32. Copyright 2006 Elsevier Ltd.

feed rate 0.233 mol min^{-1}) with 2.5 g of 0.5% Pd/Al_2O_3 diluted with 1.5 g of Al_2O_3, 0.8 mol % benzyl alcohol (0.002 mol min^{-1}), and 0.4 mol % O_2 (0.001 mol min^{-1}) revealed that the turnover frequency (TOF) reached 2500 h^{-1} with ca. 1 mol % toluene. This TOF was much higher than that obtained in the absence of toluene (1500 h^{-1}). The selectivity to benzaldehyde was ca. 95%, irrespective of whether toluene was added or not. Higher amounts of toluene led to a monotonous decrease of TOF, and the TOF dropped to 130 h^{-1} at 16 mol %. The total pressure was also crucial, because there was no difference in the reaction rate below 14.0 MPa between the oxidation in toluene-free $scCO_2$ and that in the mixed $scCO_2$−toluene (0.8 mol %) solvent system, whereas, above 14.0 MPa, higher conversions were observed in the mixed solvents. In addition, steep increases in the conversion were observed in both the $scCO_2$ and $scCO_2$−toluene media when the total pressure was increased from 14.0 to 15.0 MPa. The causes of above results were uncovered by the parallel phase behavior observation and *in situ* transmission-IR and ATR-IR spectroscopy with the cell shown in Figure 4. Thus, the drop of TOF above 1 mol % toluene was caused by the phase separation from single to biphasic, while the phase transition from biphasic to single led to drastic increases of the conversion in the pressure range 14.0−15.0 MPa. Both of these facts indicate that a single homogeneous phase is a necessary prerequisite for higher oxidation rate. The biphasic system composed of a benzyl alcohol-rich phase and a dense CO_2 phase is unfavorable, probably due to the gas−liquid mass transfer resistance, increased viscosity, and decreased diffusivity of the fluid inside the catalyst pores, and higher complexity of the multiphase flow. Note that the importance of a single homogeneous phase to achieve the highest oxidation rate has been mentioned also for the cosolvent-free $scCO_2$ media.[30,31] Although the role of toluene cosolvent was not elucidated entirely, it probably promoted mass transfer of the reactant alcohol and the products in dense CO_2 by improving the miscibility of the reaction mixture.

3.1.2.5. Oxidation of Cinnamyl Alcohol over Pd/Al_2O_3 and Its *In Situ* Spectroscopy. Baiker and co-workers investigated the continuous catalytic oxidation of cinnamyl alcohol with molecular oxygen using the flow-reactor system depicted in Figure 6.[34] Typically, the reaction was performed at 80 °C using Al_2O_3-supported 0.5% transition-metal catalyst (2.5 g) prereduced at 100 °C with H_2. The catalyst was then diluted with 1.5 g of Al_2O_3 to avoid the formation of hot spots due to the exothermic oxidation. Solid cinnamyl alcohol (10 g) was dissolved in toluene (100 mL), and the solution

Scheme 6. Products Observed during the Aerobic Oxidation of Cinnamyl Alcohol in $ScCO_2$ over Supported Pd Catalysts and Their Plausible Formation Pathways

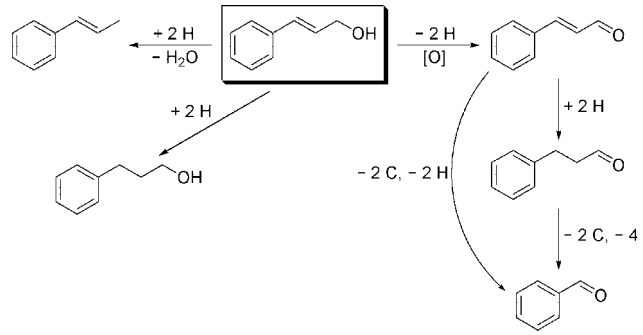

was fed into the reactor with an alcohol feed rate of 0.355 mmol min^{-1}. On the other hand, the flow rate of CO_2 was set to 0.233 mol min^{-1}. Catalyst screening was performed with a reactant/O_2/toluene molar ratio of 1:1:13 at a total pressure of 15.0 MPa, revealing that 0.5% Pd/Al_2O_3 exhibited the highest activity for the oxidation, affording 60% conversion and 72% selectivity to cinnamaldehyde. Scheme 6 shows the reaction network observed during the oxidation of cinnamyl alcohol over the palladium catalyst. Note that hydrogenation, hydrogenolysis, decarbonylation, and C=C bond cleavage also took place, yielding the corresponding byproducts in appreciable amounts, leading to the lower selectivity to cinnamaldehyde. In contrast, no product was formed over 0.5% Ru/Al_2O_3 and 0.5% Pt/Al_2O_3 under identical conditions. Replacing the cosolvent toluene with acetone or THF for the 0.5% Pd/Al_2O_3-catalyzed oxidation resulted in lower conversion and selectivity, indicating that the combination of the Pd catalyst and apolar hydrocarbon cosolvent is crucial for the aerobic oxidation in $scCO_2$. The activity of 0.5% Pd/Al_2O_3 in $scCO_2$−toluene, however, was found to gradually decrease over several working days with a slightly increased selectivity, and the conversion and selectivity on the fifth day became 14.9 and 79.0%, respectively, after which no further deactivation was observed. As shown in Figure 17, the conversion and selectivity in the 0.5% Pd/Al_2O_3-catalyzed reaction strongly depended on the total pressure. A maximum conversion was observed at 12.0 MPa, where the TOF and selectivity were 400 h^{-1} and 58.4%, respectively. Under the conditions, the mixture was composed of two phases, i.e., a CO_2-rich phase and a CO_2-expanded liquid phase. Thus, gas−liquid mass transfer was unlikely to be the rate-determining step in the oxidation. The

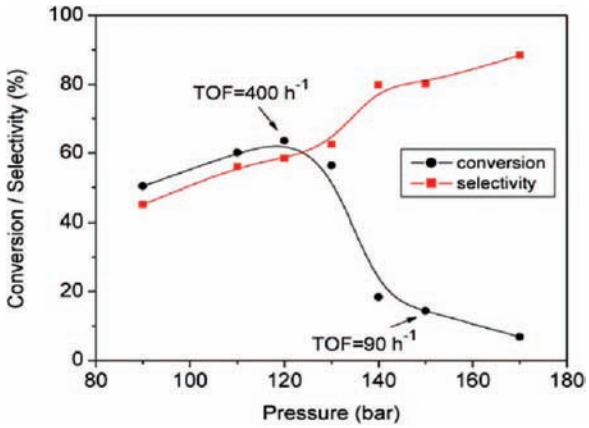

Figure 17. Variation of the conversion and selectivity as a function of total pressure for the continuous catalytic aerobic oxidation of cinnamyl alcohol in $scCO_2$. Reaction conditions: Reaction temperature, 80 °C; composition of the reactant upstream, 0.15 mol % cinnamyl alcohol, 0.15 mol % O_2, 1.9 mol % toluene, CO_2 with a feed rate of 0.233 mol min^{-1}; catalyst, 2.5 g of 0.5% Pd/Al_2O_3. Reprinted with permission from ref 34. Copyright 2006 Elsevier Ltd.

major byproducts were 3-phenyl-1-propanol and β-methylstyrene, of which formations were enhanced, particularly in the lower total pressure region; the selectivity to 3-phenyl-1-propanol exceeded 30% below 13.0 MPa. The O_2 concentration in the feed was also a crucial parameter for the oxidation, and its effect on the conversion and selectivity was different when the operating total pressure was changed as shown in Figure 18. It is noteworthy that the catalyst showed no significant deactivation even at an O_2 concentration of 10 mol %. This result is in contrast to that obtained in the oxidation of benzyl alcohol, in which the same Pd catalyst typically showed a drastic decrease in activity just above a certain pressure below 10 mol %, possibly due to overoxidation of the palladium particles (see sections 3.1.1.2, 3.1.2.3, and 3.1.2.4). As a typical trend, an increase in the O_2 concentration suppressed the formation of the hydrogenated products, leading to higher selectivity to cinnamaldehyde but also promoting the formation of benzaldehyde (selectivity in the range 10−15 and 20−30% at 12.0 and 15.0 MPa, respectively, above 5 mol % of O_2 in the feed). The phase behavior inside the catalyst pores was inspected using the cell previously employed for the benzyl alcohol oxidation (Figure 4). For this purpose, the ZnSe ATR-IR crystal was coated with the 0.5 or 5% Pd/Al_2O_3 catalyst, and the oxidation was performed at 12.0 MPa and 80 °C with a mixture composed of 0.15 mol % cinnamyl alcohol, 0.15 mol % O_2, 1.9 mol % toluene, and CO_2. These investigations revealed that the mixture existed as a single

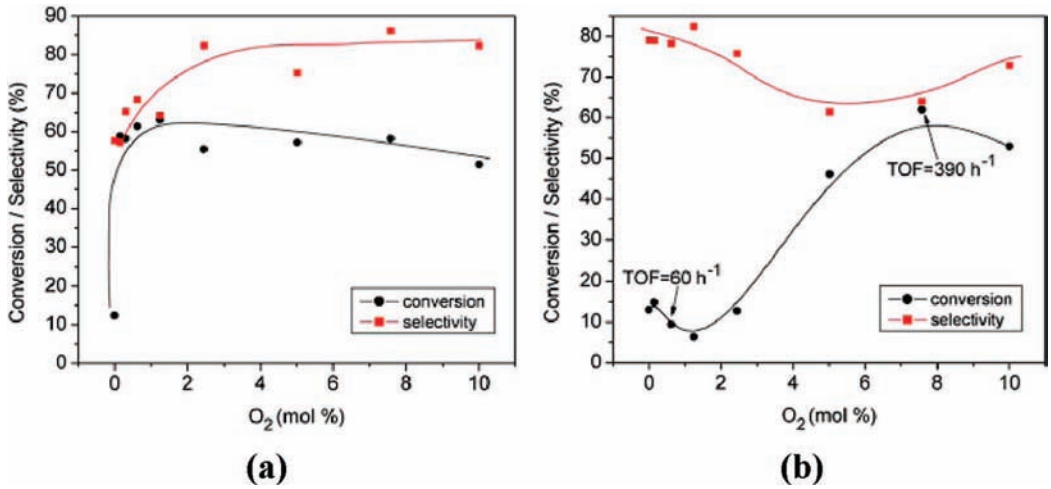

Figure 18. Variation of the conversion and selectivity as a function of O_2 content for the continuous catalytic aerobic oxidation of cinnamyl alcohol in $scCO_2$. Reaction conditions: Reaction temperature, 80 °C; total pressure, 12.0 MPa (a), 15.0 MPa (b); composition of the reactant upstream, 0.15 mol % cinnamyl alcohol, 1.9 mol % toluene, CO_2 with a feed rate of 0.233 mol min^{-1}; catalyst, 2.5 g of 0.5% Pd/Al_2O_3. Reprinted with permission from ref 34. Copyright 2006 Elsevier Ltd.

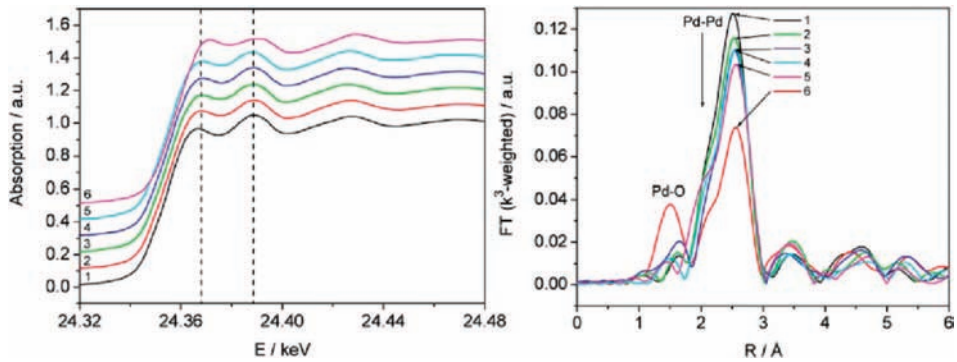

Figure 19. *In situ* EXAFS spectra of the 0.5% Pd/Al_2O_3 catalyst. (a) Energy-calibrated and background-corrected XANES spectra. (b) Fourier-transformed EXAFS spectra. Spectrum 1, in 5% H_2/He at 100 °C; 2, in CO_2 at 12.0 MPa and 80 °C; 3, in 0.15% cinnamyl alcohol, 0.15% O_2, and CO_2 with a total pressure of 12.0 MPa at 80 °C; 4, in 0.15% cinnamyl alcohol, 0.15% O_2, and CO_2 with a total pressure of 15.0 MPa at 80 °C; 5, in 0.15% cinnamyl alcohol, 7% O_2, and CO_2 with a total pressure of 15.0 MPa at 80 °C; 6, in 5% O_2 and CO_2 with a total pressure of 15.0 MPa at 80 °C. Reprinted with permission from ref 34. Copyright 2006 Elsevier Ltd.

Scheme 7. Preparation of the Palladium Nanoparticles Supported on Poly(ethylene glycol) (PEG)-Modified Silica

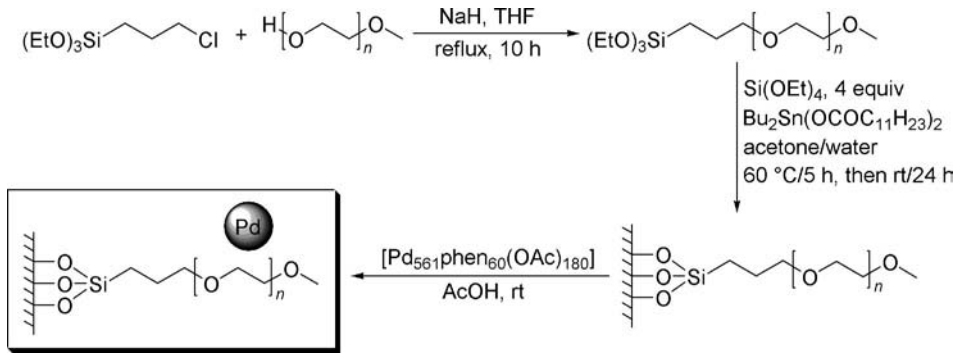

homogeneous phase in the pores of the catalyst even at a pressure lower than that required for rendering the outer bulk phase homogeneous. In addition, the C═O stretching vibration band of the product, cinnamaldehyde, could be observed by ATR-IR spectroscopy during the oxidation. These results are in contrast to the trend observed for the catalyst−benzyl alcohol−O_2−CO_2 mixture.[31] Particularly, it is interesting to note that under the optimal conditions the mixture inside the catalyst pores was homogeneous, whereas the outer bulk phase was composed of two phases, as previously mentioned. *In situ* X-ray absorption spectroscopy was also applied to reveal the oxidation state of palladium particles during the oxidation, using the flow cell shown in Figure 7. The catalyst was first reduced in a stream of H_2/He, followed by its exposure to pure CO_2, benzyl alcohol/O_2/CO_2, and O_2/CO_2 flows in that order. The results are shown in Figure 19. The point of the spectra is that no significant change in the Pd oxidation state occurred when the pressure was increased from 12.0 to 15.0 MPa, corresponding to the transition from biphasic to homogeneous single phase, and even when the O_2 concentration was increased up to 7 mol %. The weak effect of O_2 concentration on the oxidation state of palladium would account for the slight decrease in the oxidation rate at higher O_2 concentrations (Figure 18). The authors proposed that the overoxidation of palladium could be suppressed because a large number of surface hydrogen atoms were constantly provided by the dehydrogenation processes shown in Scheme 6 during the oxidation. This explanation was also supported by the significant change in the Fourier-transformed EXAFS spectra when the feed was changed from the cinnamyl alcohol/O_2/CO_2 flow to O_2/CO_2 flow, indicating that palladium was oxidized to a considerable extent in the absence of cinnamyl alcohol, which serves as a reducing agent.

3.1.2.6. Palladium Nanoparticle Catalysts Stabilized in Poly(ethylene glycol)-Modified Silica. Leitner's group conducted the aerobic oxidation of alcohols to the corresponding carbonyl compounds in $scCO_2$ using palladium nanoparticles immobilized on poly(ethylene glycol) (PEG)-modified silica as catalyst.[35] The preparation method of this catalyst is depicted in Scheme 7. For comparison, a reference catalyst was prepared without using $(EtO)_3Si(CH_2)_3\{O(CH_2)_2\}_nOMe$. The catalytic performances were first compared in the oxidation of cinnamyl alcohol, which was performed at 80 °C in a 36-mL batch-type reactor using 90 mg of 5% Pd catalyst, 1.95 mmol of the alcohol, 36 mmol of O_2, and 414 mmol of CO_2. The superiority of the PEG-modified silica was evident from the much shorter induction period compared to that observed for the reference catalyst, indicating that the PEG chains offer the best environment for immobilization of the Pd_{561} particles. The Pd/PEG-modified silica catalyst was also successfully applied to the oxidation of primary allylic and benzyl alcohols, yielding the corresponding aldehydes in high conversions and selectivities (Table 3). In Table 3 are also given the results of the oxidation of secondary alcohols performed under otherwise similar conditions. The secondary alcohol oxidations were highly selective but proceeded much slower compared to the oxidation of primary alcohols. 1-Butanol was also tested but converted mainly to butyric acid and the corresponding ester with very low rate. The catalytic performances were also evaluated in the continuous oxidation of benzyl alcohol. In this experiment, 0.20 g of catalyst was used, and the CO_2/O_2 stream with a molar ratio of 92:8 (total pressure 15 MPa) and the reactant alcohol were fed into a tubular reactor heated at 80 °C with a rate of 7.5 L h^{-1} and 1.0 mL h^{-1}, respectively. Under these conditions, the Pd/PEG-modified silica catalyst maintained its high performance for at least 30 h, showing >98% selectivities to benzaldehyde and conversions within the range of 50−60%. The turnover number (TON) and turnover frequency (TOF) were then estimated to be 1750 and 58 h^{-1}, respectively. In contrast, the reference catalyst without PEG modifier, even though it afforded 50−60% conversions at the initial stage of the continuous operation, was gradually deactivated with time-on-stream. For both batch and continuous operations, palladium could be loaded on the same PEG-modified silica also by thermal decomposition of $[Pd(\eta^3\text{-}C_3H_5)(\eta^5\text{-}C_5H_5)]$ at 60 °C. The performance of the resultant catalyst was comparable to that prepared by wet-impregnation using $[Pd_{561}phen_{60}(OAc)_{180}]$ as Pd precursor (Scheme 7). TEM images revealed that no agglomeration of Pd nanoparticles occurred for the Pd/PEG-modified silica, whereas significant agglomeration was observed for the reference catalyst possessing no PEG modifier. Thus, even though no data on the oxidation state of palladium was shown, it is reasonable to conclude that the high stability of the nanoparticles realized by the PEG chains could be related to the high catalytic performance of the Pd/PEG-modified silica catalyst.

3.2. Supported Ruthenium Catalysts

3.2.1. Modified Silica-Captured Tetrapropylammonium Perruthenate (TPAP)

Tetrapropylammonium perruthenate (TPAP) is a versatile oxidizing agent effective for the conversion of primary alcohols to aldehydes and of secondary alcohols to ketones.[36] With an appropriate co-oxidant such as *N*-methylmorpholine-*N*-oxide[36a] or molecular oxygen,[36c] TPAP can be used in catalytic amounts. The attempt to perform the aerobic oxidation of alcohols with TPAP catalyst in dense CO_2 was

Table 3. Aerobic Oxidation of Alcohols in $ScCO_2$ Using the Palladium Nanoparticles Stabilized on PEG-Modified Silica as Catalyst (Data Taken from Ref 35)[a]

entry	substrate	product	time (h)	conversion (%)	selectivity (%)	TON[b]
1	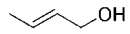	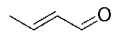	4	98.9	98.0	45
2	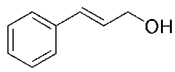	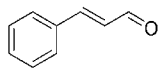	5	96.8	98.5	47
3	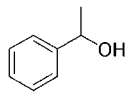	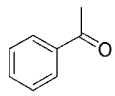	12	58.8	99.5	29
4	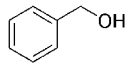	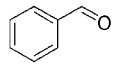	16	96.5	98.8	45
5	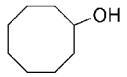	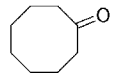	18	46.4	98.2	22

[a] Reaction conditions: reaction temperature, 80 °C; batch reactor volume, 36 mL; catalyst (see Scheme 7), 90 mg; substrate, 1.95 mmol; d (CO_2/O_2) = 0.55 g mL^{-1}; molar ratio, CO_2/O_2 = 92:8. [b] Turnover number (TON) = (mol of product)/(mol of Pd).

started by Pagliaro and co-workers. They found that the simple mixing of benzyl alcohol, O_2, TPAP (0.1 equiv), and $scCO_2$ at 75 °C and 22.0 MPa required 11 h for the completion of the oxidation,[37] whereas in conventional CH_2Cl_2 solvent, benzaldehyde is formed quantitatively in just 30 min at room temperature.[36c] It was assumed that the insolubility of TPAP in $scCO_2$ accounts for the much lower oxidation rate. Pagliaro's group, however, succeeded in enhancing the activity of TPAP by dispersing it on surface-modified silica gels. In the following, the results with the heterogenized TPAP catalysts are described.

3.2.1.1. Methyl Group-Modified Silica-Encapsulated TPAP Catalysts. Pagliaro and co-workers prepared TPAP encapsulated in organically (methyl group-) modified silicas (denoted ORMOSILs) and applied them for the aerobic oxidation of alcohols in $scCO_2$.[37] Several types of the ORMOSILs were prepared by varying the $MeSi(OMe)_3$/$Si(OMe)_4$ ratio as well as the Si/H_2O/MeOH ratio in the sol−gel mixture. In addition, the effect of the presence of NaF as a condensation catalyst was examined. Typically, the use of NaF lowered the activity of the resultant catalysts, and the catalyst prepared with a Si/H_2O/MeOH molar ratio of 1:8:1 exhibited higher activity than that with the ratio of 1:4:4. Particularly, the catalyst prepared with the former ratio using a $MeSi(OMe)_3$/$Si(OMe)_4$ ratio of 1:1 (denoted **A-Me2**) was most active for the oxidation of benzyl alcohol in $scCO_2$. The correlation between the catalytic activity and the structural properties was not simple, but the above best catalyst possessed the largest pore volume among the catalysts prepared. In addition, the catalyst possessed surface methyl groups originating from $MeSi(OMe)_3$, most of which were suggested to be present on the internal surface, rendering the environment hydrophobic. Hence, large pore volume and internal surface hydrophobicity were suggested to be crucial factors for high activity. Although the activity of the ORMOSILs-encapsulated TPAP in $scCO_2$ was still considerably lower than that in liquid solvents, some benefits of using $scCO_2$ may be obtained during the workup process; the $scCO_2$ phase contained no TPAP as well as ORMOSILs, while dissolving the organic reactant and products, allowing us to perform the selective product extraction using dense CO_2.

Detailed mechanistic investigations were performed with the catalyst prepared with a Si/H_2O/MeOH ratio of 1:8:1 and a $MeSi(OMe)_3$/$Si(OMe)_4$ ratio of 75:25 (denoted **A-Me3**).[38] The kinetic analysis implied that RuO_4^- is the catalytically active species and that an ester-type intermediate, $RCH_2-O-Ru(OH)O_3^-$, exits in the catalytic cycle. The role of oxygen was suggested not to reoxidize the Ru intermediate in a reduced form but to dehydrogenate the alcohol coordinated to the metal. The rate-determining step was proposed to be the dehydrogenation step.

Later, the activity of the **A-Me3** catalyst was found to increase several months after its preparation date.[39] The oxidations performed at 75 °C in a 10-mL reactor, using 0.048 mmol of benzyl alcohol, 10 mol % of entrapped TPAP catalyst, 0.1 MPa O_2, and CO_2 at a total pressure of 22 MPa revealed that the **A-Me3** after 18 months of its preparation (denoted **A-Me3-18m**) afforded a pseudo-first-order kinetic rate constant of 4.66×10^{-2} mol^{-1} min^{-1}, which was about ten times higher than that achieved with the freshly prepared **A-Me3** (4.92×10^{-3} mol^{-1} min^{-1}). Electron-probe microanalysis revealed that the external surface Ru/Si molar ratio decreased with aging time. It was therefore suggested that further hydrolysis of the unreacted $-Si(OMe)_3$ group and condensation of the silanol group took place during the several-month aging, resulting in the formation of new microporosity in the catalyst. Then the TPAP existing as aggregates in larger pores of the freshly prepared **A-Me3** was dispersed into the newly formed micropores with the help of methanol which also formed by the hydrolysis of the $-Si(OMe)_3$ group. The isolated TPAP thus formed in the aged catalyst could exhibit much higher activity than the aggregated TPAP in the freshly prepared catalyst.

Scheme 8. Surface Model of the FluoRuGel Catalyst

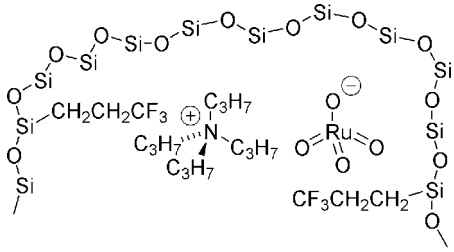

3.2.1.2. Fluoroalkyl Group-Modified Silica-Encapsulated TPAP Catalysts. Pagliaro and co-workers prepared fluoroalkyl group-modified silicas entrapping TPAP.[40] The oxidation of benzyl alcohol was chosen as a model reaction and performed at 75 °C in a 10-mL autoclave using 0.05 mmol of benzyl alcohol, 0.1 equiv of entrapped TPAP, 1 mmol of *n*-decane as GC internal standard, 0.1 MPa of O_2, and 22.0 MPa of CO_2. The most active catalyst was prepared by the sol−gel method, in which a mixture of $Si(OMe)_4$ and $CF_3(CH_2)_2Si(OMe)_3$ with a ratio of 9:1 in methanol solvent was hydrolyzed in the presence of TPAP. The catalyst yielded benzaldehyde exclusively, and no further oxidation products such as benzoic acid were detected. It is also noteworthy that the *in situ* sampling of the CO_2-rich phase during the reaction revealed no sign of ruthenium leaching, indicating that TPAP stayed in the pores of the catalyst in stable form. Apparently, the highest activity of this catalyst was related to the highest surface area (691 $m^2\ g^{-1}$) and large pore volume (0.53 mL g^{-1}), which are favorable for mass transfer of the reactants and products in the porous network where the reaction would mainly take place. The N_2 adsorption−desorption isotherm of this catalyst was type I, indicating that the catalyst was a zeolite-like microporous material with a large internal surface area. The terminal trifluoromethyl group of the catalyst support was assumed to concentrate mainly at the internal surface, promoting the diffusion of dense CO_2 solvent by the attractive interaction between CO_2 and fluorine atoms, enhancing the mass transfer of the reactant and product in the porous network. The support silicas with a longer fluoroalkyl chain were also synthesized similarly using $CF_3(CF_2)_5(CH_2)_2Si(OMe)_3$, mixed with TPAP, and applied for the oxidation. However, these catalysts typically possessed much smaller surface areas compared to those synthesized from $CF_3(CH_2)_2Si(OMe)_3$. In addition, the long fluorinated carbon chain was unstable and decomposed during the reaction. The activities were also inferior to those of the catalysts with the shorter fluoroalkyl chain.

Pagliaro's group also prepared a hybrid fluorinated silica glass doped with TPAP as an oxidation catalyst (denoted FluoRuGel).[41] The FluoRuGel catalyst was prepared using the sol−gel method by adding $Si(OMe)_4$ and

Table 4. Aerobic Alcohol Oxidations in $ScCO_2$ Using the FluoRuGel Catalyst (Data Taken from Ref 41)[a]

entry	substrate	product	$k \times 10^4$ [b] (min^{-1})
1	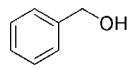	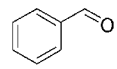	49
2	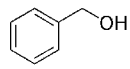	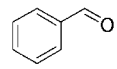	5.88, 6.50[c]
3	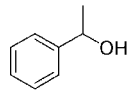	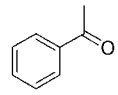	6.46
4	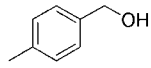	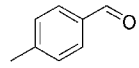	8.27
5	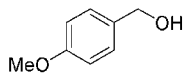	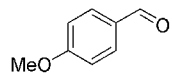	9.67
6	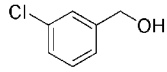	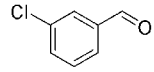	8.27
7	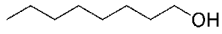		5.02
8	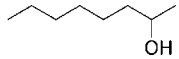	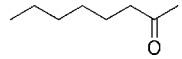	2.03

[a] Reaction conditions: reaction temperature, 75 °C; batch reactor volume, 10 mL; catalyst (see Scheme 8), 156 mg; substrate, 0.05 mmol; O_2, 0.1 MPa at room temperature; CO_2, 22 MPa/10 mL. [b] *k* was obtained from integrated pseudo-first-order plots: $\ln(1 - [\text{aldehyde}]_{t=t})/[\text{aldehyde}]_{t=\infty})$ vs time. [c] The catalyst was washed with CH_2Cl_2.

Scheme 9. Preparation of the Silica-Supported Ionic Liquids Doped with Perruthenate Catalyst (Silc 2)

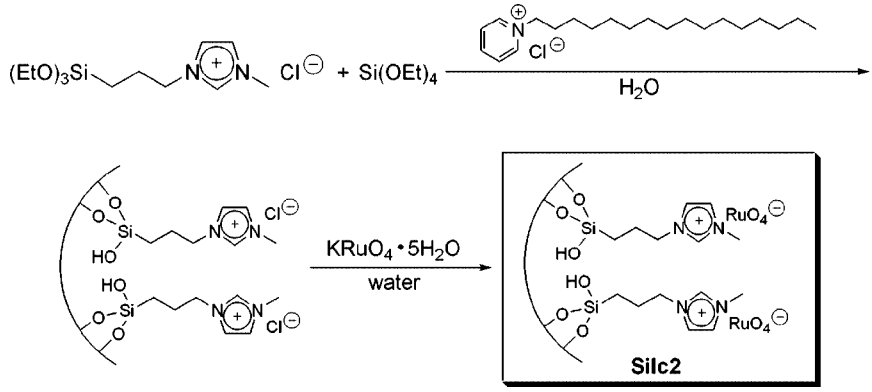

Scheme 10. Preparation of the Silica-Supported Ionic Liquids Doped with Perruthenate Catalyst (Silc 1)

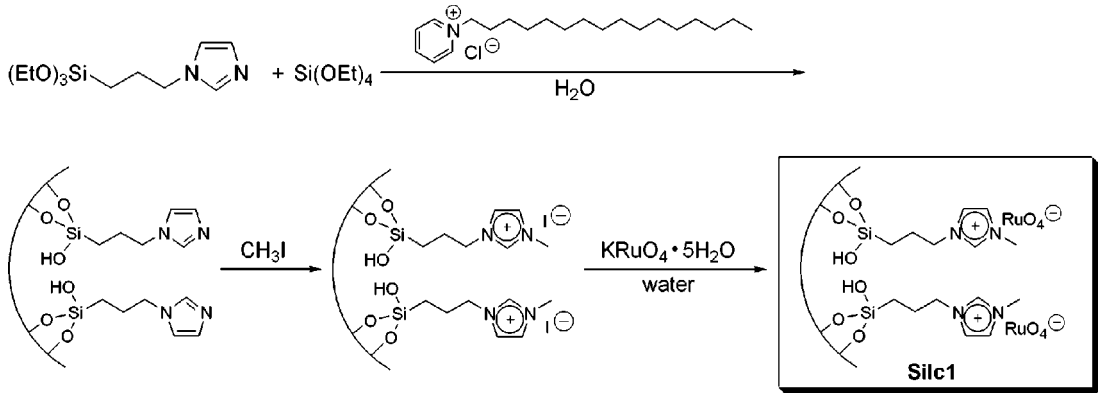

$CF_3(CH_2)_2Si(OMe)_3$ to a solution of TPAP in methanol, followed by hydrolysis of the mixture, aging, and drying. This preparation resulted in a Si/MeOH/H_2O molar ratio of 1:8:4. A surface model of this catalyst is depicted in Scheme 8. The aerobic alcohol oxidation was performed at 75 °C in a 10-mL reactor using 0.05 mmol of alcohol, 0.1 equiv of FluoRuGel, 0.1 MPa of O_2, and 22 MPa of CO_2, under which conditions the mixture formed a single homogeneous phase. The activity was analyzed by applying integrated pseudo-first-order kinetic plots, i.e., $\ln(1 - [\text{aldehyde}]_{t=t}/[\text{aldehyde}]_{t=\infty})$ vs time. Table 4 shows the kinetic constant for each substrate, which demonstrates that not only benzyl but also aliphatic alcohols could be oxidized to the corresponding carbonyl compounds without overoxidation to acids. For the aerobic oxidation with FluoRuGel catalyst, dense CO_2 seems to be the best solvent, because the use of conventional organic solvents resulted in the oxidation of the solvents, which was accompanied by the reduction of the catalytic activity. Particularly, CH_2Cl_2 rapidly decomposed when contacted with FluoRuGel under an oxygen atmosphere, generating Cl_2. Even *n*-hexane could gradually deactivate the catalyst, possibly during its oxidation process. Another important role of dense CO_2 seems to be the suppression of the leaching of perruthenate species, because no Ru was observed in the sample withdrawn from the $scCO_2$ phase during the oxidation. In contrast, CH_2Cl_2 readily dissolved TPAP, and its use can lead to the dissolution of the encapsulated TPAP in FluoRuGel. The advantage of encapsulation of TPAP in the fluorinated silica could clearly be seen in the activity comparison between FluoRuGel and free TPAP. Although free TPAP exhibited much higher activity than FluoRuGel at the initial stage of the reaction (0 min to ca. 25 min), the latter afforded higher conversion after ca. 225 min. This indicates that the aggregation of the intermediate perruthenate species into the inactive RuO_2 occurred in the free TPAP-catalyzed reaction, whereas this could be prevented with FluoRuGel due to the dispersive encapsulation of the perruthenate in the inner porosity of the sol−gel organosilica matrix. Finally, the cost required for the production of FluoRuGel was calculated to be equal to or even lower than that of conventional catalysts such as 5% Pt/C and 4% Pd−1% Pt−5% Bi/C. The authors thus emphasized the high potential of the FluoRuGel catalyst for industrial oxidation processes.

3.2.2. Silica-Supported Ionic Liquids Doped with Perruthenate

Besides the surface-modified silica-entrapped TPAP catalysts, Pagliaro's group developed the lamellar silica-supported ionic liquid doped with RuO_4^- as an efficient catalyst for the aerobic oxidation of alcohols in $scCO_2$, which yields the corresponding carbonyl compounds in 100% selectivity.[42] The catalyst (denoted Silc2) was prepared by the method shown in Scheme 9, which involves the formation of a lamellar phase by the action of cetylpyridinium chloride as surfactant, followed by ion-exchange, replacing the chloride ion with the catalytically active RuO_4^-. For comparison, the catalyst (denoted Silc1) prepared by the method shown in Scheme 10 was also tested. The distinct structural difference between Silc1 and Silc2 was that the former was mesoporous, while the latter had a lamellar structure, which was brought about by the difference in electronic properties between the 1-[3-(triethoxysilyl)propyl]imidazolium rings of the precursors. A significant difference in activity between Silc2 and Silc1 was observed in the oxidation of benzyl alcohol performed at 75 °C in a 10-mL reactor using 48.3 μmol of the alcohol, 2% entrapped perruthenate, O_2 (0.1 MPa at 25

Table 5. Aerobic Alcohol Oxidations in $ScCO_2$ Using the Silc2 Catalyst (Data Taken from Ref 42)[a]

entry	substrate	product	$k \times 10^2$ [b] (min^{-1})
1	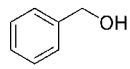	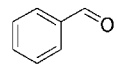	2.87
2	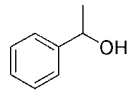	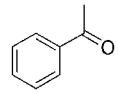	0.274
3	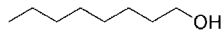		0.105
4	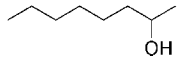	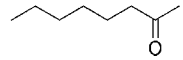	0.062

[a] Reaction conditions: reaction temperature, 75 °C; batch reactor volume, 10 mL; catalyst (see Scheme 9), 1.44 mg; substrate, 48.3 μmol; O_2, 0.1 MPa at 25 °C; CO_2, 22.0 MPa/10 mL. [b] k was obtained from integrated pseudo-first-order plots: $\ln(1 - [\text{aldehyde}]_{t=t}/[\text{aldehyde}]_{t=\infty})$ vs time.

°C), and CO_2 (22.0 MPa). Thus, the kinetic study based on the integrated pseudo-first-order plots, namely, $\ln(1 - [\text{aldehyde}]_{t=t}/[\text{aldehyde}]_{t=\infty})$ vs time, revealed that the rate constant for Silc1 was only 4.6×10^{-4} min^{-1}, whereas Silc2 afforded 2.87×10^{-2} min^{-1}, which means that Silc2 is >60 times more active than Silc1. The activity of Silc2 was also four times as high as that of the TPAP entrapped in 75% methyl-modified ORMOSIL,[39] which afforded a kinetic rate constant of 7.98×10^{-3} min^{-1} under the same conditions after 18 months of catalyst aging. It is also noteworthy that the kinetic linearity in the plots implies that the RuO_4^- species were homogeneously dispersed over the supported ionic-liquid materials Silc1 and Silc2. The reason why the Silc2 is more active than Silc1 has not been elucidated yet. However, the authors suggested that the high affinity of I^- ion with the imidazolium cation may be related to the activity difference. Actually, after the ion-exchange with RuO_4^-, Silc2 contained less than 10% of Cl^-, whereas 30% of the original I^- ions were left in the resultant Silc1. Table 5 shows the catalytic activity of Silc2 for other alcohols as well as benzyl alcohol. Note that the catalyst also exhibited high activity for the less reactive primary aliphatic alcohol, 1-octanol. Recyclability of the Silc2 catalyst was also satisfactory, showing less than 3% loss in the activity for three consecutive runs. This indicates the high stability of the catalyst under the reaction conditions. Actually, no Ru leaching as well as no breakdown of the propyl spacer of the supported ionic liquid was observed.

3.3. Other Heterogeneous Catalysts

3.3.1. Chromium-Containing Molecular Sieves

Dapurkar et al. tested chromium-doped MCM-41 catalysts (denoted CrMCM-41) in the aerobic oxidation of benzyl alcohol.[43] The chromium was loaded by adding $Cr(NO_3)_3 \cdot 9H_2O$ into the precursor gel mixture of MCM-41. The characteristic XRD patterns observed for the hexagonal MCM-41 structure were observed also for the CrMCM-41 catalyst. The oxidation was typically performed at 80 °C for 14 h in a stainless-steel reactor equipped with a 40-mL Teflon insert, using 0.1 g of the catalyst, 1 mmol of alcohol, 0.5 MPa of O_2, CO_2 at a total pressure of 16 MPa, and, if necessary, 0.5 mL of cosolvent or poly(ethylene glycol) 400 (denoted PEG400). Although the oxidation in $scCO_2$ as the sole solvent took place very slowly (<10% conversion in the CO_2 pressure range 10−18 MPa), the addition of PEG400 dramatically improved the reaction rate. Thus, in the $scCO_2$−PEG400 biphasic system, the conversion and the benzaldehyde yield reached 91 and 84%, respectively. These values were also much higher than those obtained in $scCO_2$−acetone, CO_2-free PEG400, and CO_2-free acetonitrile. It is noteworthy that the CrMCM-41 catalyst could be used three times with no degradation of catalytic performance in $scCO_2$−PEG400. The CrMCM-41/$scCO_2$−PEG400 system was also successfully applied for the oxidation of benzyl and aliphatic secondary alcohols, yielding the corresponding ketones in >99% selectivity at high (∼100%) and moderate conversions (∼40%), respectively.

3.3.2. Supported Gold

Baiker and co-workers used metal oxide-supported gold catalysts for the oxidation of alcohols to the corresponding aldehydes.[44] The used supports were TiO_2, Fe_2O_3, and C, while the gold was loaded on them from the aqueous colloidal Au or $HAuCl_4$ solutions. The resultant wet materials were dried at 80 °C for 15 h to give the catalysts, which were used for the oxidations as-prepared or after calcination at 400 °C. In addition, flame spray pyrolysis was employed for the preparation of Au-supported Fe_2O_2, in which a mixture of iron(III) acetylacetonate and $HAuCl_4$ dissolved in water, methanol, and acetic acid was sprayed in a methane/O_2 flame. Typically, the oxidation was performed in a 100-mL autoclave using 7 mmol of alcohol, 14 mmol of O_2, and 1590 mmol of CO_2 at 100 °C and a total pressure of 15.0 MPa. Under these conditions, benzyl alcohol, O_2, and CO_2 formed a single homogeneous phase, and the 1% Au-loaded TiO_2 synthesized from colloidal gold (denoted 1% Au/TiO_2(coll)), which was used as-prepared, afforded the best results, yielding benzaldehyde in 99.0% selectivity at 16.0% conversion. The reaction rate and turnover frequency (TOF) were estimated to be 73 $mol_{product}$ mol_{Au}^{-1} h^{-1} and 161 h^{-1}, respectively. Calcination of the as-prepared 1% Au/TiO_2(coll) at 400 °C resulted in a lower conversion of 10.4%, which was caused by the sintering of gold particles, as evidenced by STEM images; the mean Au-particle size of the as-prepared catalyst increased from 1.9 to 2.8 nm after calcination. The effect of changing reaction temperature was

examined using the 1% Au/TiO_2(coll) catalyst at 80, 100, and 120 °C, while the other reaction parameters were kept the same as under the standard conditions. Not only the conversion but also the selectivity increased as the temperature was raised, reaching 34.7 and 99.2% at 120 °C, respectively. The selectivity increase was attributed to the enhanced diffusion of benzaldehyde at higher temperature, leading to the suppression of further reactions of the aldehyde. Variation of the conversion as a function of reaction time was investigated under the standard conditions at 100 °C. The conversion increased with time, but the reaction rate gradually decreased; the conversion after 20 h was only 30%. However, since there were no indications for changes of the Au particle size as well as the oxidation state (demonstrated by XANES measurements) and also for leaching of the gold after the reaction, the authors proposed that the water generated blocked the active sites or changed the surface properties. Actually, another experiment conducted under the typical conditions but with intentionally added water (11 mmol) showed a decrease of the conversion from 16.0 to 9.1%. The O_2 concentration also affected the conversion. The highest conversion was achieved with 14 mmol of O_2 when the reaction was conducted under the same conditions as those of the standard conditions except for the changed O_2 (7−122 mmol) and CO_2 pressures (1020−1610 mmol CO_2); the latter was altered to render the total pressure constant (15.0 MPa). On the other hand, the effect of changing the CO_2 amount under the standard conditions revealed that the use of 680 mmol of CO_2 led to the highest conversion of 23.6% with a selectivity of 97.0%. Under these conditions, the system was composed of two phases, i.e., a CO_2-expanded benzyl alcohol phase and a CO_2-rich phase, indicating that a single homogeneous phase is not crucial for the oxidation. Although the reaction conditions were not optimized, other alcohols such as 1-octanol and geraniol were similarly oxidized over 1% Au/TiO_2(coll) to give the corresponding aldehydes, 1-octanal and citral, in 90.4 and 30.6% selectivity at 4.1 and 10.9% conversion, respectively.

3.3.3. Supported Multi-Metals

Baiker's group conducted the continuous catalytic aerobic oxidation of various alcohols in $scCO_2$ using a commercially available Pd−Pt−Bi/C catalyst.[45] A flow-reactor system similar to that depicted in Figure 6 was used. Table 6 shows the results of the oxidation of various alcohols to the corresponding aldehydes or ketones. The oxidation of benzyl alcohol (entry 1), 1-phenylethanol (entries 3 and 4), 2-octanol (entry 8), and cinnamyl alcohol (entries 9 and 10) occurred selectively, and the corresponding carbonyl compounds were obtained in synthetically satisfactory yields. Control of the oxidation of the aliphatic primary alcohol, 1-octanol, was much more difficult, because many byproducts, i.e., octanoic acid, octyl octanoate, 2-octenal, and dioctyl ether were formed. The ester and ether would be formed by the catalytic action of octanoic acid. The reaction parameters were investigated in detail with 2-octanol, revealing that the yield of 2-octanone can be increased by applying a higher amount of catalyst, lower flow rate, higher temperature, and longer contact time. The O_2 concentration in the feed was also found to be crucial, and 5 mol % of O_2 afforded the highest 2-octanone yield when the reaction was performed using 2 g of the catalyst and 5 mol % of 2-octanol at 100 °C and a total pressure of 9.5 MPa with a CO_2 flow rate of 2.46 mol h^{-1}. The decrease in yield above this O_2 concentration was attributed to overoxidation of the catalyst, because the oxidative dehydrogenation usually proceeds faster on the reduced metal surface. Another plausible reason for the yield decrease is the change in phase behavior, which was caused by the lowered CO_2 density accompanied by the increase of O_2 concentration. For solid alcohols, butanone was employed as cosolvent, but its concentration had to be kept at a low level to achieve higher yields.

3.3.4. Supported Iron Oxide

Wang and Willey performed the aerobic partial oxidation of methanol over supported Fe_2O_3 catalysts at 225−300 °C.[46] The MeOH/O_2 molar ratio was 1:1.6, and the CO_2 pressure was 9.0 MPa. As a trend observed when SiO_2 was used as support, higher Fe_2O_3 loading (20−100%) and lower temperature (225−250 °C) gave dimethyl ether as the main product, while lower Fe_2O_3 loading and higher temperature (250−275 °C) afforded methyl formate in highest selectivity. Formaldehyde was the major product when MoO_3 was used as support. Based on the reaction results and FT-IR spectroscopy of the catalysts adsorbing methanol, formic acid, methyl formate, and dimethyl ether, the authors proposed the mechanisms shown in Scheme 11 for each case. When the Fe_2O_3 loading was high, Lewis acidic Fe_2O_3 aggregates would form on the surface, yielding dense Fe−OMe species which finally condensed to give dimethyl ether and water. On the other hand, with the low Fe_2O_3 loading, the Fe−OMe species were relatively isolated and hence not likely to undergo similar condensation. Instead, the C−H bond breaking in the methyl group would occur to give formaldehyde as well as water, which was driven by the inherent redox property of the highly dispersed Fe_2O_3. At higher temperature, surface formate, Fe−OC(O)H, was formed, possibly via the further dehydrogenation of formaldehyde adsorbed. The condensation between the Fe−OC(O)H and surface methoxy groups such as Si−OMe and Fe−OMe could lead to the formation of methyl formate, which was the main product at higher temperature up to 275 °C over the catalyst with lower Fe_2O_3 content. When MoO_3 was used as support, iron molybdenate, $Fe_2(MoO_4)_3$, was formed on the surface, which was assumed to be the catalytically active species converting methanol into formaldehyde and water in the presence of O_2. The lattice oxygen in $Fe_2(MoO_4)_3$ is considered to be labile and to actively participate in the reaction.

3.3.5. Polyoxometalate

Leitner, Neumann, and co-workers found that the polyoxometalate, $H_5PV_2Mo_{10}O_{40}$, catalyzes the aerobic oxidation of benzyl alcohols to the corresponding aldehydes in $scCO_2$.[47] Typically, the reaction was performed at 100 °C for 16 h in a 10-mL autoclave, using 5 μmol of the catalyst, 0.5 mmol of alcohol, 0.2 MPa of O_2, and 6 g of CO_2, which led to a total pressure of 17.0 MPa. Under these conditions, benzaldehyde and its derivatives were formed in quantitative yield, regardless of the presence of electron-withdrawing or electron-donating substituents on the aromatic ring (Scheme 12). For comparison, $H_5PV_2Mo_{10}O_{40}/Al_2O_3$, $H_5PV_2Mo_{10}O_{40}$−PEG/Al_2O_3, and $H_5PV_2Mo_{10}O_{40}$−PEG were also tested, but their performances were inferior to $H_5PV_2Mo_{10}O_{40}$ alone in activity and selectivity. Another interesting feature of the $H_5PV_2Mo_{10}O_{40}$ catalyst is its high recyclability. A sequence of reaction, extraction of organic compounds with a dense-

Table 6. Aerobic Alcohol Oxidations in $ScCO_2$ Using the Pd−Pt−Bi/C Catalyst (Data Taken from Ref 45)[a]

entry	substrate amount (mol %)	O_2 (mol %)	total pressure (MPa)	reactor temp. (°C)	product	residence time (s)	yield (%)	select. (%)
1	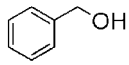 5	2.5	9.5	80	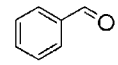	13	26	99
2	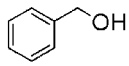 2	2	12.0	100	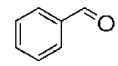	9.5	65	78
3[b]	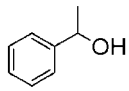 2.7	2.7	11.0	140	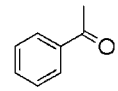	13	95	>99.5
4[b]	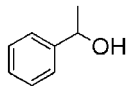 2.7	5.3	11.0	140	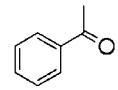	13	98	99
5[c]	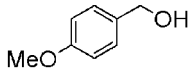 2	2	12.0	110	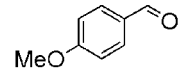	9.5	70	87
6	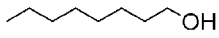 3	6	12.0	110		9.5	18	34
7	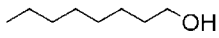 5	2.5	9.5	80		25	11	82
8	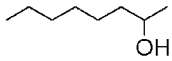 2	4	11.0	140	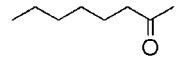	17	68	>99.5
9[c]	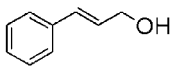 2	4	12.0	110	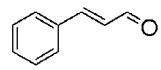	9.5	78	98
10[d]	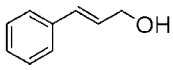 2	4	12.0	110	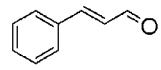	9.5	61	96

[a] Catalyst: Degussa, CEF 196 RA/W, 4% Pd + 1% Pt + 5% Bi, 3 g. The catalyst was pretreated with H_2 at 100 °C for 2 h. Flow rate of CO_2: 1.84−4.92 mol h^{-1}. [b] 5.3 mol % of butanone was used as cosolvent. [c] 4 mol % of butanone was used as cosolvent. [d] 8 mol % of butanone was used as cosolvent.

CO_2 stream, and recharge of benzyl alcohol, O_2, and $scCO_2$ could be repeated at least seven times with the same reactor containing the same catalyst without any loss in catalytic performance. The high stability of the catalyst was supported by ICP analysis, which showed the absence of molybdenum and vanadium in the extracted benzaldehyde after the seventh cycle. Visual inspection of the reaction mixture revealed that benzyl alcohol, O_2, and $scCO_2$ formed a single homogeneous phase and that $H_5PV_2Mo_{10}O_{40}$ was present as a free floating powder. As the reaction proceeded, however, small water drops were found on the wall. In contrast to benzyl alcohols, secondary alcohols were not oxidized with the $H_5PV_2Mo_{10}O_{40}$−O_2−$scCO_2$ system but converted into alkenes through the acid-catalyzed dehydration and subsequent double-bond migration. The catalytic system was also successfully applicable to the oxidation of activated aromatic

Scheme 11. Plausible Mechanisms of the Methanol Oxidation over Supported Fe_2O_3 Aerogels in $ScCO_2$

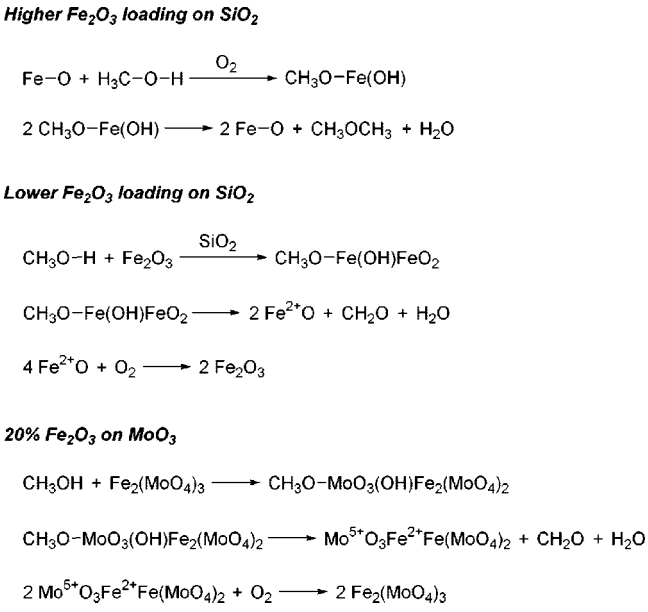

Scheme 12. Selective Aerobic Oxidations over the $H_5PV_2Mo_{10}O_{40}$ Polyoxometalate Catalyst in $ScCO_2$

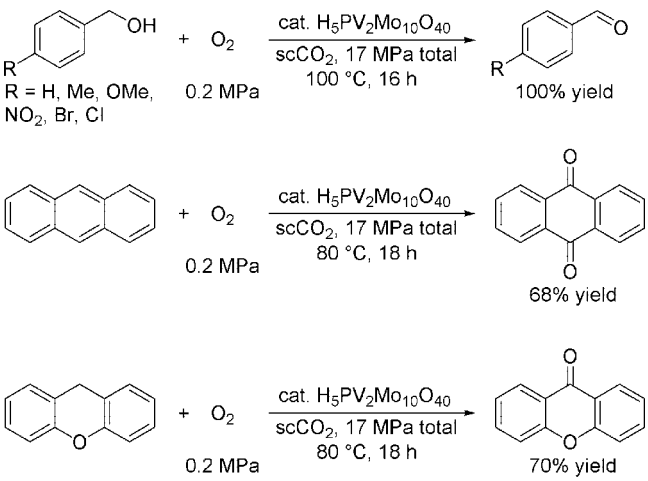

hydrocarbons such as anthracene and xanthene (Scheme 12). Thus, the corresponding carbonyl compounds were formed in 68 and 70% yield, respectively, under identical conditions except for a reduced amount of catalyst (0.5 μmol) as well as lowered reaction temperature (80 °C).

3.4. Enzyme Catalysis

Randolph and Prausnitz used enzyme catalysts for the aerobic oxidation of cholesterol to cholest-4-ene-3-one and found that cholesterol oxidases isolated from *Streptomyces* sp., *Norcardia* sp., *Pseudomonas* sp., and *Gloeocysticum chrysocreas* were active in $scCO_2$.[48] The oxidations were performed at 35 °C and 10 MPa using either a batch or a continuous-flow reactor. For batchwise experiments, the reaction mixture was composed of 0.2 mmol of cholesterol, 2.0 mL of 0.1 M $NaHCO_3$ (pH = 9), 0.8 MPa O_2 (at 22 °C), and either 0.036 or 0.072 mg of cholesterol oxidase from *Streptomyces* sp. On the other hand, the continuous operation was performed not by constantly feeding the substrate with a pump but by feeding pure $scCO_2$ into a saturation chamber containing cholesterol (1 g)-dispersed glass wool and 10 mL of water. The dense CO_2 flow thus dissolving cholesterol as well as water then entered a packed-bed reactor containing the enzyme immobilized on glass beads. Molecular oxygen also was not fed at a constant feed rate, but 0.8 MPa of O_2 (at 35 °C) was introduced at one time from the cylinder into the reaction system. Note that, for both reactor systems, the reaction mixture contained water which wetted cholesterol oxidase; enzymes usually need at least a shell of water to function catalytically. Cholesterol oxidase from *Streptomyces* sp. underwent thermal denaturation even at a temperature around the critical temperature of CO_2 (30.9 °C) and lost its activity with reaction time in $scCO_2$. On the other hand, cholesterol oxidase from *Gloeocysticum chrysocreas* was extremely stable at 35 °C and 10 MPa. The results with this oxidase are shown in Table 7. In contrast to aqueous medium (entry 1), $scCO_2$ afforded much higher turnover frequency (TOF) (entry 3). In addition, the use of branched butanols as cosolvents enhanced the TOF drastically (entries 6 and 7). EPR spectroscopy revealed that aggregation of cholesterol was greatly promoted by the use of branched butanols, which was suggested to cause the high oxidation rates. On the other hand, other cosolvents such as methanol, ethanol, acetone, and 1-butanol gave lower local concentrations of cholesterol, leading to smaller increases in oxidation rate.

Table 7. Turnover Frequencies for the Aerobic Oxidation of Cholesterol to Cholest-4-ene-3-one with Cholesterol Oxidase from *Gloeocysticum Chrysocreas* (Data Taken from Ref 48)

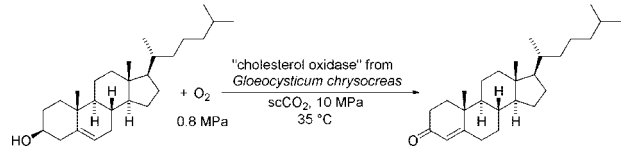

entry	solvent	TOF (s^{-1})
1	water	not measurable
2	water (5 mM phosphate, pH 7.0) + 5% v/v isopropanol	1
3	CO_2, 10 MPa	75
4	CO_2 + 2.0% v/v MeOH	62
5	CO_2 + 2.0% v/v EtOH	165
6	CO_2 + 2.0% v/v *t*-BuOH	274
7	CO_2 + 2.0% v/v ^{i}BuOH	238
8	CO_2 + 2.0% v/v acetone	86
9	CO_2 + 2.0% v/v *n*-BuOH	100

3.5. Photocatalytic Oxidations

Photocatalytic oxidation of organic pollutants over TiO_2 involves the excitation of electrons (e^-) jumping from valence band to conduction band by photoirradiation. The e^- in the conduction band reduces O_2 to give superoxide (O^{2-}), while the hole formed in the valence bond oxidizes the OH^- in water to hydroxyl radical (•OH). Organic pollutants undergo oxidative decomposition, ultimately to CO_2, through reactions with O^{2-} and •OH. Fox's group performed photocatalytic oxidation of 1-octanol in $scCO_2$ using hydrophobic TiO_2, which had been prepared by treating normal TiO_2 with trimethoxyoctylsilane (Degussa T805).[49] Unmodified normal TiO_2 with surface hydroxyl groups was not suitable, because coagulation under air moisture led to adherence of the catalyst to the sapphire windows of the reactor, disturbing the penetration of the light. This problem might be solved by employing moisture-free conditions, but this approach is not practical. Typically, the oxidation was performed at 32 °C in a 15-mL reactor, using 0.03 g of T805 TiO_2 catalyst, 25 μL of 1-octanol (ca. 0.01 M), 2.8 MPa air, and 10 MPa CO_2. Irradiation was carried out by focusing the emission of a 100-W Hg−Xe arc lamp

on the window of the vessel with a quartz focusing lens. Under these conditions, 1-octanol was oxidized to octanal, octanoic acid, and octyl octanoate. From the early stage of the reaction until 7 h, the yield of octanal monotonously increased with reaction time, but then sharply decreased, although the alcohol conversion continuously increased up to 9 h. Thus, the alcohol oxidation to the aldehyde competed with the surface desilanation at the initial stage, while after 7 h not only the alcohol oxidation but also the aldehyde oxidation to octanoic acid and ultimately to CO_2 and water took place. The photocatalytic oxidation was hardly influenced by the CO_2 pressure in the range 9−14 MPa. Reaction temperature also was not an important parameter if it was changed near the critical temperature; the reaction performed at a lower temperature of 23 °C with a CO_2 pressure of 10 MPa (liquid CO_2) only resulted in a slight decrease in the oxidation rate. However, higher temperature (≥45 °C) resulted in surface desilanation even during the early stage of the reaction, causing unfavorable adhesion of the catalyst to the wall and windows of the reactor. Thus, the optimal temperature was suggested to be that near or slightly above the critical temperature.

Later, the same group investigated in detail the effect of pressure and temperature on the same photocatalytic oxidation.[50] The reaction was carried out in a 15-mL reactor, using 50 mg of T805 TiO_2, 0.2 MPa of O_2, and 0.08 mmol of 1-octanol at various CO_2 pressures and reaction temperatures under the irradiation of light from a 100-W Hg−Xe lamp. Quantitative analysis was performed *in situ* by sampling a part of the mixture except for the solid catalyst during the reaction. The plot of the pseudo-first-order rate constant against CO_2 pressure in the range 8−20 MPa at 36 °C revealed that the reaction rate (the conversion of 1-octanol) monotonously decreases with increasing pressure, while the yield of the initial oxidation product, octanal, increased monotonously until 15 MPa, above which it reached a plateau until 20 MPa. The authors suggested that increased CO_2 pressure (density) lowered the concentration of 1-octanol in the vicinity of the catalyst surface by the dissolution of the alcohol into the CO_2-rich phase, and this led to the decrease of the reaction rate. On the other hand, the enhanced aldehyde yield up to 15 MPa was explained by its facilitated desorption from the catalyst surface at higher CO_2 density. Hence, in the *in situ* quantitative analysis, the rate of the product desorption from the catalyst surface to the CO_2-rich phase also affects the reaction results. The marginal change of the aldehyde yield at 15−20 MPa would be a balance among increased production of initial and secondary oxidation products and an enhanced mass transfer. The products except for octanal were octanoic acid and heptanal, which were suggested to form by the oxidative decarboxylation of octanoic acid. Since the solubility of octanoic acid in the apolar dense CO_2 medium is low and thus the acid would stay on the catalyst surface or precipitate at the bottom of the reactor, the online GC detected it only at higher CO_2 pressure. Another reaction parameter investigated, reaction temperature, afforded a similar CO_2 density-related trend. Increasing the temperature from 26 to 46 °C at a constant CO_2 pressure of 10 MPa resulted in an increase of the rate constant, and the value at 56 °C was almost equal to that obtained at 46 °C. The former increase in the rate can be explained in terms of the decreased CO_2 density at higher temperature at a constant pressure, rendering the concentration of 1-octanol in the vicinity of the catalyst surface high due to the lowered solubility of the alcohol at lower CO_2 density. On the other hand, the yield of octanal monotonously decreased as the temperature was raised from 26 to 56 °C at 10 MPa of CO_2, and this again could be explained by the decreased aldehyde solubility in the dense CO_2 medium. In addition, higher temperature could promote further oxidation of octanal, lowering its yield. In conclusion, the unique solvent properties of $scCO_2$, such as the low polarity, tunable density (solubilizing power) by changing the pressure and temperature, high diffusivity, and low viscosity, allow us to control the contents of products in the CO_2-rich phase beyond the level possible with conventional aqueous media. The $scCO_2$ with higher CO_2 density also played a crucial role in the successful dispersion of T805 TiO_2 in the medium, because at lower CO_2 density the catalyst precipitated on the window of the reactor, disturbing the light penetration.

4. Aerobic Oxidation of Phenols

4.1. Cobalt Complex Catalysts

Phenols undergo catalytic oxidation to give the corresponding quinones under the influence of cobalt(III) Schiff base complexes. Busch's group applied $scCO_2$ medium for the oxidation of 2,6-di-*tert*-butylphenol (denoted DTBP) and provided additional insights into the established reaction mechanism that had been well-studied in conventional solvents.[51] Due to the low solubility of the conventional Co(salen) complex in $scCO_2$, a modified salen ligand was employed (the catalyst denoted Co(salen*); see Scheme 13), which resulted in a single homogeneous phase. Typically, the oxidation was performed at 70 °C and a total pressure of 20.7 MPa for 21 h using 0.46 mM of Co(salen*), 9.2 mM of DTBP, 690 mM of O_2, and 0.59 mM of methylimidazole. One of the parameters was modified to see its effect on the catalysis. The effect of temperature was investigated in the range 50−90 °C. While the conversion monotonously increased from 50 to 100% with temperature, the selectivity to 2,6-di-*tert*-butyl-1,4-benzoquinone (denoted DTBQ) was almost constant, implying that there is only little difference in activation energy between the formation of DTBQ and the dimerization product, 3,5,3′,5′-tetra-*tert*-butyl-4,4′-diphenoquinone (denoted TTBDQ), possibly due to the very small activation energies of both processes, which are considered to be radical reactions. The authors also proposed that the temperature-independent selectivity indicates the smaller influence of transport properties in the temperature range applied. On the other hand, when the $[O_2]$/[DTBP] molar ratio was increased from 0 to 200, both conversion and selectivity increased until the ratio reached 100, above which they became constant. This behavior is typical for the reactions driven by an oxygen complex (here $LCo^{III}OO\bullet$) but is rarely observed for the reactions promoted by free oxygen. The catalyst concentration was not crucial for the selectivity in the range 0.1−0.7 mM. However, the conversion increased with increasing concentration, reaching a maximum at ca. 0.6 mM. The drop of conversion at 0.7 mM was explained in terms of the formation of inactive dimeric dicobalt species. In addition to the above parameters, the amount of methylimidazole was also found to be crucial for the reaction. It was proposed that methylimidazole binds to the cobalt center, altering the reactivity of the catalyst. In addition, it also could serve as cosolvent, enhancing the solubility of the catalyst in $scCO_2$. The beneficial role of methylimidazole, however, could be seen only up to its molar

Scheme 13. Plausible Mechanism for the Aerobic Oxidation of 2,6-Di-*tert*-butylphenol with a Cobalt(III) Schiff Base Complex Catalyst in $ScCO_2$

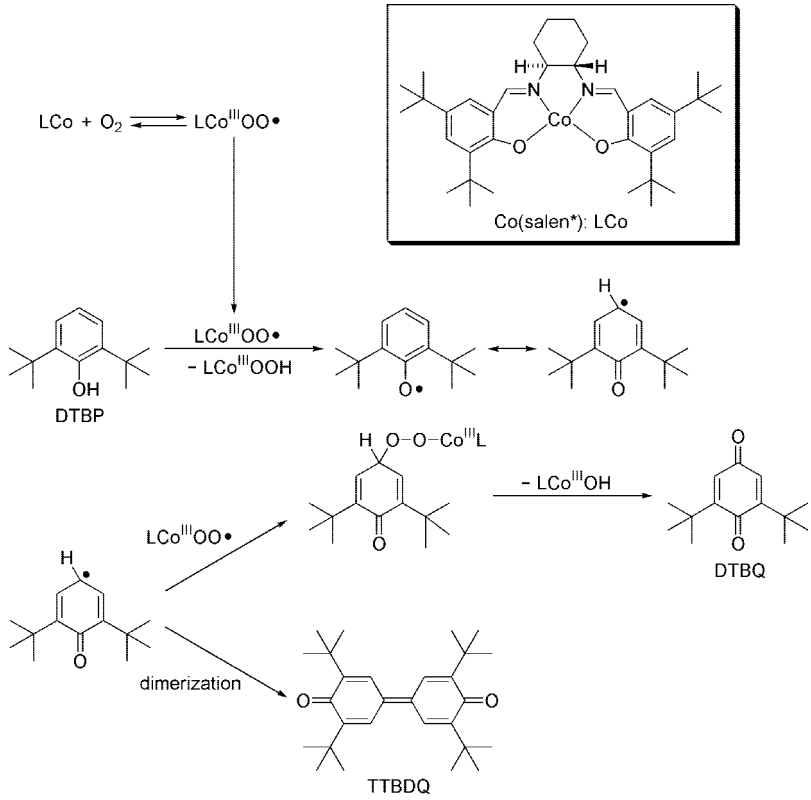

Scheme 14. Catalytic Aerobic Oxidation of 2,6-Di-*tert*-butylphenol in $ScCO_2$ Using Immobilized Co(II) Complex Catalysts

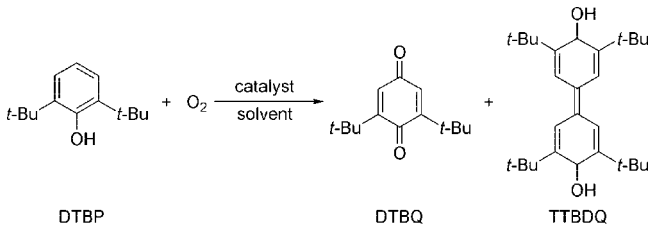

concentration equal to the catalyst concentration. Adding excess methylimidazole led to the formation of a coordinately saturated, six-coordinated cobalt complex which no longer has a site available for binding to oxygen. On the basis of these parameter studies, the authors concluded that the oxidation in $scCO_2$ takes place also by the mechanism depicted in Scheme 13. However, there still remains a question as to how the $LCo^{III}OOH$ and $LCo^{III}OH$ were reconverted to LCo^{III} or $LCo^{III}OO\bullet$ species. Although the work mainly focused on the elucidation of the mechanism, we also should pay attention to the fact that a DTBQ selectivity of more than 90% could be achieved in $scCO_2$ under optimal conditions, indicating the high potential of the medium as a replacement for conventional liquid solvents.

Subramaniam and co-workers carried out the oxidation of DTBP using molecular oxygen and immobilized Co complexes as oxidant and heterogeneous catalysts, respectively, which affords 2,6-di-*tert*-butyl-1,4-benzoquinone (DTBQ) and 3,5,3′,5′-tetra-*tert*-butyl-4,4′-diphenoquinone (TTBDQ) as products (Scheme 14).[52] The catalysts were prepared by the template copolymerization method, in which precursor Co complexes possessing polymerizable ligand were treated with ethylene glycol dimethacrylate in the presence of azobisisobutyronitrile (AIBN) as radical initiator. Figure 20 shows the models for the immobilized metal sites which are isolated enough to prevent detrimental intermolecular interactions. The catalysts were mesoporous, with average pore diameters in the range 2.5−5.0 nm, which can bind O_2 with

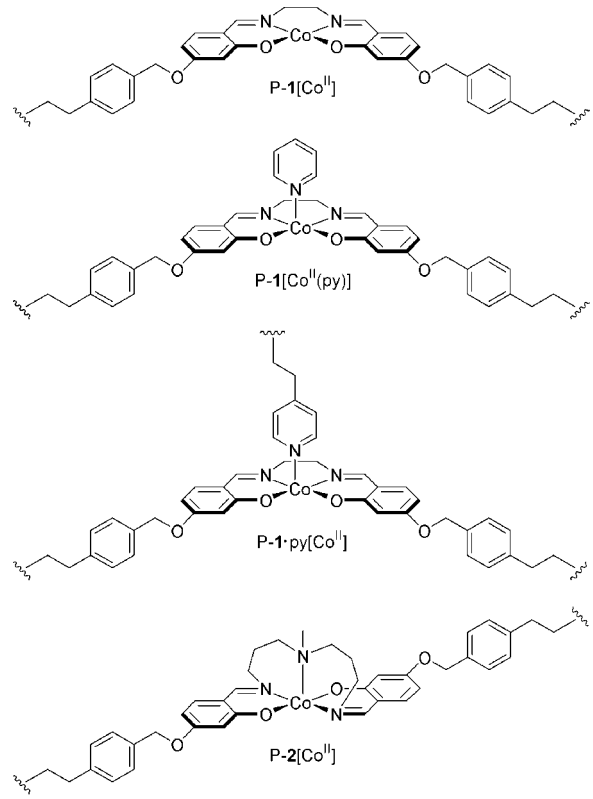

Figure 20. Models of the immobilized metal sites in P-**1**[Co^{II}], P-**1**[Co^{II}(py)], P-**1**•py[Co^{II}], and P-**2**[Co^{II}] catalysts.

different affinities at atmospheric pressure; the percentage of the Co sites binding O_2 increased in the order P-**1**[Co^{II}] (10%) < P-**1**[Co^{II}(py)] (60%) < P-**1**·py[Co^{II}], P-**2**[Co^{II}] (90%). The affinities of P-**1**·py[Co^{II}] and P-**2**[Co^{II}] for O_2 were high because they have immobilized sites containing the requisite five endogenous donors around the Co(II) ions required for O_2 binding. The oxidation was performed at various temperatures (35−80 °C) for 21 h in a 15-mL reactor with a catalyst/substrate/O_2 molar ratio of 1:80:800. All the catalysts afforded higher conversion and slightly lower selectivity to DTBQ in $scCO_2$ (CO_2 mole fraction: 0.979) than in acetonitrile and CO_2-expanded acetonitrile (CO_2 mole fraction: 0.695), regardless of the reaction temperature. This behavior implies that $scCO_2$, which is completely miscible not only with DTBP but also with O_2, enhanced the mass transfers in the porous network of the catalysts by virtue of its intrinsic low viscosity and high diffusivity. Comparison of the performance of the catalysts revealed that the high affinity of the Co sites for O_2 is a necessary prerequisite to achieve higher conversions. Thus, the conversions given by P-**1**·py[Co^{II}] and P-**2**[Co^{II}] were higher than that achieved with P-**1**[Co^{II}], regardless of the medium and reaction temperature. The reusability of P-**1**·py[Co^{II}] was also investigated at 50 °C in $scCO_2$, acetonitrile, and CO_2-expanded acetonitrile. In all the media, the catalyst gradually lost its activity and selectivity with recycling time. ICP analysis showed some loss of cobalt in the used catalyst, which could be one of the reasons for the relatively low reusability of the catalyst.

4.2. Enzyme Catalysis

Klibanov and co-workers applied mushroom polyphenol oxidase (tyrosinase) for the aerobic oxidation of *p*-cresol and *p*-chlorophenol in $scCO_2$.[53] The oxidations were performed at 36 °C and 34 MPa, and then CO_2 containing 2% O_2 was used. Although both static and flow systems afforded a *p*-cresol conversion of 70−80%, the flow system allowed the isolation of more catecholic product (4.8 vs 2.4%). The yield of 4-methylcatechol was low, because it easily underwent further oxidation to 4-methyl-*o*-benzoquinone and then smoothly polymerized under the conditions applied. The molecular weights of the polymerized products ranged from about 200 to 6500 with a maximum at ca. 300, indicating that the major products were dimers and trimers. It was suggested that 4-methyl-*o*-benzoquinone remained on the surface of wet polyphenol oxidase after its formation due to its low solubility in $scCO_2$, thereby undergoing the polymerization. *p*-Chlorophenol also polymerized in $scCO_2$ (22.5% based on the initial substrate) under otherwise similar conditions, while a trace amount (0.15%) of 4-chlorocatechol was detected. Although the polyphenol oxidase was relatively stable in the $scCO_2$−O_2 system, it gradually lost its activity in the presence of the substrates, that is, as the oxidation proceeded. The reason for this behavior was not clarified.

5. Oxidation of Alkenes

The oxidation of alkenes with peroxides or molecular oxygen is catalyzed by metal catalysts, yielding epoxides, alcohols, and carbonyl compounds.[54] The use of dense CO_2 as solvent seems to be promising, particularly when molecular oxygen is used as oxidizing agent, because it can eliminate the gas−liquid boundary, greatly enhancing the miscibility of alkenes and O_2. In contrast to the work reported so far on alcohol oxidations in dense CO_2, the oxidation of alkenes has mainly been performed with nonsupported, complex-type metal catalysts, which are termed "homogeneous" catalysts in conventional organic solvents. In compressed CO_2 media, however, complex catalysts often do not dissolve completely, and the oxidations are catalyzed only by a part of the added complex which is present in the dense CO_2 phase or by the surface of the precipitated complex.[1g] In the following, the examples of the use of complex catalysts and supported metal catalysts are separately introduced in the order of the year of publication.

Scheme 15. Generally Accepted Mechanism for the Molybdenum-Catalyzed Epoxidations

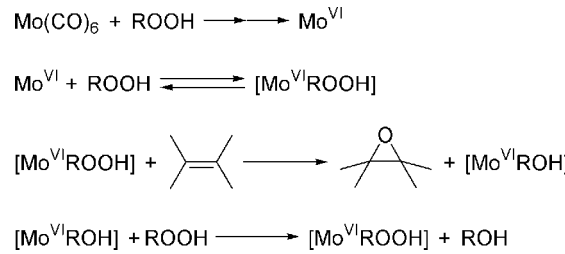

5.1. Metal Complex Catalysts

5.1.1. Molybdenum-Based Catalysts

5.1.1.1. $Mo(CO)_6$ Catalyst. This complex, $Mo(CO)_6$, catalyzes the epoxidation of alkenes with alkyl hydroperoxides not only in conventional organic solvents but also in $scCO_2$. The generally accepted reaction mechanism is depicted in Scheme 15. Early results of this oxidation in $scCO_2$ obtained by Noyori et al.,[55] Walther et al.,[56] and Tumas et al.[57] are comprehensively introduced in the former review.[1g] Noyori's group found that the epoxidation of 2,3-dimethyl-2-butene with cumene hydroperoxide proceeded at 85 °C and 22.7 MPa without producing cyclic carbonates.[1e,g,55] Walther and co-workers, on the other hand, reported that cyclooctene is epoxidized with *t*-BuOOH at 45 °C and a CO_2 pressure of 8.5 MPa in 100% selectivity with a TON of 27.[56] In contrast, the oxidation of cyclohexene with aqueous *t*-BuOOH at 95 °C in $scCO_2$ did not afford the corresponding epoxide but afforded 1,2-cyclohexanediol (73%), 2-cyclohexen-1-one (10%), and 2-cyclohexen-1-ol (10%).[57]

More systematic study was done by Haas and Kolis, who used *t*-BuOOH as oxidizing agent.[58] As shown in Table 8, the $Mo(CO)_6$−*t*-BuOOH−$scCO_2$ system was successfully applied for several alkenes. Particularly, cyclic alkenes tend to cleanly afford the corresponding oxidized products in high yields, indicating that the fixed two alkyl groups bearing the C═C bond carbons allow for an unhindered approach to the active Mo species. In addition, the electron-donation from the two alkyl groups would be important, because the Mo atom in the active species is highly oxidized and thus strongly electrophilic. It is noteworthy that $Mo(CO)_6$ could be recycled for numerous times without loss of its activity in the oxidation of cyclohexene. In contrast, acylic alkenes were less reactive, possibly due to their floppy side chains causing steric hindrance. The retardation of the oxidation rate by steric hindrance could be more clearly reflected in the difference in reactivity between *cis*-2-heptene (entry 5) and *trans*-2-heptene (no reaction under otherwise similar conditions). To elucidate the role of $scCO_2$ medium, the $Mo(CO)_6$-catalyzed oxidation of cyclohexene and 2-vinylnaphthalene was performed also in benzene or under solvent-free condi-

Table 8. Homogeneous Catalytic Oxidation of Alkenes Using $Mo(CO)_6$ Catalyst in $ScCO_2$ (Data Taken from Ref 58)[a]

entry	substrate	oxidant	subs:ox	temp. (°C)	time (h)	product yield/%
1		70% aq. *t*-BuOOH	1:1	95	3	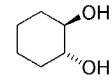 100
2		70% aq. *t*-BuOOH or 5.0–6.0 M *t*-BuOOH in decane	1:3	86	3	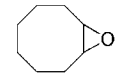 100
3		70% aq. *t*-BuOOH	1:3	92	3	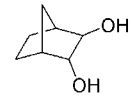 66
4	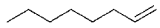	70% aq. *t*-BuOOH	1:3	103	4	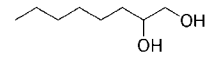 80
5	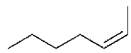	5.0–6.0 M *t*-BuOOH in decane	1:3	95	3	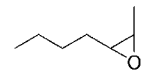 20
6	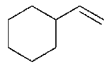	5.0–6.0 M *t*-BuOOH in decane	1:3	90	3	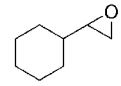 20
7	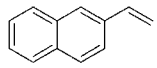	70% aq. *t*-BuOOH	1:3	92	3	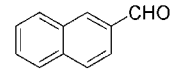 80
8	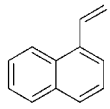	70% aq. *t*-BuOOH	1:3	92	3	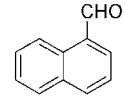 80
9	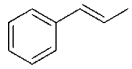	70% aq. *t*-BuOOH	1:3	90	3	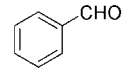 30
10	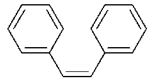	70% aq. *t*-BuOOH	1:3	95	3	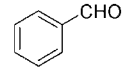 50

[a] All reactions were performed with 0.02 equiv of catalyst. 22 MPa of CO_2 was initially loaded into the reaction vessel at room temperature.

tions under the same time/temperature conditions, revealing that these media are inferior to $scCO_2$ in yield and selectivity. The uses of other catalysts such as $MoO_2(acac)_2$ and $VO(acac)_2$ were also attempted for the oxidation of cyclohexene in $scCO_2$, but the corresponding diol was obtained in trace amounts. Since these complexes were insoluble in $scCO_2$ in contrast to $Mo(CO)_6$, the authors concluded that catalyst solubility is a serious limitation in the catalytic system. Another interesting feature of the oxidations is that different oxidized products were obtained depending on the conditions and substrate. Diols were predominantly formed when the aqueous oxidant was used at higher temperature. It was proposed that the epoxides first formed were subsequently hydrolyzed by the water solvent of the oxidant and that the hydrolysis would be promoted by the acidic CO_2-H_2O environment. However, in several cases where the epoxide products were quite stable, further hydrolysis did not occur (e.g., entry 2). Temperature was found to also be a crucial reaction

Scheme 16. Oxidations with the (η^5-$Me_3SiC_5H_4$)MoO_2Cl Catalyst

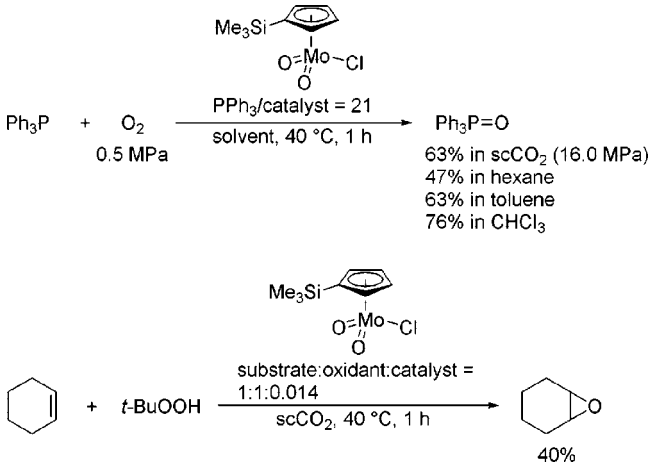

parameter. Thus, when the reaction was performed at a temperature above 100 °C, $Mo(CO)_6$ was converted into an inactive dark blue solid, which is most likely a reduced molybdenum oxide cluster. In addition, the epoxides underwent alcoholysis with the reduced oxidant, *t*-BuOH, at higher temperature. On the other hand, temperature below 75 °C led to no oxidation. Since $Mo(C_8H_{14})(CO)_5$ with easily dissociable C_8H_{14} ligand was in contrast active even at a much lower temperature of 65 °C, it was concluded that the dissociation of CO ligand from $Mo(CO)_6$, which is an initial step of the catalysis, requires a temperature above 75 °C.

5.1.1.2. (η^5-$Me_3SiC_5H_4$)MoO_2Cl Catalyst. Most metal complexes are used as homogeneous catalysts in conventional liquid solvents. However, this is not always the case in $scCO_2$, which shows high solubilizing power only for nonpolar, nonionic, and low molecular weight compounds. To increase the solubility of complexes, several methods have been developed, including the use of cosolvents, surfactants, and ligands bearing fluorinated alkyl groups.[1g] The ligand modification with fluorinated group is, however, usually difficult and expensive. Montilla and co-workers found that the introduction of a $-SiMe_3$ (TMS) group as a substituent at the cyclopentadienyl ligand also enhances the solubility of the corresponding complexes in $scCO_2$ without changing the parent reactivity.[59] Thus, (η^5-$Me_3SiC_5H_4$)MoO_2Cl catalyst was applied for the aerobic oxidation of PPh_3 and the oxidation of cyclohexene with *t*-BuOOH in $scCO_2$ (Scheme 16). The results obtained in $scCO_2$, however, were not always better than those obtained in conventional solvents. Further reactions must be explored to make the best use of this newly designed catalyst in $scCO_2$.

5.1.2. Vanadium- and Titanium-Based Catalysts

Tumas' group reported results of the vanadium and titanium complex-catalyzed epoxidation of alkenes with *t*-BuOOH in liquid CO_2.[57] These epoxidations were typically performed below room temperature in organic solvents, owing to the lower selectivity at higher temperatures, and hence, $scCO_2$ (critical temperature 30.9 °C) was not applied. Both allylic and homoallylic alcohols with alkyl group-substituted olefin moieties were selectively converted to the corresponding epoxides (conversions >96%, selectivity from 85 to >99%), when 0.42 mM substrate was treated with 100 mM decane-dissolved *t*-BuOOH and 1.47 mM $VO(OPr^i)_3$ catalyst in liquid CO_2 at 25 °C for 24 h. The reagents then

Scheme 17. Katsuki–Sharpless Epoxidation in Liquid CO_2

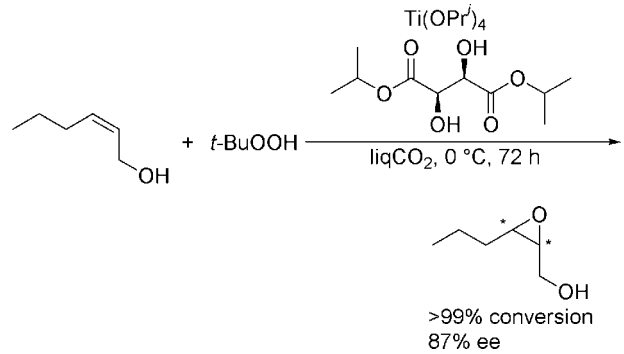

Scheme 18. Pd(II)-Catalyzed Wacker-Type Acetalization of Acrylate Esters to Acetals in $ScCO_2$

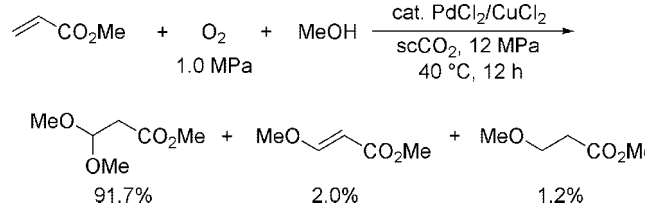

completely dissolved in liquid CO_2. The trends of reaction results in liquid CO_2 were parallel to those observed in conventional organic solvents; activated alkenes react faster than simple alkenes, and allylic alcohols react faster than homoallylic alcohols. However, the epoxidation in liquid CO_2 does not always take place with the same rate as in conventional solvents. Another kinetic study performed with 42 mM of (*Z*)-non-3-en-1-ol at 24 °C using 100 mM of *t*-BuOOH and 1.47 mM of the vanadium catalyst revealed that the rates increased in the order *n*-C_6H_{14} (relative rate 0.3) < CCl_4 (0.6) < CO_2 (1.0) < PhMe (1.9) < MeCN (2.0) < CH_2Cl_2 (3.3), respectively.

The Katsuki–Sharpless epoxidation[60] could also be achieved in liquid CO_2. Thus, at 0 °C, (*E*)-hex-2-en-1-ol could be epoxidized enantioselectively to afford the corresponding product in 87% ee at >99% conversion, although the conditions were not optimized (Scheme 17).

5.1.3. Palladium(II) Chloride

The Pd(II)-catalyzed aerobic oxidation of terminal alkenes in the presence of CuCl is known as Wacker oxidation, which yields the corresponding aldehydes.[61] When this oxidation is performed with alcohols, acetals can be obtained in a "one-pot" pathway. Jiang's group found that this type of reaction takes place efficiently in $scCO_2$.[62] For example, treatment of methyl acrylate (5 mmol) with O_2 (1.0 MPa) and methanol (24.7 mmol) in the presence of 3 mol % $PdCl_2$ and 0.4 equiv of $CuCl_2$ at 40 °C for 12 h in $scCO_2$ (12 MPa) resulted in the formation of the corresponding acetal in 91.7% yield (Scheme 18). These CO_2 and O_2 pressures were optimized ones, because lower pressures led to decreased conversion and selectivity. $PdCl_2(MeCN)_2$ could also be used as catalyst but afforded a slightly lower oxidation rate. Note that different from the usual Wacker-type oxidations, $CuCl_2$ was used as cocatalyst here instead of CuCl, affording, in some cases, even better results.

Jiang's group later used polystyrene-supported benzoquinone (denoted PS–BQ) as cocatalyst instead of conventional copper chlorides.[63] Representative results are shown in Table 9. The $PdCl_2$/PS–BQ catalytic system functioned

Table 9. Wacker-Type Acetalization of Various Alkenes with Methanol Using $PdCl_2$/PS−BQ Catalyst in $ScCO_2$ (Data Taken from Ref 63)[a]

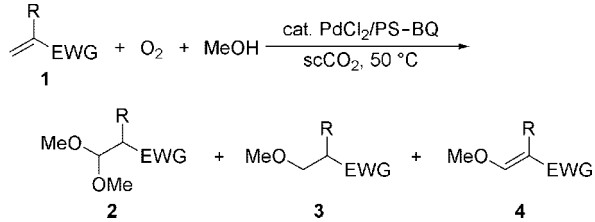

entry	1	total pressure (MPa)	conversion (%)	yield of 2[b] (%)	yield of 3[b] (%)	yield of 4[b] (%)
1	CO_2Me	10	99.8	95.5	0.5	3.1
2	CO_2Et	10	100	84.5	0	9.1
3	CO_2Bu-*n*	8	78.9	77.8	0	1.1
4[c]	CO_2Me	8	0	0	0	0
5	CO_2H	9	0	0	0	0
6	CN	9	100	79.1	0	0
7[c]	$CONH_2$	8	0	0	0	0
8	COMe	8	100	76.8	13.4	0

[a] Reaction conditions: $PdCl_2$, 0.15 mmol (3 mol %); PS−BQ, 2 mmol; **1**, 5 mmol; O_2, 0.5 MPa; methanol, 25 mmol; reaction time, 12 h. [b] Determined by GC. [c] Reaction time, 24 h.

Table 10. Wacker Oxidation in Various Reaction Media (Data Taken from Ref 66)[a]

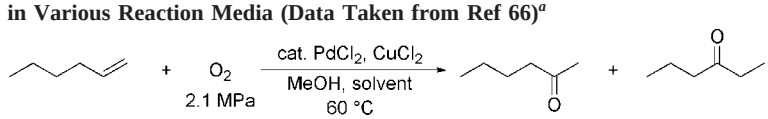

entry	solvent	pressure (MPa)	conversion (%)	selectivity to 2-hexanone (%)
1	$scCO_2$	12.5	98.9	70.5
2	$scCO_2$-[bmim][PF_6]	12.5	98.2	91.9
3	[bmim][PF_6]		97.0	64.2
4	no solvent		99.9	63.2

[a] Reaction conditions: volume of the stainless-steel reactor, 18 mL; 1-hexene, 1 mL; $PdCl_2$, 0.032 g; $CuCl_2$, 0.25 g; MeOH, 2 mL; reaction time, 17 h.

very well in $scCO_2$, and the yields of the desired acetal were comparable to or even higher than those obtained with the $PdCl_2/CuCl_2$ catalytic system. In contrast to copper chlorides, which generate HCl during the reaction, benzoquinone does not afford any strong acids or bases, thereby allowing us to perform the acetalization of $CH_2{=}CHCO_2R^1$ with R^2OH, giving $(R^2O)_2CHCH_2CO_2R^1$ without causing transesterifications (entries 2 and 3). In addition, by supporting it on a polystyrene matrix, the workup process becomes much simpler. The performance of $PdCl_2$/PS−BQ catalyst, however, was greatly influenced by the steric hindrance of substrates (entry 1 vs entries 2 and 3; entry 4). It is noteworthy that acrylonitrile also underwent the Wacker-type acetalization in an excellent selectivity (entry 6).

Dense CO_2−ionic liquid (denoted IL) systems afford unique reaction media, owing to the fact that ILs dissolve a large amount of CO_2, whereas dense CO_2 does not dissolve ILs.[64] These properties allow us to perform highly efficient hydrogenation with molecular hydrogen and, possibly also, aerobic oxidations using metal complex catalysts which are insoluble in $scCO_2$ but soluble in ILs.[65] In addition, it is also attractive that selective extraction of organic compounds (i.e., substrates and products) is possible by just exposing the product mixture to dense CO_2 flow, which, on the other hand, leaves the ILs containing the catalysts in the reactor.[64,65] Han and co-workers performed the selective Wacker oxidation of 1-hexene to 2-hexanone by employing the $scCO_2$−1-*n*-butyl-3-methylimidazolium hexafluorophosphate (denoted [bmim][PF_6]) medium.[66] As can be seen in Table 10, the mixed $scCO_2$−[bmim][PF_6] afforded significantly higher selectivity compared to $scCO_2$, [bmim][PF_6], and solventless conditions. Since $PdCl_2$ and $CuCl_2$ are insoluble in $scCO_2$,

Scheme 19. Aerobic Oxidation of Styrene Catalyzed by $PdCl_2$ in a $ScCO_2$−PEG System in the Presence or Absence of CuCl

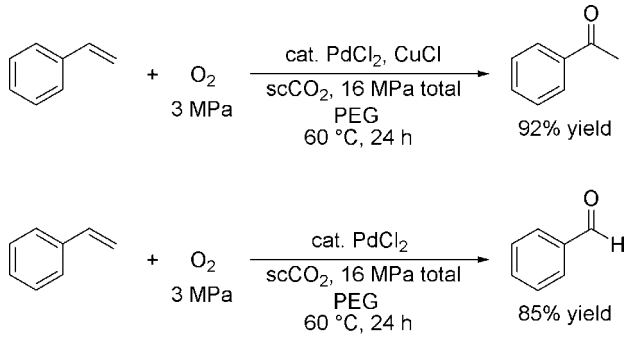

they would stay in the CO_2-expanded [bmim][PF_6], while 1-hexene could exist in both the CO_2-expanded IL and dense CO_2 phase. The low concentration of 1-hexene in the vicinity of the Pd and Cu salts thus realized would suppress the undesirable double-bond migration to 2-hexene which leads to the formation of 3-hexanone. In addition, the contact of 1-hexene with the salts would further be reduced by the lower viscosity of the IL dissolving CO_2. Thus, higher CO_2 pressure is expected to give higher selectivity, and this was actually observed. The six-time reuse of the $PdCl_2$ and $CuCl_2$ in $scCO_2$−[bmim][PF_6] by employing the extraction of the product mixture with dense CO_2 showed that the conversion and selectivity dropped monotonously, although the decrease was not significant. Elemental analysis revealed that the extracted samples did not contain Pd and Cu. Hence, the Pd and Cu salts would be gradually deteriorated during the reaction.

He and co-workers found that the $scCO_2$−PEG system acts as an efficient medium for the $PdCl_2$-catalyzed aerobic oxidation of styrene.[67] The reaction was typically performed at 60 °C for 24 h in a 25-mL reactor, employing 2.6 mmol of styrene, 3 MPa O_2, 2 mL of PEG-300, 27 mg of $PdCl_2$, and, if necessary, 200 mg of CuCl. The oxidation selectivity could be switched with CuCl; under the optimized conditions, the presence of CuCl led to the formation of acetophenone in 92% yield, while its absence resulted in the formation of benzaldehyde in 85% yield (Scheme 19). Although the phase behavior was not reported, the reaction mixture would be composed of two phases, i.e., a PEG-rich phase (CO_2-expanded PEG) and a CO_2-rich phase. The $PdCl_2$ catalyst and CuCl promoter would mainly stay in the CO_2-expanded PEG phase, whereas styrene and the product carbonyl compounds were present in both phases. The merit of using a $scCO_2$−PEG medium could be seen in the results obtained in other media, such as $scCO_2$, PEG, $scCO_2$−H_2O, $scCO_2$−MeOH, and $scCO_2$−PEG−H_2O, which afforded much lower product yields. In addition, the effect of changing the CO_2 pressure revealed that the optimal CO_2 pressure was 16 MPa, indicating that the use of dense CO_2 has a beneficial effect on the catalysis. Under otherwise similar conditions except for the lowered O_2 pressure (2 MPa), the $PdCl_2$−CuCl−$scCO_2$−PEG catalytic system was also successfully applied for the oxidation of other substrates such as *p*-methylstyrene, *p*-chlorostyrene, *p*-methoxystyrene, 1-octene, and 1-hexene, yielding the corresponding methyl ketone in 87, 72, 85, 58, and 99% yield, respectively. The role of PEG was suggested to stabilize the Pd catalyst, because no significant loss of the activity was observed for at least five-time reuses. This was also attributed to the least

Scheme 20. $PdCl_2$-Catalyzed Aerobic Oxidation of Terminal Alkenes with Electron-Withdrawing Groups in the Presence of Methanol in $ScCO_2$

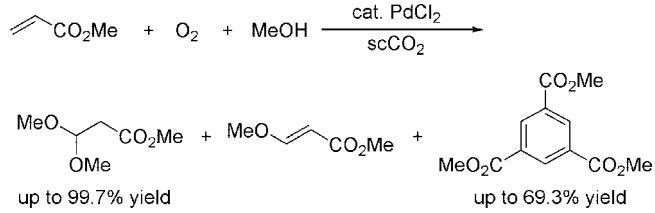

loss of the Pd species during the workup procedures; the reactants and products could be selectively extracted from the product mixture by using dense CO_2 (20 MPa, 50 °C), leaving the PEG phase containing the inorganic complexes which were used for the subsequent reaction.

Jiang et al. performed the $PdCl_2$-catalyzed aerobic oxidation of terminal alkenes with electron-withdrawing groups in $scCO_2$.[68] Methyl acrylate was converted into a dimethoxy-adduct, a monomethoxy-adduct, and a 1,3,5-trisubstituted benzene as shown in Scheme 20. Although the monomethoxy-adduct was usually formed in trace amounts, the other two products were given in synthetically satisfactory yields under optimized conditions. Thus, treatment of 5 mmol of methyl acrylate with 0.15 mmol of $PdCl_2$, 1.0 MPa of O_2, and 25 mmol of methanol in 14 MPa of CO_2 at 50 °C for 15 h in a 25-mL autoclave yielded the dimethoxy-adduct in almost quantitative yield, while changing the catalyst amount, O_2 pressure, CO_2 pressure, temperature, and reaction time to 0.25 mmol, 0.7 MPa, 20 MPa, 120 °C, and 32 h, respectively, resulted in the formation of the benzene derivative in 69.3% yield (Scheme 20). As a trend, higher CO_2 pressure, lower O_2 pressure, and higher reaction temperature favored the formation of the trisubstituted benzene, whereas the opposite tendency was observed for the formation of the dimethoxy-adduct. Interestingly, methanol was the best cosolvent also for the formation of trisubstitued benzene. One crucial role of methanol is the enhancement of the solubility of $PdCl_2$ in apolar dense CO_2. However, the alcohol also serves as promoter in other ways, because the combined use of other conventional liquid solvents with $scCO_2$, which also could increase the solubility of $PdCl_2$, resulted in worse results. The $PdCl_2$−O_2−MeOH−$scCO_2$ catalytic system was also successfully applied for other alkyl acrylates and also for methyl vinyl ketone, similarly yielding either dimethoxy acetals or trisubstituted benzene in moderate to high yields under optimal conditions.

5.1.4. Iron-Based Catalysts

Tumas' group used iron porphyrin catalysts for the aerobic oxidation of cyclohexene in $scCO_2$.[69] The oxidation was typically performed in an 18-mL batch reactor, using a catalyst (2−3 mg), 0.5 mL of cyclohexene, 3.4 MPa air, and CO_2 at 80 °C and a total pressure of 34 MPa. The catalysts possessed fluorinated phenyl rings to enhance their solubility in $scCO_2$, and they yielded several oxidation products as shown in Scheme 21. Compared to organic solvents such as benzene and CH_2Cl_2, $scCO_2$ afforded a much lower oxidation rate but different product selectivity (Table 11). The features observed for dense CO_2 medium involve the much cleaner products and higher selectivity to cyclohexene oxide, particularly when Fe(TPFPPBr$_8$)Cl catalyst was used (up to 34%). These benefits are related to the inertness of CO_2 under the oxidative conditions, because additional solvent-derived

Scheme 21. Products Observed during the Fe(TPFPP)Cl- and Fe(TPFPPBr$_8$)Cl-Catalyzed Aerobic Oxidations of Cyclohexene

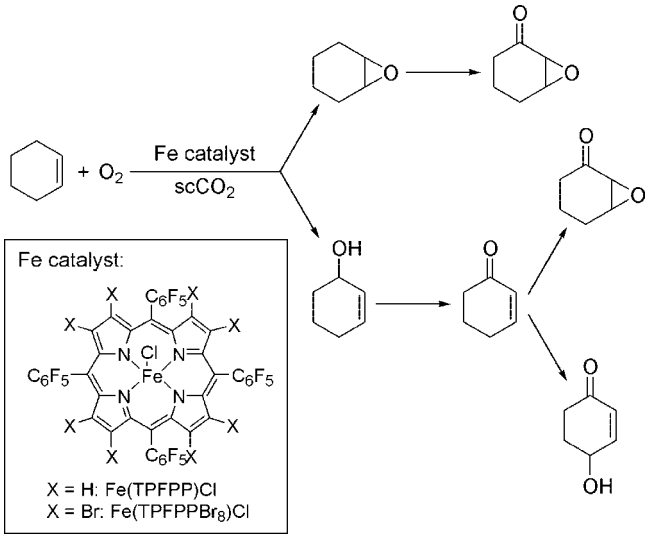

products were formed in organic solvents, where various free radicals, including those formed from solvent molecules, were present in significant amounts. It was proposed that either free radical propagation reactions are slower or termination reactions are faster in scCO_2 than in organic solvents. Degradation of the catalysts was also more significant in organic solvents than in scCO_2, which would be similarly driven by the various free radicals in large amounts. The catalysts were, however, deteriorated also in scCO_2 during the oxidation, and Fe(TPFPP)Cl was found to be inferior to Fe(TPFPPBr$_8$)Cl in stability. The authors attempted to explain the difference in product selectivity under different conditions from a viewpoint of reaction mechanism. However, a clear explanation was not given due to the very complex mechanism, which involves the decomposition of *in situ* generated peroxide and iron porphyrin-mediated epoxidation.

Porphyrin-free iron catalyst was also tested for the aerobic oxidation of cyclohexene in scCO_2. Sahle-Demessie and coworkers investigated the performance of *cis*-[Fe(DMP)$_2$(H$_2$O)$_2$](CF$_3$SO$_3$)$_2$ catalyst.[70] The oxidation was performed in a 500-mL batch reactor equipped with a spinning dynamic basket in which catalyst was loaded. Ten milliliters of substrate and 0.55−20 MPa of O_2 were used, and CO_2 was added until the total pressure reached 20.7 MPa at the reaction temperature (60 or 100 °C). Lower O_2 concentration, higher reaction temperature, and shorter reaction time tended to afford higher conversion. Thus, a maximum conversion (3.98%) could be achieved in 6 h when the reaction was performed at 100 °C with an O_2 pressure of 0.55 MPa (Scheme 22). Note that 2-cyclohexen-1-one was predominantly formed not only under these conditions but also under all the conditions applied. The authors also tested heterogeneous catalysts such as 0.5% Pd/Al$_2$O$_3$ and 0.5% Pt/Al$_2$O$_3$ for the same oxidation, but the major products were benzene and phenol, indicating that cyclohexene undergoes dehydrogenation rather than oxidation over these catalysts. However, the results obtained only with 0.48 MPa of O_2 at 100 °C were shown. The selectivity to oxygenated products would probably increase even with the supported metal catalysts if a higher O_2 concentration were applied.

Koda's group investigated the kinetics of the oxidation of cyclohexene using the Fe(TPFPP)Cl catalyst.[71] The reaction was typically carried out at 50 °C for 8 h in a 2.7-mL reactor using 120 μL of cyclohexene, 56 μg of catalyst, 1.65 equiv of O_2 to the substrate, and dense CO_2 at a total pressure of 16.7 MPa. Under these conditions, 2-cyclohexen-1-hydroperoxide, C$_6$H$_9$OOH, as well as the products observed by Tumas's group (Scheme 21)[69] was also detected. The most prominent product was 2-cyclohexen-1-one. The effect of changing the O_2 concentration was investigated in the O_2/substrate range 0.43−2.06, revealing that the total product yield and the selectivity to each product were almost independent of this ratio. Thus, the great miscibility of O_2 in scCO_2 cannot be beneficial in this case, although the use of the CO_2 medium leads to the prevention of possible explosion. On the other hand, the total product yield was found to be dependent on the initial cyclohexene concentration with ca. second order, when the substrate amount was changed in the range 30−150 μL. Hence, the following kinetics was proposed for the conditions applied:

$$\text{reaction rate} \propto [\text{cyclohexene}]^2[\text{catalyst}]^{\leq 1}[O_2]^0$$

The oxidation was retarded in the presence of a radical inhibitor (2,6-di-*tert*-butyl-4-methylphenol), indicating that the oxidation principally took place by the radical chain reaction mechanism.

Table 11. Homogeneous Catalytic Oxidation of Cyclohexene Using Iron Porphyrin Catalysts: Comparison of Activity and Selectivity in Different Reaction Media (Data Taken from Ref 69)[a]

entry	catalyst	solvent	selectivity (%)					TON	conversion (%)
							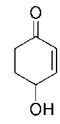		
1	TPFPP	CO_2	17	5.5	38	38	1.6	350	9.0
2	TPFPP	benzene/N_2	6.1	5.1	51	27	11	1320	32
3	TPFPP	CH_2Cl_2/N_2	21	4.0	40	29	5.7	1340	38
4	TPFPPBr$_8$	CO_2	34	5.2	35	23	1.9	580	8.9
5	TPFPPBr$_8$	benzene/N_2	8.8	6.8	50	24	10	1520	20
6	TPFPPBr$_8$	CH_2Cl_2/N_2	16	9.2	45	25	5.3	2170	29

[a] All reactions were run at 80 °C and a total pressure of 34 MPa for 12 h using 3.4 MPa of air.

Scheme 22. Aerobic Oxidation of Cyclohexene Catalyzed by *cis*-[Fe(DMP)$_2$(H$_2$O)$_2$](CF$_3$SO$_3$)$_2$

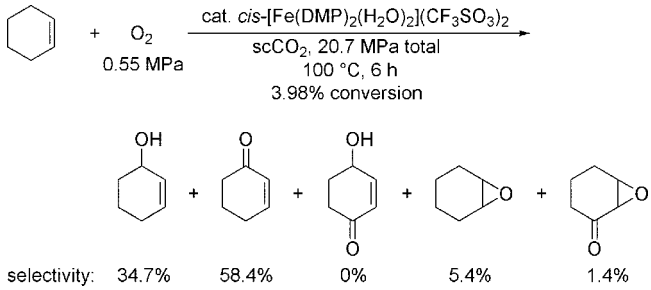

5.1.5. Manganese-Based Catalysts

Campestrini and Tonellato found that hexafluoroacetone hydrate-catalyzed epoxidation of alkenes is remarkably accelerated by using an appropriate manganese porphyrin complex and $scCO_2$ as additional catalyst and reaction medium, respectively.[72] The crucial role of the Mn complex could be seen in the initial test performed at 40 °C and a total pressure of 20.0 MPa in a 10-mL stainless-steel reactor, using 3.80×10^{-2} M cyclooctene, 0.22 M H_2O_2, 3.38×10^{-3} M 4-*tert*-butylpyridine, 3.60×10^{-2} M $(CF_3)_2CO \cdot 3H_2O$, and 1.28×10^{-4} M Mn(TDCPP)Cl. The epoxide yield under the given conditions reached ~70% in 470 min, while in the absence of Mn(TDCPP)Cl the yield dropped to ~20%. On the other hand, the merit of using $scCO_2$ medium was demonstrated by comparing the results with those obtained in *n*-hexane, which in contrast afforded higher epoxide yield in the absence of the Mn complex in the same reaction time (~67%; ~28% with Mn(TDCPP)Cl). The reaction mixture was heterogeneous in the nonpolar *n*-hexane, which has a dielectric constant close to that of $scCO_2$, and thus, the mixture in $scCO_2$ would be also heterogeneous. The heterogeneous conditions are unfortunately not beneficial for the epoxidation, because the use of $CHCl_3$ solvent rendering the mixture homogeneous resulted in a much higher epoxidation rate under otherwise similar reaction conditions (100% yield in 30 min). Under the conditions of the initial test with $scCO_2$, except for the lowered 4-*tert*-butylpyridine concentration (1.69×10^{-2} M), the concentrations of the reagents other than the Mn complex were modified to see the effects on the catalysis. The concentration of 4-*tert*-butylpyridine was changed in the range 3.38×10^{-3}–3.38×10^{-2} M, revealing that the epoxide yield reached a maximum at 1.69×10^{-2} M. The nitrogen base binds to Mn of the complex as an axial ligand, resulting in the formation of a more effective catalyst. Hence, a larger concentration of the base would accelerate the reaction. However, addition of an excess amount of the base inhibits the alkene epoxidation, because the base competes with the alkene for the oxidant. On the other hand, a monotonous increase in the epoxidation rate was observed with an increase in the concentration of hexafluoroacetone hydrate in the range 7.2×10^{-3}–0.144 M, indicating that $(CF_3)_2C(OH)OOH$ formed by the addition of H_2O_2 to hexafluoroacetone served as an oxygen-transferring agent for cyclooctene and/or the Mn complex. The effect of changing the H_2O_2 concentration was much more difficult to explain, although the higher concentration seems to favor the epoxidation (97% yield at 0.44 M; 49% yield at 0.11 M). Finally, the wall of the stainless-steel reactor was found to cause the unfavorable decomposition of H_2O_2, because the use of a Teflon-coated reactor gave a higher epoxidation rate. Thus, under the best conditions, which also include the use of a Teflon-coated reactor, a maximum yield of 98% could be achieved in $scCO_2$.

5.2. Supported Metal Catalysts

5.2.1. Catalytically Active Wall of a Stainless-Steel Reactor

It sometimes happens that the wall of a stainless steel reactor can act as a catalyst or a promoter. In some cases, even synthetically satisfactory results can be obtained with such "unusual" concepts. Loeker and Leitner found that the aerobic oxidation of alkenes to the corresponding epoxides using aldehyde as co-oxidant takes place smoothly in a stainless steel reactor.[73] The use of a stainless-steel reactor was crucial, because, for instance, the oxidation of *cis*-cyclooctene in toluene hardly proceeded in a normal glass flask, whereas the same reaction in a stainless-steel reactor resulted in high conversion. Selected results are shown in Table 12, which indicates that this uncommon catalytic system is effective particularly for internal alkenes and long-chain terminal alkenes. For some alkenes, the choice of co-oxidant aldehyde was also crucial (entry 4). Epoxidation of the double bonds bearing aromatic rings was unsuccessful, but indene afforded some other oxidation products. Although toluene solvent afforded higher conversion than $scCO_2$ for the oxidation of (*R*)-(+)-limonene, other substrates underwent epoxidation much faster in $scCO_2$ than in toluene. The complete miscibility of substrates as well as O_2 in $scCO_2$ would account for the higher oxidation rate in $scCO_2$. It is also notable that the product mixture is relatively clean when $scCO_2$ was used as solvent due to the inertness of CO_2 toward oxidative conditions, whereas the use of toluene solvent led to the formation of significant amounts of benzaldehyde, benzyl alcohol, benzyl hydroperoxide, and benzoic acid, which are the oxidation products of toluene. A brief kinetic study of the stainless-steel-promoted oxidation of *cis*-cyclooctene in $scCO_2$ revealed a significant induction period, which is typical for the mechanism involving acylperoxy radicals (Scheme 23).

5.2.2. Supported Palladium

Beckman performed batchwise production of H_2O_2 from H_2 and O_2 over a 0.47% Pd supported on titanium silicate, TS-1 (1.6% Ti), catalyst and applied the *in situ* generated oxidant for the epoxidation of propylene.[74] Typically, the reaction was performed in a 4×10^{-5}-m^3 stainless-steel reactor at 45 °C for 4.5 h with 4 mM propylene, 1.26 mM H_2, 8.3 mM O_2, and compressed CO_2 or N_2 (13.1 MPa total). Three solvent systems, CO_2, MeOH–H_2O–CO_2 (MeOH/H_2O = 75/25; 1.0×10^{-5} m^3), and MeOH–H_2O–N_2 (MeOH/H_2O = 75/25; 1.0×10^{-5} m^3), were employed, and the highest selectivity of 94.3% at a conversion of 7.5% was achieved in dense CO_2 without protic solvents. The amount of catalyst was 0.2998 g, below which the selectivity decreased. The use of MeOH and H_2O in dense CO_2, on the other hand, afforded additional solvent-derived byproducts, lowering the selectivity. This was consistent with the former observation by Baiker et al. (see section 5.2.3.1). Changing the dense CO_2 to N_2 gas further lowered the selectivity, which could be attributed to the lower solubility of reactant gases (propylene, O_2, and H_2) in the N_2-expanded liquid than in the CO_2-expanded liquid.

5.2.3. Supported Multi-Metals

5.2.3.1. Titanium Silicate-Supported Pd and Pt Catalysts. Supported Pd–Pt catalysts promote the formation of H_2O_2

Table 12. Aerobic Epoxidation of Alkenes Using 2-Methylpropionaldehyde in the Presence of Stainless Steel (Data Taken from Ref 73)[a]

entry	substrate	solvent	conversion (%)	product	selectivity (%)	runs
1		$scCO_2$	95–99.6	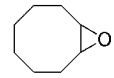	>99	15
2		toluene	50–84	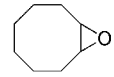	>99	4
3		$scCO_2$	95		91	1
4[b]		$scCO_2$	26		94 (6[c])	1
5	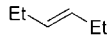	$scCO_2$	96	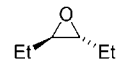	>98	1
6	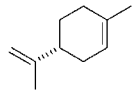	$scCO_2$	30–51	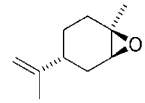	59–60 (30–32[d]) (9–10[e])	2
7	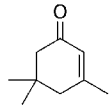	$scCO_2$	16	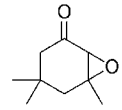	30	1

[a] Reaction conditions: reaction temperature, 55 °C; volume of the stainless-steel reactor, 100 mL; substrate, 2.50 mmol; O_2, 25.0 mmol; aldehyde, 5.00 mmol; CO_2, 75 g. [b] 2,2-Dimethylpropionaldehyde was used as co-oxidant. [c] Selectivity to 3,4-epoxyoctane. [d] Selectivity to *trans*-1,2-epoxylimonene. [e] Selectivity to *cis*- and *trans*-8,9-epoxylimonene.

Scheme 23. Plausible Reaction Mechanism of the Aerobic Epoxidation of Alkenes over the Wall of the Stainless Steel Reactor in the Presence of an Aldehyde as Co-oxidant

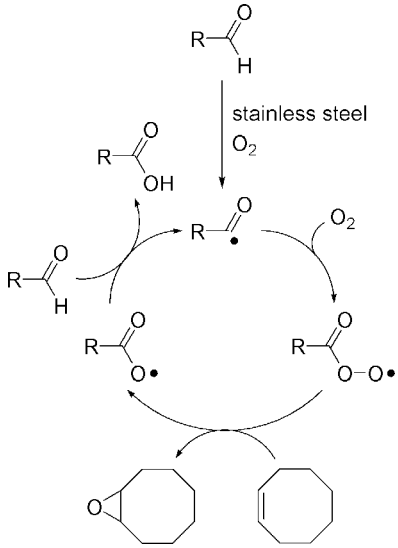

from a mixture of H_2 and O_2. This can be the initial step of several oxidations. Baiker and co-workers prepared Pd- and Pt-doped TS-1 (Si/Ti = 40) and applied it for the continuous catalytic oxidation of propylene to propylene oxide.[75] The reaction is shown in Scheme 24 with the main byproducts detected. Typically, the oxidation was performed with 3.8 g of the catalyst, employing the reactant upstream composed of propylene (18.7 mol %), O_2 (7.2 mol %), H_2 (4.6 mol

Scheme 24. Oxidation of Propylene with H_2 and O_2 over Pd−Pt/TS-1 Catalyst

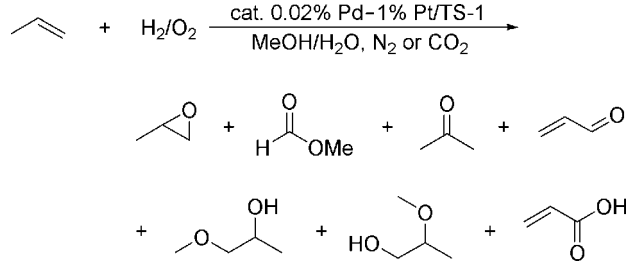

%), methanol (23 mol %), water (13.2 mol %), and N_2 (33.3 mol %). Under these conditions, a significant drop of propylene oxide yield was observed with time-on-stream. Surface analysis of the spent catalysts revealed the formation of both volatile and nonvolatile byproducts. It was proposed that formic acid, which was also a byproduct from methanol solvent, further promoted many side reactions, including the oligomerization of volatile products. The resultant nonvolatile organic compounds would gradually block the catalyst pores, resulting in the decrease in epoxidation rate. Intriguingly, replacement of N_2 gas diluent with CO_2 under otherwise similar conditions led to an increased propylene oxide yield, and the yield could be further improved by increasing CO_2 pressure from 5 to 12 MPa (supercritical state) by 20 relative %. The authors attributed this favorable effect of $scCO_2$ to the enhanced mass transfer, resulting in higher concentration of the reactant in the vicinity of active sites; however, this would not be the sole reason. Additional studies including

Scheme 25. Oxidation of Styrene with H_2O_2 over Supported Pd and Au Catalysts

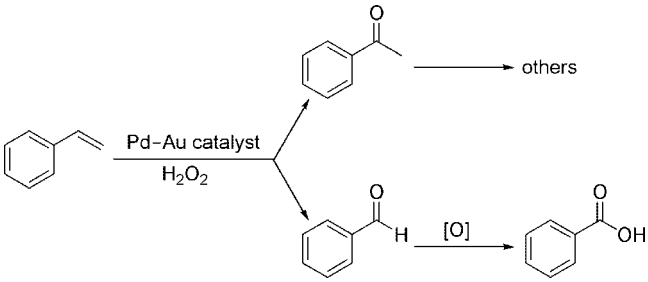

phase behavior observation would be necessary for a better understanding of the CO_2 pressure (density) effect.

5.2.3.2. Alumina-Supported Pd and Au Catalysts. Wang et al. observed that Pd- and Au-doped alumina promotes the oxidation of styrene with H_2O_2, giving acetophenone in high selectivity.[76] The metal deposition was achieved by an impregnation method from the aqueous solution of $HAuCl_4 \cdot 3H_2O$ and $PdCl_2$, and the final calcination temperature was 400 °C. The oxidation of styrene was typically carried out at 120 °C for 3 h in a 50-mL reactor, using 0.4 g of catalyst, 1 mmol of styrene, 4 mmol of H_2O_2, and 9 MPa of CO_2. The products are shown in Scheme 25. Under these conditions, 2.5% Pd- and 2.5% Au-doped alumina exhibited the highest selectivity to acetophenone (87%) at reasonable conversion (68%), while 5% Au/Al_2O_3, 5% Pd/Al_2O_3, and 2.5% Pd/Al_2O_3 afforded 35, 81, and 83% selectivity at 4, 54, and 53% conversion, respectively, indicating that Au atoms are not active sites but assist the Pd catalysis. Similarly, *p*-methylstyrene and 3-nitrostyrene were also converted to the corresponding ketones in 88 and 61% selectivity at 79 and 55% conversion, respectively. In the reaction of 3-nitrostyrene, a relatively large amount of 3-nitrobenzaldehyde was formed. Both 2.5% Pd and 2.5% Au were loaded also on other supports such as ZrO_2, CeO_2, SiO_2, and TiO_2 and tested in the oxidation. However, the yields of acetophenone were lower than that obtained with alumina. The effect of changing CO_2 pressure was investigated in the range 0−16 MPa. The conversion increased from 53 to 69% when the pressure was increased from 0 to 4 MPa, indicating that the presence of CO_2 enhances the reaction rate. However, the conversions were almost constant above 4 MPa. On the other hand, the selectivity to acetophenone increased with CO_2 pressure, reaching a maximum at 9 MPa (87%). Below 9 MPa, the selectivity to acetophenone decreased due to the increased selectivities to benzaldehyde and others, while the pressure above 9 MPa promoted the formations of benzaldehyde and benzoic acid, lowering the selectivity to acetophenone. The effect of temperature was also investigated in the range 90−130 °C, revealing that higher temperature favors the acetophenone formation. Unfortunately, the reusability of the 2.5% Pd−2.5% Au/Al_2O_3 catalyst was low; both conversion and selectivity dropped significantly after the first run. The authors did not clarify the reason for the catalyst deactivation.

6. Oxidation of Alkanes Including Alkylaromatic Compounds

The aerobic oxidation of alkanes is more difficult than those of alcohols and alkenes due to their lower reactivity. However, in the presence of a proper catalyst and an oxidant, alkanes undergo oxidations at relatively low temperatures, but still exceeding 100 °C. The temperatures required are thus far beyond the critical temperature of CO_2 (30.9 °C). Since extremely high pressures are required to obtain liquid-like CO_2 densities at such high temperatures,[1g] CO_2 in a gaslike state with lower density has been applied as diluent gas rather than as solvent for the oxidation of alkanes. The volatility of alkanes, however, increases with temperature, and thus, in most cases, alkanes, O_2, and CO_2 formed a single homogeneous phase under the reaction conditions applied. Most oxidations have been performed using molecular oxygen as oxidant, though a few examples on the use of diluted peroxides are known. Solids as well as metal complex catalysts have been applied, but solid catalysts seem to be more appropriate, because complexes encounter the solubility problem at lower CO_2 densities.[1g] In addition, the high temperatures could decompose metal complexes, most of which are thermally unstable. In the following, we consider examples of alkane oxidations in high-pressure CO_2.

6.1. Catalyst-Free Autocatalytic Aerobic Oxidations

Catalyst-free aerobic oxidation of cyclohexane to cyclohexanone and cyclohexanol in $scCO_2$ has been investigated by Srinivas and Mukhopadhyay.[77] Although this oxidation appears to be out of the scope of the present review focusing on the use of catalysts, it was assumed that the oxidation takes place by "autocatalytic" free-radical mechanisms under the conditions applied (Scheme 26). The oxidation in $scCO_2$ was carried out in a microreactor (low carbon, stainless steel; internal diameter 16 mm) with 10 mol % cyclohexane, 10 mol % O_2, and 80 mol % CO_2 at 137, 150, or 160 °C and 17.0 or 20.5 MPa. The mixture formed a single homogeneous phase at the start of the reaction, regardless of the temperature and pressure applied. However, the mixture became cloudy as the reaction proceeded, indicating the occurrence of phase separation, owing to the formation of insoluble water.[78] Under all the conditions applied, cyclohexanone formed more selectively than cyclohexanol, and the cyclohexanone yield monotonously increased with temperature at any pressure. On the other hand, the effect of temperature on the cyclohexanol formation was less drastic, and even a decrease of yield was observed when the temperature was raised from 150 to 160 °C. The effect of pressure was also more pronounced for cyclohexanone than for cyclohexanol at each of the three temperatures. These results imply that $C_6H_{11}O_2\bullet$ formed in larger proportion than $C_6H_{11}O\bullet$ and that pathway (R1) → (R4) in Scheme 26 prevailed over (R1) → (R2) → (R3) → (R4), particularly at higher temperature and pressure. Important reaction parameters as well as rate constants obtained are shown in Table 13. At 160 °C, a drastic 1.7-time increase of the rate constant was observed with increasing the pressure from 17.0 to 20.5 MPa, which was explained in terms of the following equation on the effect of pressure on reaction rate:[79]

$$\left(\frac{\partial \ln k_c}{\partial P}\right)_{T,x} = -\frac{\Delta V^{\ddagger}}{RT} - \kappa_T$$

where k_c is the rate constant, $\Delta V^{\ddagger}$ is the activation volume, and κ_T is the isothermal compressibility. However, the large isothermal compressibility often offset the large negative activation volumes. This is the reason why the rate enhancements with pressure were not so striking, and even rate retardation at higher pressure was observed in spite of the negative activation volume (the case at 150 °C). On the other

Scheme 26. Plausible Reaction Mechanism for the Catalyst-Free Autocatalytic Aerobic Oxidation of Cyclohexane to Cyclohexanone and Cyclohexanol

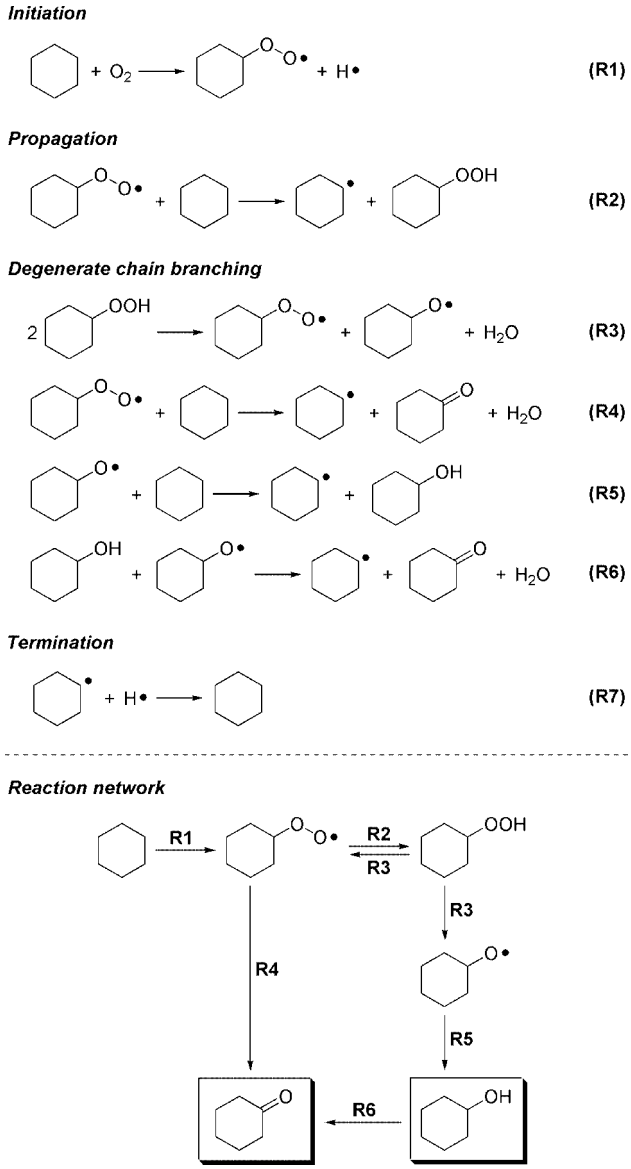

hand, the kinetic analysis based on the Arrhenius plots indicated that the activation energy at 20.5 MPa (94.6 kJ mol^{-1}) was greater than that at 17.0 MPa (54.4 kJ mol^{-1}). The authors attributed this result to the cage effect wherein the free radicals and cyclohexane were surrounded by the solvent (CO_2) molecules. Although the conventional liquid phase oxidation still affords a much higher oxidation rate than the oxidation in $scCO_2$, it is important to note that the tunable physical properties of $scCO_2$ allow us to control the outcomes of the oxidation by pressure and temperature. The authors later described the phase behavior−oxidation rate relationship, based on their kinetic analysis of the oxidation results obtained with various cyclohexane/O_2/CO_2 ratios.[80] As a trend, the oxidation was observed to be faster at lower CO_2 mole fraction, reaching a maximum in the CO_2-dissolved liquid (cyclohexane) phase. The main reason for this seems to be the reduced dilution effect at lower CO_2 content. The effect of the metal components of the reactor wall was not reported (see section 6.3.1).

6.2. Metal Complex Catalysts

6.2.1. Iron(III) Porphyrins

Koda and co-workers performed the aerobic oxidation of cyclohexane to cyclohexanol and cyclohexanone using an iron fluorinated-porphyrin catalyst in $scCO_2$.[81] Typically, the oxidation was performed in a 2.65-mL reactor with 1.0 mmol of cyclohexane, 1.0 MPa (1.0 mmol) O_2, 0.25 mmol of acetaldehyde as coreductant, and 0.5 μmol of Fe(TPFPP)Cl. Increasing the reaction temperature from 22 to 70 °C at a total pressure of 6 MPa resulted in a monotonous increase of the product yields. On the other hand, the yields reached a maximum at a certain total pressure when the pressure was changed at a constant temperature in the range 22−70 °C (e.g., Scheme 27). The yield increase with total pressure up to a certain pressure would be related to the increased solubility of the catalyst as well as substrate in dense CO_2. It was expected that the fluorinated phenyl groups in the porphyrin ligand could enhance the solubility of the catalyst through the attractive interaction between CO_2 and fluorine atoms. However, the phase behaviors under the conditions applied were not entirely investigated.

Cardozo-Filho's group performed the oxidation of cyclohexane to cyclohexanol and cyclohexanone using *meso*-tetraphenylporphyrin iron(III) chloride (denoted Fe(TPP)Cl).[82] They did not use molecular oxygen but used aqueous 70% *tert*-butyl hydroperoxide (*t*-BuOOH) and 30% hydrogen peroxide (H_2O_2) as oxidants. The two oxidants, however, did not perform equally, and *t*-BuOOH typically afforded better results. The results are summarized in Table 14. The oxidation using *t*-BuOOH in $scCO_2$ led to higher turnover number and product yields than those obtained in acetonitrile (entry 2 vs 4), though the reaction temperatures were different. The oxidation in $scCO_2$ strongly depended on the CO_2 density, and the highest cyclohexanol yield as well as turnover number was obtained at 0.724 g mL^{-1}. Note that higher CO_2 density favored the formation of cyclohexanol (entries 4 and 5 vs 6). In acetonitrile, the activity of Fe(TPP)Cl could further be increased by its "ship-in-bottle"-type encapsulation in zeolite Y (entry 2 vs 8). However, this was not observed in $scCO_2$ (entries 4 and 5 vs 9). Reusability of the heterogenized complex catalyst was also inferior in $scCO_2$. The actual phase behaviors of the reaction mixtures, including the solubility of the metal complex, were not reported.

6.2.2. Cobalt(II) Fluorinated Acetate

The aerobic oxidation of alkylaromatic compounds to the corresponding acids using cobalt salts is a principal method in industry. This reaction is homogeneously performed in acetic acid−water media under pressurized air in the presence of ionic promoters such as manganese ions and bromide. However, several drawbacks originate from the use of acetic acid as solvent, including difficulty in the separation of products from the solvent, decarboxylation of acetic acid, which proceeds during the oxidation, the corrosive and toxic nature of acetic acid, and the explosion hazards associated with acetic acid and molecular oxygen at high concentrations. Tsang and co-workers succeeded in replacing acetic acid with $scCO_2$ by using fluorous surfactant-like species.[83] The oxidation was typically performed at 120 °C for 12 h in a ca. 111-mL Teflon cup placed in a 160-mL stainless-steel reactor, using 18.8 mmol of toluene, 1.0 MPa O_2, 0.25 mmol of $[CF_3(CF_2)_8COO]_2Co\cdot nH_2O$ (denoted F−Co), 0.2 mmol

Table 13. Physical Properties and Rate Constants of the Catalyst-Free Autocatalytic Aerobic Oxidation of Cylohexane to Cyclohexanone and Cyclohexanol in $ScCO_2$ (Data Taken from Ref 77)

conditions	density ($\times 10^3$ mol cm^{-3})	isothermal compressibility ($\times 10^3$ MPa^{-1})	rate constant ($\times 10^3$ h^{-1})	activation volume (cm^3 mol^{-1})
137 °C/17.0 MPa	7.11	6.43	1.95	36
137 °C/20.5 MPa	8.50	4.69	1.50	96
150 °C/17.0 MPa	6.46	6.41	2.30	−217
150 °C/20.5 MPa	7.92	4.81	2.28	−161
160 °C/17.0 MPa	6.09	6.39	3.61	−775
160 °C/20.5 MPa	7.35	4.86	6.13	−720

Scheme 27. Iron Fluorinated-Porphyrin Complex-Catalyzed Aerobic Oxidation of Cyclohexane to Cyclohexanol and Cyclohexanone in $ScCO_2$

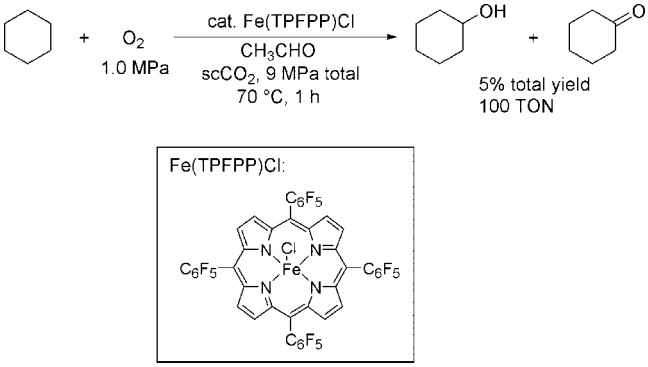

of NaBr, 100 μL of H_2O, and compressed CO_2 at a total pressure of 15.0 MPa. Under these conditions, the mixture formed an aqueous emulsion due to the enhanced miscibility of ionic species in the apolar $scCO_2$ medium by virtue of the attractive interaction between CO_2 and fluorine atoms in the Co catalyst. Excellent conversion (98.2%) and selectivity to benzoic acid (99.1%) were achieved with the formations of benzaldehyde and benzyl alcohol in trace amounts. The oxidation rate was roughly 10-times higher than that obtained in conventional acetic acid−water solvent systems (Scheme 28). Use of the Co catalyst with a fluorinated tag was crucial, because Co(II) acetate was inactive under otherwise similar conditions (conversion 0.1%), owing mainly to its poor solubility in $scCO_2$. The presence of water and NaBr were also indispensable, because their absence led to a drastic decrease in the conversion. The influence of changing the quantity of water was investigated in the range 100−500 μL, revealing that the induction period was shortened with increasing amount of water. The authors therefore concluded that some water (at least 270−310 μL) is required to saturate the $scCO_2$ phase before the formation of emulsion droplets. On the other hand, more than 0.05 mmol of NaBr was necessary for higher conversion. The effects of changing O_2 and CO_2 pressure were also investigated under the typical conditions but with the changed amounts of toluene (14.1 mmol) and water (400 μL). No change in TOF was observed in the O_2 pressure range 0.5−1.0 MPa, whereas lower CO_2 pressure afforded better results in the range 10.0−17.0 MPa (total pressure). Since toluene dissolved in $scCO_2$ under all the conditions applied, a dilution effect may account for the lower oxidation rate at higher CO_2 pressure. Intriguingly, the combined use of Co(II) acetate with $[CF_3(CF_2)_8COO]_2Mg$ (denoted F−Mg) was also successful, affording a high oxidation rate equal to that obtained with F−Co. In contrast, however, a much slower rate was observed for the combination of Co(II) acetate with $[CF_3(CF_2)_8COO]K$ (denoted F−K). The detailed reason for these phenomena was not elucidated, but cation-exchange would smoothly take place in the emulsion droplets for the Co(II) acetate−F−Mg system. The $[CF_3(CF_2)_8COO]_2Co$−NaBr catalyst in a water−$scCO_2$ medium was also successfully applied for other alkylaromatic compounds such as *p*-xylene (90.3% conversion), ethylbenzene (49.2%), 9,10-dihydroanthracene (99.2%), and 2-methylanthracene (62.4%) under conditions similar to those employed for toluene, yielding terephthalic acid (89.1% selectivity), a mixture of acetophenone (83.7%) and *sec*-phenylethyl alcohol (16.3%), a mixture of anthracene (67.6%) and anthraquinone (32.4%), and a mixture of 2-methylanthraquinone (76.3%) and 2-methylanthrone (23.7%), respectively.

6.3. Heterogeneous Catalysts

6.3.1. Catalytically Active Wall of a Stainless-Steel Reactor

Leitner's group performed the aerobic oxidation of alkanes in the presence of acetaldehyde as sacrificial coreductant.[84] No catalyst was intentionally added. The oxidation was typically performed at 52 °C for 27 h in a 205-mL stainless-steel reactor, using 50 mmol of substrate, 105 mmol of O_2, 100 mmol of acetaldehyde, and 800 mmol of CO_2. In addition to gas chromatography, *in situ* ATR-IR spectroscopy was used to trace the oxidations. The use of a stainless-steel reactor (austenitic steel no. 1.4571) was crucial, because the metal components of the reactor wall heterogeneously initiated and maybe also catalyzed the oxidations. Actually, when a glass liner was inserted in the stainless-steel reactor, a longer induction period was observed. Selected oxidation results are shown in Table 15. Note that the oxidations were conducted under multiphase conditions composed of a CO_2-rich phase and a substrate-rich phase (CO_2-expanded liquids), which was found to be most effective. The oxidations were faster in the concentrated substrate phase with lower concentration of coreductant acetaldehyde, which was suggested to be present mainly in the CO_2-rich phase due to its high volatility. In addition, the use of dense CO_2 lowers the melting point of solid substrates, thereby allowing us to perform the oxidation of cyclododecane (mp 60.4 °C) even at 45 °C (entry 5). Then, cyclododecane mainly existed as a CO_2-expanded liquid. The substrates which were solid even under dense CO_2 were not effectively oxidized (entry 1). Based on the product distributions and the control experiments using cyclooctane derivatives, the authors concluded that the mechanism shown in Scheme 29, involving an alkyl hydroperoxide intermediate, was the major pathway to oxygenated products under the conditions applied. Other compressed gases such as N_2 and Ar were also tested as media instead of CO_2 under otherwise identical conditions, however, resulting in significantly lower conversions and product yields.

In contrast to the above favorable effect of a stainless-steel reactor, there is one report describing a negative

Table 14. Oxidation of Cyclohexane Using Fe(TPP)Cl and Zeolite Y-Encapsulated Fe(TPP)Cl (Fe(TPP)Y) Catalysts (Data Taken from Ref 82)[a]

entry	catalyst	solvent	oxidant	yield of cyclohexanol (%)	yield of cyclohexanone (%)	TON	TOF (h^{-1})
1	Fe(TPP)Cl	CH_3CN	H_2O_2	2.0	3.5	47	23
2	Fe(TPP)Cl	CH_3CN	*t*-BuOOH	0.61	1.2	15	8
3	Fe(TPP)Cl	$scCO_2$[b]	H_2O_2	not detected	not detected	0	0
4	Fe(TPP)Cl	$scCO_2$[b]	*t*-BuOOH	13	not detected	43	22
5	Fe(TPP)Cl	$scCO_2$[c]	*t*-BuOOH	15	not detected	53	27
6	Fe(TPP)Cl	$scCO_2$[d]	*t*-BuOOH	3.0	6.8	28	14
7	Fe(TPP)Y	CH_3CN	H_2O_2	0.47	0.25	12	6
8	Fe(TPP)Y	CH_3CN	*t*-BuOOH	0.93	2.0	25	12
9	Fe(TPP)Y	$scCO_2$[e]	*t*-BuOOH	2.5	not detected	9	4

[a] Reactions in CH_3CN were performed at room temperature for 2 h with a catalyst/oxidant/cyclohexane ratio of 1/1100/1100 (cyclohexane: 0.77 M), while those in $scCO_2$ were carried out at 40 °C for 2 h with a catalyst/oxidant/cyclohexane ratio of 1/1100/1100 (cyclohexane: 0.33 M). [b] CO_2 density 0.741 g mL^{-1}. [c] 0.724 g mL^{-1}. [d] 0.341 g mL^{-1}. [e] 0.732 g mL^{-1}.

Scheme 28. Aerobic Oxidation of Toluene Using Cobalt Catalysts

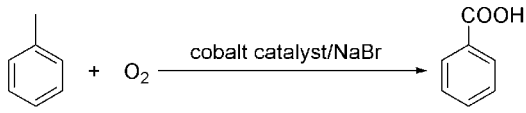

Co(III) acetate, acetic acid–water, 87 °C: 2.4 × 10^{-4} s^{-1} TOF

$[CF_3(CF_2)_8COO]_2Co$, $scCO_2$–water, 100 °C: 2.86 × 10^{-3} s^{-1} TOF

catalytic effect of the reactor wall on alkane oxidation. McHugh's group performed the noncatalytic aerobic oxidation of cumene to cumene hydroperoxide in three different supercritical fluids.[85] The oxidation was performed at 110 °C using 12 mol % cumene, 0.1 mol % cumene hydroperoxide as radical initiator, 0.4−30 mol % O_2, and compressed CO_2, Xe, or Kr at a total pressure in the range 20.0−41.4 MPa. The mixture then formed a single homogeneous phase. Kinetic investigations based on a radical mechanism revealed that the oxidation was slower in the stainless-steel reactor (316SS) and in the corresponding gold-plated reactor in SCFs than in a Pyrex reactor in neat cumene. In addition, the selectivity to cumene hydroperoxide in SCFs with the metallic reactors was inferior to that obtained under the metal-free neat conditions. The authors thus concluded that the metallic reactors catalyze the termination step of the radical reactions in SCFs, thereby resulting in lower product yield in the supercritical fluids. The effects of solvent polarity and viscosity were suggested to be minimal. Further optimization of the reaction conditions is necessary, including the elimination of the catalytic influence of the reactor wall to ascertain the benefit of operating the oxidation in SCFs. Nevertheless, it is noteworthy that isolation of the thermally unstable cumene hydroperoxide can easily be performed by isothermal depressurization after the oxidation in SCFs, which could be one advantage of using SCFs as reaction media.

6.3.2. Supported Cobalt Oxides

6.3.2.1. Partial Oxidation of Toluene to Benzaldehyde with O_2 over CoO/Al_2O_3 Catalyst. Dooley and Knopf performed the aerobic oxidation of toluene in $scCO_2$ using a continuous-flow reactor.[86] Various catalysts were examined, including alumina-supported CoO, MoO_3, and CoO−MoO_3, a commercial Ni−W hydroprocessing catalyst, and a commercial Y-zeolite (Si/Al = 2.37) of which Na^+ ions were exchanged with protons. The reaction mixture was composed of 1.5 wt % (0.7 mol %) toluene, 1.5 wt % (2.0 mol %) O_2, 1.2 × 10^{-3} mol % benzoic acid as co-oxidant, 5 wt % N_2, and the balance CO_2, and its temperature and pressure were adjusted to 127−227 °C and 8 MPa, respectively. Under these conditions, the mixture formed a single homogeneous phase at the reactor entrance. Among the catalysts tested, 5% CoO/Al_2O_3 prepared by impregnation from aqueous solution of $Co(NO_3)_2 \cdot 6H_2O$ and calcined at 197 °C afforded the highest activity (TOF 10^{-5} s^{-1}) and selectivity to benzaldehyde. On the other hand, the fact that 5% CoO−10% MoO_3/Al_2O_3 and a mixture of 5% CoO−10% MoO_3/Al_2O_3 and protonated Y-zeolite exhibited lower activity indicates that molybdenum oxide and Brønsted acid sites did not participate in the oxidation. The authors proposed that Co^{2+}/Co^{3+} redox pairs on the 5% CoO/Al_2O_3 catalyst are catalytically active sites for the partial oxidation of toluene. However, *in situ* X-ray absorption spectroscopic investigations would be necessary to fully understand the oxidation state of the metals (see section 3.1.2.4). Finally, the authors suggested that the reaction mechanism over 5% CoO/Al_2O_3 in $scCO_2$ is different from that of the classical vapor phase oxidations over a series of oxides including MoO_3, WO_3, and V_2O_5. This speculation was based on the facts that the activity of the 5% CoO/Al_2O_3 catalyst in $scCO_2$ was much higher than those of the latter three oxides under vapor-phase conditions and that the product distributions were considerably different; the condensation products observed under vapor-phase oxidations were not observed for the supercritical oxidation (Scheme 30). The vapor-phase oxidations involve a Mars−van Krevelen mechanism in which the lattice oxygen atoms are incorporated into the organic substrates and dissociatively adsorbed molecular oxygen compensates for the lattice vacant spaces thus formed. On the other hand, the oxidation over 5% CoO/Al_2O_3 in $scCO_2$ was suggested to take place by direct insertion of molecular oxygen into free radical intermediates to give the corresponding peroxides, which decomposed to the products.

6.3.2.2. Partial Oxidation of Propane with O_2 over Co_3O_4/SiO_2 Catalyst. Kerler and Martin investigated the partial oxidation of propane.[87] The reaction was carried out in a 305-mL batch reactor which contained 2 mL of catalyst and 21 mL of glass beads filled in a wire basket. Various active components, such as Co_3O_4, CuO, MnO_2, MoO_3, Pd, and Pt, were supported on SiO_2, ZrO_2, and γ-Al_2O_3 by impregnation, precipitation, and coprecipitation methods and used as catalysts. The support materials as well as the reactor wall did not catalyze the oxidation. Important trends observed were (i) cobalt in low content was most effective for the partial oxidation, and (ii) less acidic support afforded higher selectivity to the partially oxidized products. Thus, 2.4% Co_3O_4/SiO_2 prepared by a precipitation method exhibited the

Table 15. Aerobic Oxidation of Alkanes in the Presence of Acetaldehyde as Coreductant in $ScCO_2$ (Data Taken from Ref 84)[a]

entry	reactant	phase number[b]	main products (yields)	ROOH[c] ($mmol^{-1}$)
1		2 (solid/ $scCO_2$)	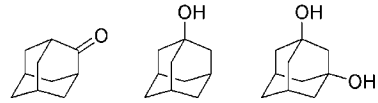 0.3% 1.5% 1.3%	0.53
2		1	 0.4%	not detected
3		2	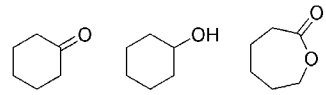 4.2% 1.2% 1.8%	0.17
4		2	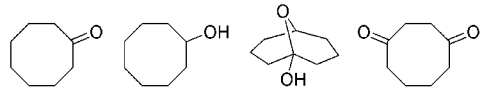 18.4% 2.3% 1.0% 2.2%	1.31
5		2	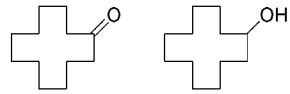 9.5% 2.4%	0.42
6	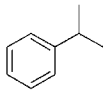	2	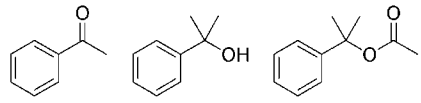 5.8% 22.2% 2.9%	>1.90
7	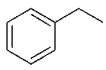	2	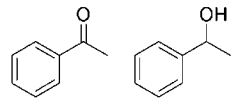 15.5% 0.7%	0.87

[a] Reaction conditions: reactor volume, 205 mL; substrate, 50 mmol; acetaldehyde, 100 mmol; O_2, 105 mmol; CO_2, 800 mmol; reaction temperature, 50 °C; reaction time, 27 h. [b] 1, a single homogeneous phase; 2, CO_2-rich phase and substrate-rich (CO_2-explanded liquid) phase. [c] Determined by iodometric analysis (demonstration for the presence of alkyl hydroperoxide intermediates; see Scheme 29).

Scheme 29. Plausible Mechanism for the Aerobic Oxidation of Alkanes Using Acetaldehyde as Coreductant

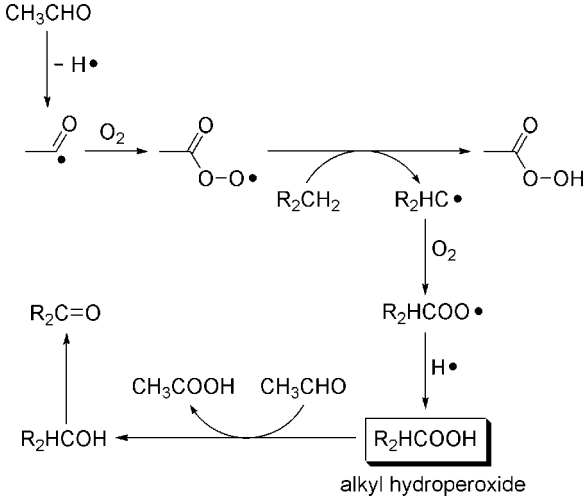

best catalytic performance. This catalyst was prepared by adding 1 N KOH dropwise to a $Co(NO_3)_2 \cdot 6H_2O-SiO_2$ suspension until the pH reached 9, followed by separation of the resulting solid, washing, drying, and calcination at 250 °C for 6 h and subsequently 350 °C for 6 h. Treatment of the catalyst with a mixture of propane, air, and CO_2 at a molar ratio of 1:2.5:112 at 300 °C for 353 min resulted in the formation of oxygenated compounds such as acetic acid (major), methanol, acetone, and acetaldehyde in 59% total selectivity at 12% conversion; then, propene also formed in 21% selectivity. The effect of changing the reaction parameters at 280 °C was investigated within narrow ranges, and the results were reported. However, further data are necessary to systematically understand the $Co_3O_4/SiO_2-propane-O_2-CO_2$ system. Intriguingly, the addition of water as cosolvent could increase the selectivity to the partially oxidized compounds.

6.3.2.3. Partial Oxidation of Cyclohexane with O_2 over CoO_x/SiO_2 and FeO_x/SiO_2 Catalysts. Martin and coworkers performed the partial oxidation of cyclohexane over cobalt, manganese, and iron oxide supported on alumina and silica with both batch and continuous-flow reactors.[88] Batch-operation was performed in a 300-mL stainless-steel autoclave with a cyclohexane/air/CO_2 molar ratio of 1:5:94,

Scheme 30. Reaction Pathways of the Aerobic Oxidation of Toluene in $ScCO_2$ and under Gas-Phase Conditions

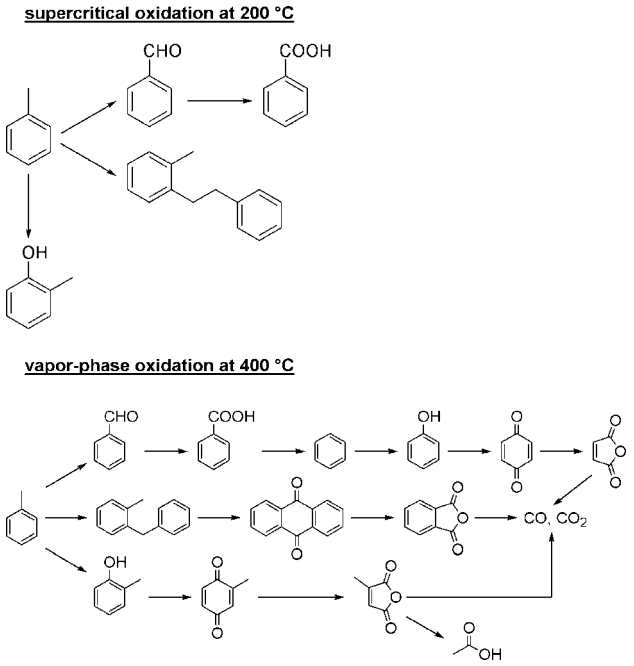

corresponding to a 2-fold excess of O_2 compared to the stoichiometry of the reaction. It was confirmed by another blank experiment that the reactor wall and the catalytic support materials, namely, alumina and silica, were inactive for the oxidation. High total selectivity exceeding 20% to cyclohexanol and cyclohexanone was observed at ca. 10% conversions for 5% CoO_x/SiO_2 and 5% FeO_x/SiO_2 catalysts, when the oxidation was performed at 230 °C and a total pressure of 16.0 MPa for 4 h. Although higher reaction temperature (290 °C) was required to obtain similar conversions, even better selectivity was observed when the oxidation was performed in a continuous-flow mode. Thus, with the same pressure (16.0 MPa) and cyclohexane/air/CO_2 molar ratio (1:5:94), the total selectivity to cyclohexanol and cyclohexanone reached ca. 40% at 7% conversion with 5% CoO_x/SiO_2 catalyst. As a general trend, the decisive parameter for the selectivity was the conversion of cyclohexane, and the conversion must be kept low to obtain the partially oxidized products in higher selectivities.

6.3.2.4. Partial Oxidation of Cyclohexane with O_2 over Cobalt-Incorporated Aluminophosphate Catalysts. Wang and co-workers prepared cobalt-incorporated aluminophosphate (denoted CoAPO-5) and used it as catalyst for the aerobic oxidation of cyclohexane.[89] This catalyst was prepared hydrothermally from the gel mixture of $0.05Co_2O_3 \cdot 0.95Al_2O_3 \cdot P_2O_5 \cdot 1.4Et_3N \cdot 35H_2O$, where Et_3N served as organic template. UV−vis and XANES revealed that the solid obtained by aging the gel contained tetrahedral Co^{2+} ions, which were partially (i.e., 22%) oxidized to Co^{3+} ions by calcination at 550 °C, thereby leading to the formation of redox active sites. The oxidation was performed at 121 °C for 15 h in a 14-mL stainless-steel batch reactor, using a mixture composed of 15 mol % cyclohexane, 15 mol % O_2, and 70 mol % CO_2. Then, 0.2 wt % of *tert*-butyl hydroperoxide (TBHP; initiator) as well as 2.0 wt % of the catalyst was also added. Under these conditions, the apparent density of the mixture greatly influenced the conversion and selectivity to cyclohexanol and cyclohexanone. Thus, the conversion monotonously decreased from 8.7 to 3.7% with

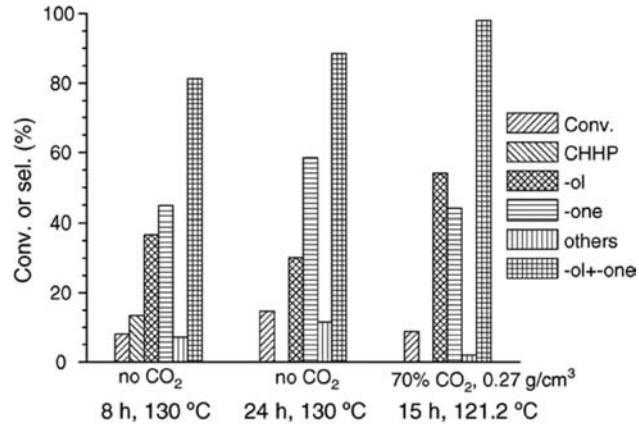

Figure 21. Comparison of the conversion and selectivity in the absence and presence of CO_2. CHHP, an intermediate of the cyclohexane oxidation; -ol, cyclohexanol; -one, cyclohexanone; others, adipic acid, valeric acid, etc. The CO_2-free oxidations were performed in a 100-mL reactor at the specified temperatures for the specified reaction times, using 50 g of cyclohexane, 0.5 g of CoAPO-5, 0.1 g of TBHP as initiator, and 1.5 MPa of O_2. Reprinted with permission from ref 89. Copyright 2005 Elsevier Ltd.

increasing the density from 0.27 to 0.61 g cm^{-3}. The selectivity to cyclohexanol also decreased from 54.0 to 37.4% with the density increase, whereas the selectivity to cyclohexanone increased from 44.0 to 62.1%. The merit of using dense CO_2 could be clearly seen in the higher total selectivity to cyclohexanol and cyclohexanone compared to that obtained under CO_2-free conditions (Figure 21).

6.3.3. Other Heterogeneous Catalysts

6.3.3.1. Total Oxidation of Toluene and Tetralin over Pt/Al_2O_3 Catalyst. Akgerman's group investigated the total oxidation of toluene and tetralin over a commercially available 0.5% Pt/Al_2O_3 catalyst (5−35 mg, diluted with glass beads).[90] The toluene oxidation was performed at 345−390 °C at 7.93−10.7 MPa, while the oxidation of tetralin was carried out at 300−375 °C and 8.96 and 10.0 MPa. The total flow rate was within the range 3.69−8.83 mol h^{-1}, and the CO_2/O_2 molar ratio was 98:2 for both substrates. The O_2/toluene molar ratio and O_2/tetralin molar ratio were 25:1 and 15:1, respectively. Under these conditions, particularly due to the high temperatures, no catalyst deactivation was observed for at least 12 h time-on-stream. In addition, no partially oxidized products such as organic oxygenates and carbon monoxide were formed, indicating that only the total oxidation took place for both substrates under the conditions applied. The results revealed that the oxidations were surface reaction-controlled, and internal as well as external mass transfer limitation was negligible. The best fitting rate expression was one with half-order dependence on O_2 partial pressure and a fractional order dependence on toluene and tetralin partial pressures. Thus, dissociative adsorption of O_2 as well as toluene and tetralin was suggested to be involved in the reaction mechanism. The authors proposed rate expressions for both toluene and tetralin oxidation, on the basis of a plausible stepwise Langmuir−Hinshelwood-type mechanism. These rate expressions well agreed with the experimental data. A pressure effect on the oxidation rate was also examined for toluene at 345 and 360 °C in the range 7.93−10.7 MPa. The rates were increased with pressure, but the changes were only marginal.

6.3.3.2. Partial Oxidation of Propane with O_2 over $(VO)_2P_2O_7$ Catalyst. Martin's group also used $(VO)_2P_2O_7$

catalyst for the aerobic oxidation of propane, which led to the formation of acetic acid and acrylic acid besides the total oxidation products (CO_2 and H_2O).[91] A continuous-flow-reactor system with a 5-mL fixed-bed reactor was employed. The oxidation was performed under both gas phase and supercritical phase conditions. Under all the conditions applied, the reaction mixtures formed a single homogeneous phase, regardless of the presence of polar oxygenated products (acetic acid and acrylic acid), as revealed by visual inspection using a cell equipped with sapphire windows. The total pressure was found to be a crucial parameter for the oxidation. Thus, when a mixture composed of propane, synthetic air, and CO_2 with a constant molar ratio of 1:13:86 was reacted over $(VO)_2P_2O_7$ at a residence time of 19 s at 400 °C, the conversion monotonously increased from 71 to 82% with the pressure increase from 2.4 to 9.7 MPa. The selectivity to acetic acid and that to acrylic acid, on the other hand, showed a contrastive behavior. Acetic acid formation was more favored at higher pressure (1% selectivity at 2.4 MPa; 3% at 9.7 MPa), while acryl acid formation was suppressed as the pressure was increased (2.5% selectivity at 2.4 MPa; <1% at 9.7 MPa). Although the selectivity change was very small, several plots of the selectivities at the different pressures clearly showed the above trend. Supercritical fluid chromatography revealed that acrylic acid was adsorbed more strongly on the catalyst surface than acetic acid and thereby remained there longer during the oxidation. This trend was more pronounced at higher pressures. Hence, the authors concluded that the acrylic acid underwent total oxidation more readily at higher pressures, resulting in the declined selectivity. The catalyst also significantly changed its morphology under higher pressures (enhanced sintering), which would also contribute to the conversion and selectivity changes with pressure.

6.3.3.3. Partial Oxidation of Cyclohexane with O_2 over Silver Decamolybdodivanadophosphate Catalyst. Tsang and co-workers performed the oxidation of cyclohexane using molecular oxygen in $scCO_2$.[92] Two types of catalysts, namely, $Co(OAc)_2-Mn(OAc)_2-NaBr$ and $Ag_5PMo_{10}V_2O_{40}$ were applied for the reaction. Typical conditions for the use of $Co(OAc)_2-Mn(OAc)_2-NaBr$ were a C_6H_{12}/O_2 molar ratio of 1:1.32, 2.0 MPa of O_2, and a total pressure of 14.0 MPa. A 300-mL autoclave was used as reactor. Under these conditions at 215 °C, the selectivity to partially oxygenated products formed in 6 h was only 9.4% at 16% conversion. This is because the combustion products, namely, carbon oxides, were mainly formed. Addition of acetic acid and, particularly, changing the radical initiator from NaBr to *N*-hydroxyphthalimide (denoted NHPI) significantly enhanced the selectivity; the combined use of $Co(OAc)_2-Mn(OAc)_2-NHPI-AcOH$ afforded the partial oxygenates in 67% selectivity at 54.9% conversion even at a low reaction temperature of 80 °C. The role of acetic acid is the extraction of the partially oxidized polar species from the aqueous micellar catalyst, avoiding their overoxidation to carbon oxides by a prolonged contact with the catalyst. The $Ag_5PMo_{10}V_2O_{40}$ catalyst, on the other hand, was prepared using $H_5PMo_{10}V_2O_{40}$ and $AgNO_3$ as starting materials, and it was applied for the oxidation under the following conditions: a C_6H_{12}/O_2 molar ratio of 1:1.32, 2.0 MPa of O_2, and 5 mL of methanol as cosolvent. The total pressure was then 14.0 MPa. Although higher reaction temperature increased the conversion of cyclohexane, it also enhanced the combustion, yielding significant amounts of carbon oxides. At 180 °C, a high selectivity of 96% could be achieved for the partially oxygenated products at 10.0% conversion. When the oxidation was performed in the absence of catalyst or in the presence of $Na_5PMo_{10}V_2O_{40}$ under otherwise similar conditions, no reaction took place, indicating that there was a synergetic effect between Ag(I) cationic centers and the redox oxygen centers. The temperature-programmed reduction (TPR) profile revealed three reduction peaks at 200, 500, and 650 °C for the $Ag_5PMo_{10}V_2O_{40}$ catalyst, whereas its sodium salt form, $Na_5PMo_{10}V_2O_{40}$, exhibited no characteristic peaks, indicative of the crucial role of Ag(I) for the redox properties.

Scheme 31. Diastereoselective Oxidation of Chiral Sulfides in $ScCO_2$

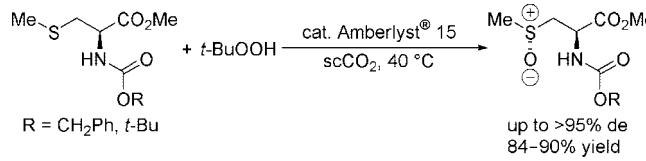

7. Oxidation of Other Compounds

7.1. Oxidation of Sulfides

Rayner and co-workers found that diastereoselectivity in the sulfoxidation of chiral sulfides derived from methionine and cysteine could greatly be controlled in $scCO_2$ by changing the CO_2 pressure.[93] Notably, treatment of Cbz methyl cystein methyl ester with TBHP over an acidic resin catalyst of Amberlyst 15 in $scCO_2$ at 40 °C and 18.0 MPa led to the formation of the corresponding sulfoxide in >95% de (Scheme 31, R = CH_2Ph), whereas no diastereoselectivity was observed in conventional organic solvents such as toluene and CH_2Cl_2. The diastereoselectivity was strongly pressure-dependent, because, above or below 18.0 MPa, the value dropped drastically. A similar pressure effect was observed also for Boc methyl cystein methyl ester which, however, afforded less impressive stereoselectivity (up to 31% de; Scheme 31, R = *t*-Bu).

Campestrini and Tonellato used various manganese porphyrin catalysts for the oxidation of sulfides.[94] A commercially available Oxone ($2KHSO_5 \cdot KHSO_4 \cdot K_2SO_4$) was employed as oxidant. In a 10-mL cylindrical reactor, the oxidation of diphenylsulfide (0.3 mmol) with the oxidant (0.65 mmol active oxygen) took place even without catalyst in $scCO_2$ at 20 MPa and 40 °C containing acetone cosolvent (1.0% w/w); the corresponding sulfoxide and sulfone were obtained in 4 and 1% yield, respectively, in 24 h. The yields, however, could be increased up to 9 and 22%, respectively, by adding Mn(TPFPP)Cl catalyst (2.4×10^{-3} mmol), 4-*tert*-butylpyridine (0.17 mmol) as axial ligand, and Aliquat 336 (tricaprylmethylammonium chloride; 0.11 mmol) as phase transfer catalyst. The presence of 4-*tert*-butylpyridine was then crucial, because the Mn complex itself acted as inhibitor for the oxidation. It was suggested that coordination of the base ligand renders the metal center prone to undergo oxidation by Oxone and that the resultant oxo-manganese porphyrin oxidizes sulfides to sulfoxides and then to sulfones. Similarly, methyl *p*-tolyl sulfide was oxidized under otherwise identical conditions to give the corresponding sulfone in 82% yield. Then, the expected sulfoxide was not obtained, but it formed in 7−14% yields at the cost of the sulfone yield when the amount of Oxone was reduced or Aliquat 336 was not added. Other manganese porphyrins such as

Scheme 32. Oxidation of Pyridine to Pyridine *N*-Oxide by H_2O_2 Formed by the Reaction between H_2 and O_2 over Pd−Pt/TS-1 Catalyst in $ScCO_2$

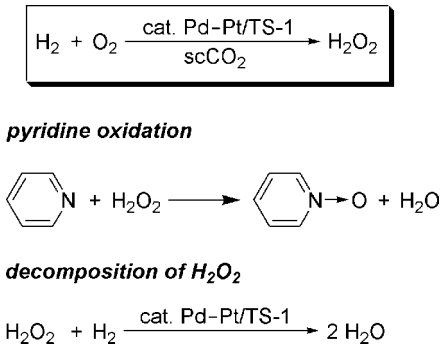

Mn(TMP)Cl, Mn(TOP)Cl, Mn(TMPBr$_8$)Cl, and Mn(THEF-PP)Cl were also tested under the conditions without Aliquat 336, affording results similar to those obtained by Mn(T-PFPP)Cl. Under all the conditions applied, the reaction mixtures formed virtually two phases, namely, a solid phase (insoluble manganese porphyrin complexes and the oxidant components) and a CO_2-rich phase. The organic components would mainly be present in the CO_2-rich phase containing acetone cosolvent and probably reacted heterogeneously over the surface of catalyst and oxidant. However, without exact partitioning data of every component in different phases, which could drastically change with reaction time under the conditions applied, it is difficult to discuss the factors governing the activity and selectivity.

7.2. Oxidation of Pyridine

Pyridine undergoes oxidation by H_2O_2 to give pyridine *N*-oxide (Scheme 32). Chen and Beckman employed this reaction to determine the amount of H_2O_2 formed during the reaction between H_2 and O_2 over titanium silicate (TS-1)-supported Pd and Pd−Pt catalysts in $scCO_2$.[95] No oxidation took place when pyridine was reacted with O_2 alone over TS-1 or Pd/TS-1 catalyst or with the mixture of H_2 and O_2 in the presence or absence of TS-1 catalyst, indicating that the H_2O_2 *in situ* generated by the reaction of H_2 and O_2 over the Pd/TS-1 catalyst oxidizes pyridine. Addition of Pt to Pd/TS-1 enhanced the formation of H_2O_2, and the yield reached 31.7% with a selectivity of 56.1% when equimolar amounts (12.4 mmol) of H_2 and O_2 were reacted over 0.05 g of the 0.2% Pd−0.02% Pt/TS-1 catalyst in water (27.8 mmol) at 60 °C and 12.5 MPa for 5 h, as shown by the coadded indicator of pyridine (6.2 mmol). The yield of H_2O_2, however, decreased when an excess amount of H_2 or a larger amount of the catalyst or loaded metal was employed. The authors attributed these results to the enhanced hydrogenolysis of H_2O_2 to H_2O which proceeds over the same catalyst. Thus, design of a new system which quickly removes H_2O_2 from the catalyst surface was suggested to be a future subject to be explored.

8. Potential and Limitations of Dense CO_2 as a Medium for Catalytic Oxidations

Based on the above survey (sections 3−7), we discuss here the potential and limitations of dense CO_2 medium, in terms of catalysts and opportunities offered by the use of the unique tunable physical properties in oxidations and separation processes.

8.1. Catalysts

Catalytic oxidations in $scCO_2$ have been performed using various well-defined supported metals, oxides, and metal complexes. Also, both favorable and unfavorable catalytic effects of the wall of a stainless-steel reactor have been reported (sections 5.1.5,[72] 5.2.1,[73] and 6.3.1[84,85]), suggesting that the strict check of inertness of the reactor or the use of a Teflon insert is a necessary prerequisite for kinetic investigations. In the following, the trends, potential, and limitations of the catalysts used are discussed.

8.1.1. Supported Metals and Oxides

8.1.1.1. Alcohol Oxidations. As clearly seen in section 3, supported palladium catalysts are promising for the aerobic oxidation of benzyl alcohols to the corresponding aldehydes, not only in conventional liquid solvents but also in $scCO_2$. Both alumina and carbon serve as good supports for Pd particles. However, examples of the use of other supports are rare, and more support-screening studies are necessary for finding new catalysts exhibiting better performance. In addition, such an approach will furnish additional mechanistic information on oxidation catalysis in dense CO_2. Intriguingly, the supported Pd particles are oxidized to a relatively larger extent during the benzyl alcohol oxidation in $scCO_2$ compared to those in conventional organic solvents (section 3.1.2.4[29]). This means that more oxygen atoms are adsorbed or incorporated in the surface and subsurface of the Pd particles during the oxidation in $scCO_2$. Such a surface environment would greatly enhance the oxidative removal of adsorbed hydrogen and/or poisoning species such as carbon monoxide, provided that the dissociative O_2 adsorption is a slow step in conventional oxidations using organic solvents. It is noteworthy that Pd/Al_2O_3 is also effective for the oxidation of aliphatic secondary alcohols to the corresponding ketones in $scCO_2$, but its use for the aliphatic primary alcohol oxidations resulted in low selectivity to the desired aldehydes (section 3.1.2.3[27]).

In contrast to palladium, platinum and rhodium, which are also suitable as oxidation catalysts in conventional liquid solvents, behave in a rather complex manner in $scCO_2$. According to Grunwaldt, Baiker, and co-workers, Pt/Al_2O_3 and Rh/Al_2O_3 catalysts are unexpectedly not usable for the continuous aerobic oxidation of benzyl alcohol (sections 3.1.2.2[26] and 3.1.2.4[32]) and cinnamyl alcohol (section 3.1.2.5[34]) in $scCO_2$. The low activity of Pt catalyst in $scCO_2$ was attributed to poisoning of active sites by strongly adsorbed species such as carbon monoxide and other carbonaceous species. On the other hand, the high propensity for oxidation of the Rh particles was proposed to be the reason for the low activity of Rh/Al_2O_3; probably, a greatly increased O_2 concentration in the vicinity of the catalyst surface in $scCO_2$ facilitates the oxidation. The alumina support also may contribute to the low activity of Pt/Al_2O_3 in $scCO_2$, because Tsang et al. (section 3.1.1.1[20]), Gläser et al. (section 3.1.1.2[22]), and Zhou and Akgerman (section 3.1.2.1[25]) successfully performed the aerobic oxidation of alcohols over Pt/C or Pt/TiO_2 catalyst in $scCO_2$. Note also that Rh/C exhibited higher activity than Rh/Al_2O_3 for the oxidation of *m*-hydroxybenzyl alcohol (section 3.1.1.4[24]). The origin of the difference in Pt and Rh catalyses when different supports were used is still unclear.

Examples of the use of other supported metals are rare; only chromium (section 3.3.1[43]) and gold (section 3.3.2[44])

were reported to be effective when loaded on proper metal oxides. More metals as well as support materials should be tested for various alcohol oxidations in $scCO_2$. Oxidation catalysis by the solid oxide catalysts with inherent redox properties such as iron oxide (section 3.3.4[46]) and polyoxometalate (section 3.3.5[47]) has also scarcely been investigated in $scCO_2$. These catalysts are superior to transition-metal-based catalysts due to their lower cost and less toxicity, and hence, more effort is required on their development.

8.1.1.2. Alkene Oxidations. In contrast to the many publications on the use of metal complex catalysts, examples of the use of solid catalysts in alkene oxidations in $scCO_2$ are rare. In addition, to our knowledge, there are still no reports on the aerobic alkene oxidation over solid catalysts. In most cases, supported Pd and/or Pt was used as catalyst, and H_2O_2 was used as oxidant (sections 5.2.2[74] and 5.2.3[75,76]). It is notable that *in situ* generated H_2O_2 from the catalytic reaction between H_2 and O_2 over supported precious metals can oxidize alkenes in $scCO_2$, giving the corresponding epoxides, diols, etc. (sections 5.2.2[74] and 5.2.3.1[75]). This protocol seems to be more preferable than that using aqueous 30% H_2O_2, because the water used for dilution of H_2O_2 could deteriorate the inherent structure of solid catalysts and enhance the leaching of supported metals. In addition, aqueous H_2O_2 liquid is relatively insoluble in $scCO_2$, bringing about unfavorable phase separation of the reaction mixtures. In contrast, gaseous H_2 and O_2 are free from such problems and suitable for use in fixed-bed continuous-flow operations. However, researchers should note that special care is needed for the use of the explosive H_2/O_2 gaseous mixture, even if dense CO_2 could more or less dilute it and improve heat dissipation. It also should be pointed out that *in situ* generated H_2O_2 could oxidize pyridine to give pyridine *N*-oxide (section 7.2[95]).

8.1.1.3. Oxidation of Alkanes and Alkylaromatic Compounds. The most widely studied system is the combination of supported cobalt oxide catalysts and molecular oxygen as oxidant. These catalytic systems are effective for the partial oxidation of toluene to benzaldehyde (section 6.3.2.1[86]), propane to several organic oxygenates (mainly acetic acid) (section 6.3.2.2[87]), and cyclohexane to cyclohexanol and cyclohexanone (section 6.3.2.3[88]) in $scCO_2$, although a very high temperature exceeding 200 °C is required. The active sites are considered to be Co^{2+}/Co^{3+} redox pairs. Dooley and Knopf suggested that Mars−van Krevelen-type direct incorporation of lattice oxygen atoms into substrate molecules is unlikely to occur over CoO/Al_2O_3 catalyst in $scCO_2$. Instead, the direct insertion of O_2 into radical intermediates was proposed (section 6.3.2.1[86]). For the propane oxidation, less acidic silica serves as the best support in $scCO_2$ (section 6.3.2.2[87]).

Other catalysts suitable for the partial oxidation of alkanes in $scCO_2$ involve $(VO)_2P_2O_7$ (section 6.3.3.2[91]) and $Ag_5PMo_{10}V_2O_{40}$ (section 6.3.3.3[92]). The former catalyst, however, possesses a relatively fragile structure, and its sintering under high-pressure $scCO_2$ conditions is serious. On the other hand, the latter exhibits an excellent selectivity for the partially oxidized products in the cyclohexane oxidation in $scCO_2$ at 180 °C. The surface Ag(I) was suggested to exhibit unique redox properties.

For the total aerobic oxidation of alkylaromatic compounds to CO_2 and H_2O, Pt/Al_2O_3 exhibits good performance in $scCO_2$, though the reaction temperature is extremely high (>300 °C) (section 6.3.3.1[90]). The catalyst is considered to promote the oxidations via the Langmuir−Hinshelwood mechanism in $scCO_2$, which involves the dissociative adsorption of both substrates and O_2.

8.1.2. Metal Complexes and TPAP

Compared to supported metal and oxide catalysts, metal complex catalysts have more limitations for the use in oxidations under dense CO_2 conditions. The $scCO_2$ medium typically dissolves only nonpolar, nonionic, and low molecular weight compounds due to its low dielectric constant close to *n*-hexane as well as insufficient density intermediate between gas and liquid. Thus, metal complexes often do not dissolve completely in $scCO_2$, leading to lower oxidation rates compared to those in conventional organic solvents. Another drawback is their thermally unstable properties, which restrict the range of applicable reaction temperature. Nevertheless, oxidation by metal complex catalysts has widely been attempted. Some groups have modified the ligands of conventional metal complexes to improve the solubility in $scCO_2$ (sections 4.1,[51] 5.1.1.2,[59] 5.1.4,[69,71] 6.2.1,[81] 6.2.2,[83] and 7.1[94]).

8.1.2.1. Phenol Oxidations. For aerobic phenol oxidations in $scCO_2$, cobalt Schiff base complexes are usable similarly as in conventional liquid solvents. However, some ligand modification may be necessary to perform the reaction under completely homogeneous conditions (section 4.1, Scheme 13[51]). Cobalt Schiff base complexes immobilized on polymer supports can also successfully be applied for the oxidations, and the results are, in some cases, even better than those obtained in organic solvents (section 4.1, Figure 20[52]), though the catalysts are gradually deteriorated as the reaction proceeds.

8.1.2.2. Alkene Oxidations. Aerobic alkene oxidations in $scCO_2$ have been performed with various kinds of metal complexes. For Wacker-type oxidations, $PdCl_2$−copper chlorides (section 5.1.3[62,66,67]) or $PdCl_2$ alone (section 5.1.3[68]) or $PdCl_2$−benzoquinone (section 5.1.3[63]) is effective, while iron porphyrins, particularly $Fe(TPFPPBr_8)Cl$, are usable for the alkene epoxidation in $scCO_2$ (section 5.1.4[69]). For the iron porphyrin-catalyzed oxidations, fully oxidized $scCO_2$ serves as an ideal solvent, because solvent-derived, additional byproducts are formed in conventional organic solvents. In the Fe(TPFPP)Cl- and *cis*-$[Fe(DMP)_2(H_2O)_2](CF_3SO_3)_2$-catalyzed aerobic oxidation of cyclohexene in $scCO_2$, 2-cyclohexen-1-one is obtained as a major product (section 5.1.4[70,71]). For alkene epoxidations with alkyl hydroperoxides in $scCO_2$ or liquid CO_2, classical $Mo(CO)_6$ (section 5.1.1.1[1e,g,55−57]), $VO(OPr^i)_3$, and $Ti(OPr^i)_4$ (section 5.1.2[57]) are successfully applied. However, it is unclear if the dense CO_2 can afford better conversion and selectivity or not, compared to conventional liquid solvents; further studies are needed to uncover the benefit of using a dense CO_2 medium. The combined use of Mn(TDCPP)Cl with $(CF_3)_2CO\cdot 3H_2O$ in the presence of 4-*tert*-butylpyridine was reported to be effective for the cyclooctene epoxidation with aqueous H_2O_2 in $scCO_2$ (section 5.1.5[72]). However, the oxidation takes place much more slowly than in $CHCl_3$, probably due to the greatly restricted mass transfers in $scCO_2$, which cannot make the reaction mixture homogeneous, due to the low solubilizing power.

8.1.2.3. Alkane Oxidations. Iron porphyrin catalysts such as Fe(TPFPP)Cl and Fe(TPP)Cl are usable for the oxidation of cyclohexane to cyclohexanol and cyclohexanone with O_2 or *t*-BuOOH in $scCO_2$ (section 6.2.1[81,82]). However, the

published reports do not specify the phase behaviors of the reaction mixtures. In the oxidation using Fe(TPP)Cl and aqueous *t*-BuOOH, there might be three phases, i.e., insoluble solid Fe(TPP)Cl, CO_2-expanded aqueous *t*-BuOOH, and CO_2-rich phase probably containing most of the cyclohexane. In such a complex system, it is very difficult to predict where the oxidation mainly takes place. Unfortunately, detailed comparison of the activity and selectivity of iron porphyrin catalysts between $scCO_2$ and conventional organic solvents has never been performed.

For the aerobic oxidation of alkylaromatic compounds, $[CF_3(CF_2)_8COO]_2Co \cdot nH_2O$−NaBr serves as a very good catalyst in $scCO_2$ containing a small amount of water (section 6.2.2[83]), affording a much higher oxidation rate than that in the classical acetic acid−water solvent. Under optimized conditions, toluene can be oxidized to benzoic acid in quantitative yield. Although the beneficial role of $scCO_2$ is still unclear, the mixture forms an aqueous emulsion under the reaction conditions applied, which enables the dispersion of catalyst in $scCO_2$. This behavior, together with the great miscibility of cyclohexane and O_2 in $scCO_2$, affords an exceedingly high-speed oxidation rate, which is hardly achievable in conventional liquid solvents possessing an inherent gas−liquid mass transfer limitation.

8.1.2.4. Alcohol Oxidations. TPAP with a proper co-oxidant has widely been used in organic synthesis with great success. However, its activity in $scCO_2$ is inferior to that in conventional CH_2Cl_2, even though it does function catalytically also in $scCO_2$ (section 3.2.1[37]). The main cause for the lower activity is considered to be the insolubility of TPAP in apolar $scCO_2$ medium. However, the activity of TPAP in $scCO_2$ can be enhanced by supporting it onto surface-modified silicas, as demonstrated by Pagliaro et al. (section 3.2.1[37−41]). These approaches are interesting in terms of material and catalysis chemistry, but they seem to not be practical due to the complicated preparation method of the catalysts. On the other hand, use of cosolvents or surfactants may enhance the solubility of TPAP in $scCO_2$, thereby improving its catalytic performance. However, we are unaware of any published reports on this topic.

8.1.2.5. Sulfide Oxidation. The oxidation of sulfides to sulfoxides and sulfones with Oxone ($2KHSO_5 \cdot KHSO_4 \cdot K_2SO_4$) in $scCO_2$ is accelerated by manganese porphyrin complex catalysts (section 7.1[94]). Under the reaction conditions, the manganese porphyrins as well as the oxidant are not soluble in $scCO_2$, and the oxidation was suggested to be catalyzed heterogeneously. The oxidation probably takes place much faster in conventional liquid solvents which can dissolve the complex catalyst and oxidant completely.

8.1.3. Enzymes

There are a few successful examples on the use of enzyme catalysts for aerobic oxidations in $scCO_2$ (cholesterol, section 3.4;[48] phenols, section 4.2[53]). Most enzymes seem to be able to withstand even under high-pressure conditions, but researchers must carefully determine the reaction temperature, because enzymes undergo fatal thermal denaturation. In addition, note that a proper amount of water is necessary to make enzymes perform at their best conditions.[96] Thus, when enzymes are applied to continuous-flow operations, wet CO_2 must be fed into the fixed-bed reactor where the enzyme exists. Enzyme catalysts are attractive due to their inherent greater selectivity, but only a limited number of enzymes (oxidases) is currently available.

8.2. Effect of Tunable Physical Properties of Dense CO_2

8.2.1. Extraction and Mass and Heat Transfer

The physical properties of $scCO_2$ are intermediate between those of gas and liquid, and they can be successively tuned from those close to gas to those of the corresponding liquid by changing pressure and temperature.[1,97] These unique properties allow us to render reactant and O_2 completely miscible in $scCO_2$, thereby eliminating the gas−liquid mass transfer limitations. This can be a benefit for the oxidation of which rate depends normally on O_2 concentration. However, for certain supported metal and metal complex catalysts, increased O_2 concentration in the vicinity of catalysts may bring about overoxidation of the metals, leading to fatal deactivation of the catalysts. On the other hand, the gaslike low viscosity and high diffusivity of $scCO_2$ greatly enhance mass transfer in the porous network of heterogeneous catalysts. For the oxidations involving relatively polar and high molecular weight substrate and/or product(s), however, more liquid-like $scCO_2$ (lower temperature and higher pressure) should be applied at the cost of diffusivity to enhance their solubility as well as desorption from the catalyst surface. Instead, if both the substrate and product(s) are thermally stable and volatile at higher temperatures, their miscibility with O_2 and CO_2 as well as mass transfer in catalyst pores can greatly be enhanced by increasing temperature. The high utility of SCFs as extractor for the adsorbed compounds was, for example, demonstrated in an earlier work by Tiltscher et al.[98] ATR-IR spectroscopy using a catalyst-coated ATR-crystal[1k,14] furnishes information on the composition of a reaction mixture in catalyst pores during the oxidation in $scCO_2$ (sections 3.1.2.4[31] and 3.1.2.5[34]), thereby helping the optimization of reaction conditions. Note here that even the state of pure dense CO_2 in catalyst pores is considerably different from that in the outer space.[14b] Hence, *in situ* ATR-IR spectroscopy is a powerful tool for a better understanding of the heterogeneously catalyzed oxidations.

$scCO_2$ also has a greater heat conductivity than gas and, hence, is expected to efficiently eliminate reaction heat during the exothermic oxidations. However, elimination of the reaction heat by $scCO_2$ is typically insufficient, and unfavorable side reactions can proceed at the increased temperature. Some researchers have used glass beads or other inactive oxides for dilution of supported metal catalysts to avoid the formation of possible hot spots. Otherwise, the oxidations should be performed under more diluted conditions with reduced amounts of catalyst, substrate, and O_2 and an increased amount of CO_2 at lower temperatures. This approach gives a slower oxidation rate but may afford better selectivity to the desired product, particularly when heat-driven side reactions of the product immediately occur (sections 3.1.1.4,[24] 3.1.2.3,[27] and 6.3.2.3[88]).

8.2.2. Phase Behavior

The phase behavior of the reaction mixtures greatly affects the oxidations in dense CO_2. This is related to the presence or absence of mass transfer limitation between different phases and to the concentration of substrate, oxidant, and catalyst in the phase where the oxidation mainly takes place. Phase behavior can be controlled by changing the pressure and temperature of CO_2. Liquid-like $scCO_2$ at lower temperature and higher pressure tends to afford a single

homogeneous phase dissolving substrate, oxidant, and metal complex catalyst, whereas $scCO_2$ with lower density at lower temperature and pressure can lead to phase separations. The following systems have been applied for catalytic oxidations in dense CO_2: (i) a single homogeneous phase with gaslike $scCO_2$, (ii) a single homogeneous phase with liquid-like $scCO_2$, (iii) gaseous CO_2−liquid CO_2, (iv) $scCO_2$−solid, (v) $scCO_2$−CO_2-expanded liquid (CXL), and (vi) $scCO_2$−CXL−solid, where the solid phase involves solid catalysts, insoluble metal complexes, insoluble solid oxidants, or other insoluble solid reagents, and CXL is either CO_2-expanded substrate or CO_2-expanded intentionally modified solvent (e.g., organic solvents, ionic liquids, poly(ethylene glycol), etc.). Substrates, oxidants, and products are distributed to each phase according to their solubility in the respective phases. Although the phase behavior is important for controlling the oxidations as well as other catalytic reactions in SCFs, only a few groups have investigated in detail the phase behavior−conversion/selectivity relationships. One of the reasons for this is the limitation of visual observation of phase behavior; human eyes can easily miss small insoluble droplets or small solid particles attached on the wall of the view cell. This problem may be circumvented by applying *in situ* ATR-IR spectroscopy, provided that the insoluble substances are deposited on the IR penetration parts of the ATR-crystal (see section 3.1.2.4).[1k,14] Another problem originates from the fact that the mixture sometimes become cloudy due to the formation of molecular clusters causing light scattering, which further renders visual phase observation difficult. Nevertheless, some clear trends were observed, for example, as follows: For continuous-flow aerobic oxidation of benzyl alcohol to benzaldehyde over Pd/Al_2O_3, a type (iv) system affords the highest conversion and selectivity (section 3.1.2.4[30,31]), while a type (vi) system is favorable for the same reaction over Au/TiO_2 (section 3.3.2[44]) and the aerobic oxidation of cinnamyl alcohol over Pd/Al_2O_3 (section 3.1.2.5[34]).

For the use of metal complexes, it is important to somehow dissolve them in $scCO_2$ to make the reaction mixture homogeneous (type (ii) system) in order to achieve a higher oxidation rate. Introduction of fluorinated groups or other CO_2-philic groups in the ligands has been attempted (sections 4.1,[51] 5.1.1.2,[59] 5.1.4,[69,71] 6.2.1,[81] 6.2.2,[83] and 7.1[94]), but the corresponding metal complexes are not always soluble in $scCO_2$. Interestingly, some researchers insist that the oxidation takes place over the surface of precipitated insoluble metal complexes (section 7.1[94]). Other solutions involve the use of additives such as cosolvents or surfactants which can increase the miscibility of metal complexes with $scCO_2$ (section 6.2.2[83]). However, few examples have been shown based on this approach. Phase behavior becomes much more complex when aqueous peroxides (sections 5.1.5[72] and 6.2.1[82]) or inorganic solid oxidant (section 7.1[94]) is used with relatively insoluble metal complex catalysts. Then the oxidation becomes mass transfer-controlled and virtually takes no advantage of the properties of dense CO_2.

CO_2-expanded liquids[7] (CXLs, types (v) and (vi)) have been shown as suitable media for catalytic oxidations (sections 3.1.1.3,[23] 3.1.2.5,[34] 3.3.1,[43] 3.3.2,[44] 4.1,[52] and 5.1.3[66,67]). Typically, solid as well as metal complex catalysts stay in CXLs rather than in the CO_2-rich phase during the oxidations. Note that a metal complex which is insoluble in $scCO_2$ can dissolve in CXLs by proper choice of the liquid (organic solvents, ionic liquids, poly(ethylene glycol), etc.). CXLs dissolve a smaller amount of O_2 than $scCO_2$, but probably a larger amount than CO_2-free liquids. Hence, a higher oxidation rate is expected in CXLs than in conventional organic solvents. For the catalysts that are easily overoxidized and thus exhibit short catalytic lifetimes, CXLs may protect the catalyst from the intense contact with O_2 compared to $scCO_2$.

Some oxidations in $scCO_2$ have been performed at extremely high temperatures in a fixed-bed continuous-flow-reactor system (sections 3.1.2.1,[25] 3.3.4,[46] 6.3.2.1,[86] 6.3.2.2,[87] 6.3.2.3,[88] 6.3.2.4,[89] 6.3.3.1,[90] 6.3.3.2,[91] and 6.3.3.3[92]). Then, CO_2 has very low density close to gas, and it serves as diluent gas rather than as solvent (type (i) system). As previously discussed in section 2.2, an oxygen-exchange reaction may take place between CO_2 and O_2 over certain metal oxide catalysts at such high reaction temperatures, along with the oxidations.

8.3. Facilitated Separation Process

Dense CO_2 provides three major benefits for the separation step after the catalytic oxidations: (i) CO_2 solvent can easily be separated from the reaction mixture by simple depressurization. The tunable CO_2 density by pressure and temperature[1,97] may allow us to precipitate unreacted substrate, oxidation product(s), and, in some cases, catalyst stepwise by careful depressurization. A prerequisite for making use of this technique is of course that there are large differences in the solubilities of these components in $scCO_2$. (ii) Depressurized gaseous CO_2 can be recycled after repressurization. (iii) $scCO_2$ selectively extracts the unreacted organic substrate and product(s) existing in ionic liquids (ILs) and poly(ethylene glycol) (PEG), leaving $scCO_2$-insoluble catalysts in the liquids which can be reused for additional runs.[64,65] This technique has been combined with the great utility of CO_2-expanded ILs and PEG as reaction media (sections 3.1.1.3,[23] 3.1.2.6,[35] 3.3.1,[43] and 5.1.3[66,67]).

9. Concluding Remarks

Work on catalytic oxidations in dense CO_2 published prior to early 2008 has been reviewed, and the potential and limitations of the medium were discussed. In addition to the inherent favorable properties, such as abundant availability, cheapness, environmental benignity, nonflammability, and high recyclability, dense CO_2 as a medium offers a number of merits for both oxidations and subsequent separation processes. The great miscibility of $scCO_2$ with substrates and O_2 eliminates the gas−liquid mass transfer limitation, often affording exceedingly high-speed oxidation rates which are unachievable in conventional liquid solvents. In addition, the inertness of CO_2 under oxidative conditions is attractive, because organic solvents sometimes undergo oxidation under these conditions, resulting in the formation of solvent-derived oxygenates, thereby lowering the selectivity to desired product(s). Separation processes are greatly facilitated by the use of dense CO_2, because CO_2 is easily separated from the product downstream by depressurization and can be recycled by repressurization. The tunable density (solubilizing power) of CO_2 by pressure and temperature may allow the precipitation of only the desirable product(s). In addition, selective extraction of organic oxygenates from ionic liquids (ILs) and poly(ethylene glycol) (PEG) is possible by using $scCO_2$ as extractor, which leaves recyclable IL and PEG containing metal complex or solid catalysts.

For beneficial use of $scCO_2$ for aerobic oxidations, $scCO_2$ probably should be completely miscible with substrate and O_2. However, CO_2-expanded liquids (CXLs) (liquids: substrates, organic solvents, ILs, PEG, etc.) are also suitable for the oxidations and, in some cases, afford even better results. Particularly, these biphasic media are favorable for metal complex catalysts, which are insoluble in pure dense CO_2 and probably also for easily overoxidized supported metal catalysts, because CXLs may avoid intense contact of O_2 with the catalyst surface.

Finally, efforts of transforming the knowledge gained in the fundamental research into practical technology are highly desired. Although the high costs generated by the use of high-pressure conditions is not negligible, some heterogeneous catalytic hydrogenation processes in $scCO_2$ have already been commercialized in industry.[2] This means that the advantages of dense CO_2, such as high reaction rates, unique product selectivities, facilitated separation, and high reusability, can compensate for the high costs, together with its environmental benignity. However, we also have to recognize that injudicious use of dense CO_2 medium in catalytic oxidations can even reduce the overall process efficiency and sustainability.

10. Abbreviations

ATR-IR	attenuated total reflection infrared spectroscopy
Boc	*tert*-butoxycarbonyl group
Cbz	benzyloxycarbonyl group
CXL	CO_2-expanded liquid
DMP	2,9-dimethyl-1,10-phenanthroline
DTBP	2,6-di-*tert*-butylphenol
DTBQ	2,6-di-*tert*-butyl-1,4-benzoquinone
Et	ethyl group
EWG	electron-withdrawing group
FT-IR	Fourier-transformed infrared spectroscopy
^{i}Bu	isobutyl group
IL	ionic liquid
^{i}Pr	isopropyl group
Me	methyl group
NHPI	*N*-hydroxyphthalimide
P_c	critical pressure
PEG	poly(ethylene glycol)
ρ_c	critical density
$scCO_2$	supercritical carbon dioxide
SCF	supercritical fluid
STEM	scanning transmission electron microscopy
TBHP	*tert*-butyl hydroperoxide
t-Bu	tertiary butyl group
T_c	critical temperature
$(TDCPP)H_2$	5,10,15,20-tetrakis(2′,6′-dichlorophenyl)porphyrin
$(THEFPP)H_2$	5,10,15,20-tetrakis(heptafluoropropyl)porphyrin
$(TMP)H_2$	5,10,15,20-tetramesitylporphyrin
$(TMPBr_8)H_2$	β-octabromo-5,10,15,20-tetramesitylporphyrin
TOF	turnover frequency
TON	turnover number
$(TOP)H_2$	5,10,15,20-tetraoctylporphyrin
TPAP	tetrapropylammonium perruthenate
$(TPFPP)H_2$	5,10,15,20-tetrakis(pentafluorophenyl)porphyrin
$(TPFPPBr_8)H_2$	β-octabromo-5,10,15,20-tetrakis(pentafluorophenyl)porphyrin
$(TPP)H_2$	5,10,15,20-tetraphenylporphyrin
TTDBQ	3,5,3′,5′-tetra-*tert*-butyl-4,4′-diphenoquinone
UV−vis	ultraviolet−visible spectroscopy
XRD	X-ray diffraction
W/*F*	contact time (*W*, catalyst weight; *F*, molar flow rate entering the reactor)
XANES	X-ray absorption near edge structure
XAS	X-ray absorption spectroscopy

11. Acknowledgments

T.S. thanks Prof. Dr. Takao Ikariya (Tokyo Institute of Technology) for supporting his activity as a Research Fellow of the Japan Society for the Promotion of Science. This work is partially supported by a grant-in-aid from the Japan Society for the Promotion of Science (project code: 070300000755). A. B. thanks past and present co-workers for their valuable contributions, their enthusiasm, and their perseverance, which have greatly stimulated our research. Their names appear in the reference list. Financial support for our research on carbon dioxide utilization by the Swiss Federal Office of Energy (SFOE) is kindly acknowledged.

12. References

(1) (a) Subramaniam, B.; McHugh, M. A. *Ind. Eng. Chem. Process Des. Dev.* **1986**, *25*, 1. (b) Savage, P. E.; Gopalan, S.; Mizan, T. I.; Martino, C. J.; Brock, E. E. *AIChE J.* **1995**, *41*, 1723. (c) Jessop, P. G.; Ikariya, T.; Noyori, R. *Science* **1995**, *269*, 1065. (d) Jessop, P. G.; Ikariya, T.; Noyori, R. *Chem. Rev.* **1995**, *95*, 259. (e) Jessop, P. G. *Top. Catal.* **1998**, *5*, 95. (f) Baiker, A. *Chem. Rev.* **1999**, *99*, 453. (g) Jessop, P. G.; Ikariya, T.; Noyori, R. *Chem. Rev.* **1999**, *99*, 475. (h) *Chemical Synthesis Using Supercritical Fluids*; Jessop, P. G., Leitner, W., Eds.; Wiley-VCH: Weinheim, Germany, 1999. (i) Licence, P.; Ke, J.; Sokolova, M.; Ross, S. K.; Poliakoff, M. *Green Chem.* **2003**, *5*, 99. (j) Grunwaldt, J.-D.; Wandeler, R.; Baiker, A. *Catal. Rev.−Sci. Eng.* **2003**, *45*, 1. (k) Grunwaldt, J.-D.; Baiker, A. *Phys. Chem. Chem. Phys.* **2005**, *7*, 3526.

(2) Seki, T.; Grunwaldt, J.-D.; Baiker, A. *Ind. Eng. Chem. Res.* **2008**, *47*, 4561.

(3) (a) Elbashir, N. O.; Dutta, P.; Manivannan, A.; Seehra, M. S.; Roberts, C. B. *Appl. Catal., A* **2005**, *285*, 169. (b) Li, X.; Liu, X.; Liu, Z.-W.; Asami, K.; Fujimoto, K. *Catal. Today* **2005**, *106*, 154. (c) Elbashir, N. O.; Roberts, C. B. *Ind. Eng. Chem. Res.* **2005**, *44*, 505. (d) Bukur, D. B.; Lang, X.; Nowicki, L. *Ind. Eng. Chem. Res.* **2005**, *44*, 6038. (e) Linghu, W.; Li, X.; Asami, K.; Fujimoto, K. *Energy Fuels* **2006**, *20*, 7.

(4) (a) Jessop, P. G.; Ikariya, T.; Noyori, R. *Nature (London)* **1994**, *368*, 231. (b) Jessop, P. G.; Hsiao, Y.; Ikariya, T.; Noyori, R. *J. Am. Chem. Soc.* **1996**, *118*, 344. (c) Kröcher, O.; Köppel, R. A.; Baiker, A. *Chem. Commun.* **1996**, 1497. (d) Kröcher, O.; Köppel, R. A.; Fröba, M.; Baiker, A. *J. Catal.* **1998**, *178*, 284. (e) Baiker, A. *Appl. Organomet. Chem.* **2000**, *14*, 751. (f) Jessop, P. G.; Joó, F.; Tai, C.-C. *Coord. Chem. Rev.* **2004**, *248*, 2425.

(5) (a) Musie, G.; Wei, M.; Subramaniam, B.; Busch, D. H. *Coord. Chem. Rev.* **2001**, *219−221*, 789. (b) Campestrini, S.; Tonellato, U. *Curr. Org. Chem.* **2005**, *9*, 31.

(6) (a) Duprez, D.; Delanoë, F.; Barbier, J., Jr.; Isnard, P.; Blanchard, G. *Catal. Today* **1996**, *29*, 317. (b) Oliviero, L.; Barbier, J., Jr.; Duprez, D. *Appl. Catal., B* **2003**, *40*, 163. (c) Ding, Z. Y.; Frisch, M. A.; Li, L.; Gloyna, E. F. *Ind. Eng. Chem. Res.* **1996**, *35*, 3257. (d) Savage, P. E. *Chem. Rev.* **1999**, *99*, 603. (e) Savage, P. E.; Dunn, J. B.; Yu, J. *Combust. Sci. Technol.* **2006**, *178*, 443.

(7) Jessop, P. G.; Subramaniam, B. *Chem. Rev.* **2007**, *107*, 2666.

(8) Ambrose, D. In *Handbook of Chemistry and Physics*, 72nd ed.; Lide, D. R., Ed.; CRC Press: Boca Raton, FL, 1991.

(9) Abdulagatov, A. I.; Stepanov, G. V.; Abdulagatov, I. M. *High Temp.* **2007**, *45*, 85.

(10) Booth, H. S.; Carter, J. M. *J. Phys. Chem.* **1930**, *34*, 2801.

(11) Zenner, G. H.; Dana, L. I. *Chem. Eng. Prog. Symp. Ser.* **1963**, *59* (44), 36.

(12) Tsang, C. Y.; Streett, W. B. *Chem. Eng. Sci.* **1981**, *36*, 993.

(13) Zosel, K. *Angew. Chem., Int. Ed.* **1978**, *17*, 702.

(14) (a) Schneider, M. S.; Grunwaldt, J.-D.; Baiker, A. *Rev. Sci. Instrum.* **2003**, *74*, 4121. (b) Schneider, M. S.; Grunwaldt, J.-D.; Baiker, A. *Langmuir* **2004**, *20*, 2890.

(15) Kiyoura, T. *Bull. Chem. Soc. Jpn.* **1966**, *39*, 2135.

(16) Iwata, R.; Ido, T.; Fujisawa, Y.; Yamazaki, S. *Appl. Radiat. Isot.* **1988**, *39*, 1207.

(17) Mallat, T.; Baiker, A. *Chem. Rev.* **2004**, *104*, 3037.

(18) (a) Dirkx, J. M. H.; van der Baan, H. S. *J. Catal.* **1981**, *67*, 14. (b) van Dam, H. E.; Kieboom, A. P. G.; van Bekkum, H. *Appl. Catal.* **1987**, *33*, 361. (c) Baba, T.; Kameta, K.; Nishiyama, S.; Tsuruya, S.; Masai, M. *Bull. Chem. Soc. Jpn.* **1990**, *63*, 255.

(19) Schneider, M. S.; Baiker, A. *Catal. Rev.−Sci. Eng.* **1995**, *37*, 515.

(20) Steele, A. M.; Zhu, J.; Tsang, S. C. *Catal. Lett.* **2001**, *73*, 9.

(21) Tsang, S. C.; Zhu, J.; Steele, A. M.; Meric, P. *J. Catal.* **2004**, *226*, 435.

(22) Gläser, R.; Josl, R.; Williardt, J. *Top. Catal.* **2003**, *22*, 31.
(23) Hou, Z.; Theyssen, N.; Brinkmann, A.; Leitner, W. *Angew. Chem., Int. Ed.* **2005**, *44*, 1346.
(24) Sato, T.; Watanabe, A.; Hiyoshi, N.; Shirai, M.; Itoh, N. *J. Supercrit. Fluids* **2007**, *43*, 295.
(25) Zhou, L.; Akgerman, A. *Ind. Eng. Chem. Res.* **1995**, *34*, 1588.
(26) Jenzer, G.; Mallat, T.; Baiker, A. *Catal. Lett.* **2001**, *73*, 5.
(27) Jenzer, G.; Schneider, M. S.; Wandeler, R.; Mallat, T.; Baiker, A. *J. Catal.* **2001**, *199*, 141.
(28) Grunwaldt, J.-D.; Caravati, M.; Ramin, M.; Baiker, A. *Catal. Lett.* **2003**, *90*, 221.
(29) Grunwaldt, J.-D.; Caravati, M.; Baiker, A. *J. Phys. Chem. B* **2006**, *110*, 9916.
(30) Caravati, M.; Grunwaldt, J.-D.; Baiker, A. *Catal. Today* **2004**, *91*−*92*, 1.
(31) Caravati, M.; Grunwaldt, J.-D.; Baiker, A. *Phys. Chem. Chem. Phys.* **2005**, *7*, 278.
(32) Caravati, M.; Grunwaldt, J.-D.; Baiker, A. *Catal. Today* **2007**, *126*, 27.
(33) Caravati, M.; Grunwaldt, J.-D.; Baiker, A. *Appl. Catal., A* **2006**, *298*, 50.
(34) Caravati, M.; Meier, D. M.; Grunwaldt, J.-D.; Baiker, A. *J. Catal.* **2006**, *240*, 126.
(35) Hou, Z.; Theyssen, N.; Leitner, W. *Green Chem.* **2007**, *9*, 127.
(36) (a) Griffith, W. P.; Ley, S. V.; Whitcombe, G. P.; White, A. D. *J. Chem. Soc., Chem. Commun.* **1987**, 1625. (b) Griffith, W. P. *Chem. Soc. Rev.* **1992**, *21*, 179. (c) Lenz, R.; Ley, S. V. *J. Chem. Soc., Perkin Trans. 1* **1997**, 3291.
(37) Ciriminna, R.; Campestrini, S.; Pagliaro, M. *Adv. Synth. Catal.* **2003**, *345*, 1261.
(38) Campestrini, S.; Carraro, M.; Ciriminna, R.; Pagliaro, M.; Tonellato, U. *Adv. Synth. Catal.* **2005**, *347*, 825.
(39) Ciriminna, R.; Campestrini, S.; Carraro, M.; Pagliaro, M. *Adv. Funct. Mater.* **2005**, *15*, 846.
(40) Ciriminna, R.; Campestrini, S.; Pagliaro, M. *Adv. Synth. Catal.* **2004**, *346*, 231.
(41) Ciriminna, R.; Campestrini, S.; Pagliaro, M. *Org. Biomol. Chem.* **2006**, *4*, 2637.
(42) Ciriminna, R.; Hesemann, P.; Moreau, J. J. E.; Carraro, M.; Campestrini, S.; Pagliaro, M. *Chem.*−*Eur. J.* **2006**, *12*, 5220.
(43) Dapurkar, S. E.; Kawanami, H.; Suzuki, T. M.; Yokoyama, T.; Ikushima, Y. *Chem. Lett.* **2008**, *37*, 150.
(44) Kimmerle, B.; Grunwaldt, J.-D.; Baiker, A. *Top. Catal.* **2007**, *44*, 285.
(45) Jenzer, G.; Sueur, D.; Mallat, T.; Baiker, A. *Chem. Commun.* **2000**, 2247.
(46) (a) Wang, C.-T.; Willey, R. J. *J. Non-Cryst. Solids* **1998**, *225*, 173. (b) Wang, C.-T.; Willey, R. J. *J. Catal.* **2001**, *202*, 211.
(47) Maayan, G.; Ganchegui, B.; Leitner, W.; Neumann, R. *Chem. Commun.* **2006**, 2230.
(48) (a) Randolph, T. W.; Clark, D. S.; Blanch, H. W.; Prausnitz, J. M. *Science* **1988**, *239*, 387. (b) Randolph, T. W.; Blanch, H. W.; Prausnitz, J. M. *AIChE J.* **1988**, *34*, 1354.
(49) Resmi, M. R.; Whitesell, J. K.; Fox, M. A. *Res. Chem. Intermed.* **2002**, *28*, 711.
(50) Hirakawa, T.; Whitesell, J. K.; Fox, M. A. *J. Phys. Chem. B* **2004**, *108*, 10213.
(51) Musie, G. T.; Wei, M.; Subramaniam, B.; Busch, D. H. *Inorg. Chem.* **2001**, *40*, 3336.
(52) Sharma, S.; Kerler, B.; Subramaniam, B.; Borovik, A. S. *Green Chem.* **2006**, *8*, 972.
(53) Hammond, D. A.; Karel, M.; Klibanov, A. M.; Krukonis, V. J. *Appl. Biochem. Biotechnol.* **1985**, *11*, 393.
(54) (a) Sheldon, R. A.; Kochi, J. K. *Metal Catalyzed Oxidation of Organic Compounds*; Academic Press: New York, 1981. (b) *Organic Syntheses by Oxidation with Metal Compounds*; Mijs, W. J., de Jonge, C. R. H. I., Eds.; Plenum Press: New York, 1986.
(55) Jessop, P. G.; Ikariya, T.; Noyori, R. Unpublished results, 1995.
(56) Kreher, U.; Schebesta, S.; Walther, D. *Z. Anorg. Allg. Chem.* **1998**, *624*, 602.
(57) Pesiri, D. R.; Morita, D. K.; Glaze, W.; Tumas, W. *Chem. Commun.* **1998**, 1015.
(58) Haas, G. R.; Kolis, J. W. *Organometallics* **1998**, *17*, 4454.
(59) Montilla, F.; Rosa, V.; Prevett, C.; Avilés, T.; Nunes da Ponte, M.; Masi, D.; Mealli, C. *Dalton Trans.* **2003**, 2170.
(60) Katsuki, T.; Sharpless, K. B. *J. Am. Chem. Soc.* **1980**, *102*, 5974.
(61) Tsuji, J. *Synthesis* **1984**, 369.
(62) Jia, L.; Jiang, H.; Li, J. *Chem. Commun.* **1999**, 985.
(63) Wang, Z.-Y.; Jiang, H.-F.; Qi, C.-R.; Wang, Y.-G.; Dong, Y.-S.; Liu, H.-L. *Green Chem.* **2005**, *7*, 582.
(64) (a) Blanchard, L. A.; Hancu, D.; Beckman, E. J.; Brennecke, J. F. *Nature (London)* **1999**, *399*, 28. (b) Brown, R. A.; Pollet, P.; McKoon, E.; Eckert, C. A.; Liotta, C. L.; Jessop, P. G. *J. Am. Chem. Soc.* **2001**, *123*, 1254. (c) Blanchard, L. A.; Brennecke, J. F. *Ind. Eng. Chem. Res.* **2001**, *40*, 287. (d) Mekki, S.; Wai, C. M.; Billard, I.; Moutiers, G.; Burt, J.; Yoon, B.; Wang, J. S.; Gaillard, C.; Ouadi, A.; Hesemann, P. *Chem.*−*Eur. J.* **2006**, *12*, 1760. (e) Saurer, E. M.; Aki, S. N. V. K.; Brennecke, J. F. *Green Chem.* **2006**, *8*, 141. (f) Kroon, M. C.; van Spronsen, J.; Peters, C. J.; Sheldon, R. A.; Witkamp, G.-J. *Green Chem.* **2006**, *8*, 246.
(65) (a) Liu, F.; Abrams, M. B.; Baker, R. T.; Tumas, W. *Chem. Commun.* **2001**, 433. (b) Ballivet-Tkatchenko, D.; Picquet, M.; Solinas, M.; Franciò, G.; Wasserscheid, P.; Leitner, W. *Green Chem.* **2003**, *5*, 232. (c) Solinas, M.; Pfaltz, A.; Cozzi, P. G.; Leitner, W. *J. Am. Chem. Soc.* **2004**, *126*, 16142.
(66) Hou, Z.; Han, B.; Gao, L.; Jiang, T.; Liu, Z.; Chang, Y.; Zhang, X.; He, J. *New J. Chem.* **2002**, *26*, 1246.
(67) Wang, J.-Q.; Cai, F.; Wang, E.; He, L.-N. *Green Chem.* **2007**, *9*, 882.
(68) Jiang, H.-F.; Shen, Y.-X.; Wang, Z.-Y. *Tetrahedron* **2008**, *64*, 508.
(69) Birnbaum, E. R.; Le Lacheur, R. M.; Horton, A. C.; Tumas, W. *J. Mol. Catal. A* **1999**, *139*, 11.
(70) Sahle-Demessie, E.; Gonzalez, M. A.; Enriquez, J.; Zhao, Q. *Ind. Eng. Chem. Res.* **2000**, *39*, 4858.
(71) Kokubo, Y.; Wu, X.-W.; Oshima, Y.; Koda, S. *J. Supercrit. Fluids* **2004**, *30*, 225.
(72) Campestrini, S.; Tonellato, U. *Adv. Synth. Catal.* **2001**, *343*, 819.
(73) Loeker, F.; Leitner, W. *Chem.*−*Eur. J.* **2000**, *6*, 2011.
(74) Beckman, E. J. *Green Chem.* **2003**, *5*, 332.
(75) Jenzer, G.; Mallat, T.; Maciejewski, M.; Eigenmann, F.; Baiker, A. *Appl. Catal., A* **2001**, *208*, 125.
(76) Wang, X.; Venkataramanan, N. S.; Kawanami, H.; Ikushima, Y. *Green Chem.* **2007**, *9*, 1352.
(77) Srinivas, P.; Mukhopadhyay, M. *Ind. Eng. Chem. Res.* **1994**, *33*, 3118.
(78) Mukhopadhyay, M.; Srinivas, P. *Ind. Eng. Chem. Res.* **1996**, *35*, 4713.
(79) (a) Asano, T.; le Noble, W. J. *Chem. Rev.* **1978**, *78*, 407. (b) van Eldik, R.; Asano, T.; le Noble, W. J. *Chem. Rev.* **1989**, *89*, 549.
(80) Srinivas, P.; Mukhopadhyay, M. *Ind. Eng. Chem. Res.* **1997**, *36*, 2066.
(81) Wu, X.-W.; Oshima, Y.; Koda, S. *Chem. Lett.* **1997**, *26*, 1045.
(82) Olsen, M. H. N.; Salomão, G. C.; Drago, V.; Fernandes, C.; Horn, A., Jr.; Cardozo-Filho, L.; Antunes, O. A. C. *J. Supercrit. Fluids* **2005**, *34*, 119.
(83) (a) Zhu, J.; Robertson, A.; Tsang, S. C. *Chem. Commun.* **2002**, 2044. (b) Tsang, S. C.; Zhu, J.; Yu, K. M. K. *Catal. Lett.* **2006**, *106*, 123.
(84) (a) Theyssen, N.; Leitner, W. *Chem. Commun.* **2002**, 410. (b) Theyssen, N.; Hou, Z.; Leitner, W. *Chem.*−*Eur. J.* **2006**, *12*, 3401.
(85) Suppes, G. J.; Occhiogrosso, R. N.; McHugh, M. A. *Ind. Eng. Chem. Res.* **1989**, *28*, 1152.
(86) Dooley, K. M.; Knopf, F. C. *Ind. Eng. Chem. Res.* **1987**, *26*, 1910.
(87) (a) Kerler, B.; Martin, A. *Catal. Today* **2000**, *61*, 9. (b) Martin, A.; Kerler, B. *Chem. Eng. Technol.* **2001**, *24*, 1.
(88) Armbruster, U.; Martin, A.; Smejkal, Q.; Kosslick, H. *Appl. Catal., A* **2004**, *265*, 237.
(89) Zhang, R.; Qin, Z.; Dong, M.; Wang, G.; Wang, J. *Catal. Today* **2005**, *110*, 351.
(90) Zhou, L.; Erkey, C.; Akgerman, A. *AIChE J.* **1995**, *41*, 2122.
(91) Kerler, B.; Martin, A.; Pohl, M.-M.; Baerns, M. *Catal. Lett.* **2002**, *78*, 259.
(92) Yu, K. M. K.; Abutaki, A.; Zhou, Y.; Yue, B.; He, H. Y.; Tsang, S. C. *Catal. Lett.* **2007**, *113*, 115.
(93) Oakes, R. S.; Clifford, A. A.; Bartle, K. D.; Pett, M. T.; Rayner, C. M. *Chem. Commun.* **1999**, 247.
(94) Campestrini, S.; Tonellato, U. *J. Mol. Catal. A* **2000**, *164*, 263.
(95) Chen, Q.; Beckman, E. J. *Green Chem.* **2007**, *9*, 802.
(96) Zaks, A.; Klibanov, A. M. *Proc. Natl. Acad. Sci. U.S.A.* **1985**, *82*, 3192.
(97) Chimowitz, E. H. *Introduction to Critical Phenomena in Fluids*; Oxford University Press: New York, 2005.
(98) Tiltscher, H.; Wolf, H.; Schelchshorn, J. *Angew. Chem., Int. Ed.* **1981**, *20*, 892.

CR8004058